

STUDIES ON THE DNA OF BACTERIOPHAGE T7

Thesis by

Frederick William Studier

In Partial Fulfillment of the Requirements

For the Degree of

Doctor of Philosophy

California Institute of Technology

Pasadena, California

1963

## ACKNOWLEDGEMENTS

I am very grateful for having had the opportunity to spend my graduate years in the stimulating atmosphere of the Caltech Biology Division. The pleasant associations with a great number of people, all of whom cannot be acknowledged here, have meant a great deal to me.

I am especially grateful to Dr. James Bonner whose helpfulness and support in every endeavor have eased the path I followed here.

Special thanks is due Dr. Paul Ts'o whose imaginative thinking and insights have influenced this work and my own development a great deal.

I appreciate very much the patient counsel and interest of Dr. Robert Sinsheimer whose acute scientific judgments have been invaluable to me in the course of this work.

Dr. Jerome Vinograd has been especially kind and helpful to me throughout my stay here both through many stimulating discussions and through generous loans of equipment when the need arose.

The help of Mr. Terry Conway in teaching me much about the ultra-violet optical system and his participation in some of the optical experiments presented here is gratefully acknowledged.

Financial support from National Science Foundation Predoctoral Fellowships and the Arthur McCallum Fund has been greatly appreciated.

I am most especially grateful to my wife, Susan, who has spiritually enriched this experience immeasurably. Thanks are due her also for patiently and carefully typing the many drafts, revisions, corrections, and the final copy of this thesis.

## ABSTRACT

The molecular weight of T7 DNA was determined to be  $15-17 \times 10^6$  by the method of sedimentation equilibrium in a CsCl density gradient. Possible sources of error in the optical reproduction of the concentration distribution in the cell were considered and evaluated. Comparison of the above molecular weight with the weight of the total DNA content of T7 phage determined by Davison and Freifelder (22) suggests: 1) that the entire DNA content of T7 bacteriophage can be released into solution as a single molecule and 2) that the density gradient method for determining molecular weights of homogeneous DNA samples is accurate within 10-20%.

The denaturation and renaturation of T7 DNA was studied using formamide as the denaturing agent. The complete cycle of denaturation and renaturation can thus be studied at room temperature without degradation of the primary structure of DNA.

Kinetics of denaturation were found to be essentially independent of concentration but were not first order, the rate falling off with time. Irreversible denaturation does not commence until the DNA has reached 80-90% of its full hyperchromicity. Samples of DNA isolated from denaturing conditions appear to be mixtures of fully denatured molecules and molecules which exhibit native characteristics to a high degree. Stirring solutions of DNA under denaturing conditions markedly accelerates the rate of denaturation. It seems possible that the molecular configuration of DNA molecules in intermediate states of denaturation may be a factor in stability to denaturation.

Optimally renatured T7 DNA has 85-90% of the native hyperchromic effect and bands at a slightly denser position than native DNA in a CsCl density gradient. Preliminary studies indicate second order kinetics for the renaturation reaction.

## INTRODUCTION

The biological importance of DNA has stimulated a substantial amount of work on its physical chemistry. It is unfortunate that the DNA samples used for much of this work have been intermolecularly heterogeneous in size and base composition. Such heterogeneity not only qualifies the interpretations of data obtained on these samples but perhaps obscures important features of DNA physical chemistry as well. The latter possibility is illustrated by the fact that renaturation has not been observed in markedly heterogeneous populations of DNA molecules.

Although valuable insights into the mechanisms of denaturation and renaturation might be provided by detailed physical chemical examination of the kinetics of these processes, such studies have not yet been reported for homogeneous DNA populations. The work to be reported here is an attempt to study by physical chemical methods the kinetics and mechanism of denaturation and renaturation of DNA prepared from bacteriophage T7.

T7 DNA was chosen for this study because of the apparent homogeneity of phage DNAs and because it was the smallest double stranded phage DNA readily available which contains no "odd" bases or attached glucose residues. The molecular weight of T7 DNA was examined by the method of sedimentation equilibrium in a CsCl density gradient to test both the homogeneity of the DNA and the accuracy of the density gradient method itself.

Denaturation and renaturation reactions were carried out in formamide solutions in order to minimize or eliminate the degradation of DNA which accompanies the heat treatment generally used to induce these

reactions. The ability to denature and renature DNA without attendant degradation of its primary structure would be especially valuable for studies of biologically active DNAs.

SECTION I. DETERMINATION OF THE MOLECULAR WEIGHT OF T7 DNA BY  
THE METHOD OF SEDIMENTATION EQUILIBRIUM IN A CsCl  
DENSITY GRADIENT

REVIEW . . . . .	4
EXPERIMENTAL . . . . .	6
METHODS . . . . .	7
Preparation of T7 DNA . . . . .	7
Density Gradient Runs . . . . .	10
Calculation of Molecular Weight . . . . .	11
STUDIES ON THE OPTICAL SYSTEM . . . . .	14
Light Source . . . . .	14
Slit . . . . .	18
Filters . . . . .	20
Camera Lens . . . . .	23
Alternator . . . . .	26
Film and Densitometer . . . . .	28
Effect of Bent Light . . . . .	33
MOLECULAR WEIGHT OF T7 DNA . . . . .	34
DISCUSSION . . . . .	38

REVIEW

Equilibrium sedimentation in a density gradient was recognized by Meselson, Stahl, and Vinograd (1) to have potential as a method for estimating molecular weights of homogeneous DNA samples. In this method a small amount of DNA is centrifuged to equilibrium at high speed in 7.7 molal CsCl (other salts may also be used (2)). The CsCl equilibrates in the centrifuge cell to form a density gradient and the DNA settles into a position centered about its buoyant density in the CsCl gradient. It was shown (1) that an anhydrous, homogeneous DNA at equilibrium in a density gradient should form a gaussian concentration distribution and that the variance of the gaussian,  $\sigma$ , should be a function of the molecular weight of the DNA. Hearst, Ifft and Vinograd (3,4,5) further expanded the theoretical treatment to include the effects of solvation and pressure on band shape and evaluated the parameters necessary for determining the molecular weight of T<sup>4</sup> DNA in a CsCl gradient. Yeandle (6) rederived the relation between molecular weight and  $\sigma$  to include the electrical effects expected from the polyanionic character of the DNA, and confirmed (1) that even if the DNA molecule were fully ionized (which is certainly far from true in 7.7 molal CsCl) the maximum error in the banding molecular weight due to electrical effects would be 15%.

It was immediately recognized (1) that density heterogeneity in DNA samples would broaden the concentration distribution found at equilibrium in a density gradient and lead to serious underestimates of the molecular weight of the sample. Generally density heterogeneity should distort the gaussian character of the concentration distribution and lead to

curvature in a  $\log C$  vs  $x^2$  plot.\* However, Baldwin (7) has shown that a sample having a gaussian distribution of effective densities will give rise to a gaussian concentration distribution at equilibrium. Such a distribution is therefore not sufficient to assure that the sample is homogeneous and the molecular weight calculated from the variance is correct. Various methods have been proposed for evaluating density heterogeneity in a sample (1,8). Density differences between DNA molecules have been shown to arise both from denaturation and from differences in G-C content (9,10,11,12,13).

Although it is difficult to estimate the molecular weight of DNA samples of doubtful homogeneity by the density gradient method, it should be straightforward to determine molecular weights on samples that are completely homogeneous. Evidence from autoradiography (14,15,16,17), electron microscopy (18) and genetics (19) indicates that the total DNA content of bacteriophages T2, T3 and  $\lambda$  can be liberated in a single piece, thus suggesting that DNA carefully prepared from these phages, and perhaps others as well, should be essentially homogeneous. Recently, banding molecular weights have been reported (20) for DNA from phages T2, T5, P22 and T7 which had been protected from shear degradation (14,23) in preparation and handling. These DNA preparations might reasonably be expected to be homogeneous, and thus the density gradient method would be expected to estimate their true molecular weight. However, Thomas and Pinkerton (20) found that the banding molecular weights for these phage

---

\* Since a gaussian concentration distribution would be  $C = C_0 e^{-\frac{x^2}{2\sigma^2}}$  where  $C$  = concentration,  $C_0$  = maximum concentration, and  $x$  = distance from band center, a plot of  $\log C$  vs  $x^2$  should be a straight line with a slope of  $-\frac{1}{2\sigma^2}$ .

DNA's were roughly a factor of two below estimates by other methods.\* They suggest that this discrepancy may be due to factors of importance in determining band shape which are as yet not fully understood, and propose that the twofold difference in molecular weights be considered a calibration factor for the density gradient method until further experimentation may resolve the issue.

#### EXPERIMENTAL

In the work to be reported here the molecular weight of T7 DNA was studied by the density gradient technique. From considerations mentioned above it seemed likely that the entire DNA content of each T7 phage could be released into solution as a single molecule, thus producing a homogeneous sample of DNA. For such a solution the molecular weight determined by the density gradient method should, in theory, equal that of the total DNA content of the phage. If this result were obtained experimentally it would demonstrate both that each T7 phage did indeed liberate a single molecule of DNA into solution and that the determination of the molecular weight by the density gradient method was not in error.

However, the findings of Thomas and Pinkerton (20) suggest that the molecular weight determined on homogeneous DNA samples by the density gradient method should equal one half the true molecular weight. An experimentally determined banding molecular weight equal to one half the molecular weight of DNA in the phage would thus be inconclusive

---

\* It should be pointed out that the molecular weight of  $10-12 \times 10^6$  obtained by Thomas and Pinkerton on T7 DNA prepared by us is distinctly lower than the  $15-17 \times 10^6$  molecular weight obtained here as well as the  $18 \times 10^6$  obtained by Meselson (21) and  $15 \times 10^6$  by Davison and Freifelder (22). It is possible that the DNA could have been degraded in transit.

without an independent molecular weight determination on the isolated T7 DNA.

In order to make as accurate a determination of the molecular weight as possible the ultraviolet absorption optical system of the ultracentrifuge was critically examined for possible sources of error in reproduction of the band shape present in the cell. Almost any optical error would tend to lower the molecular weight obtained. Factors such as light source position, slit width, focus, film and densitometer error, as well as other possible sources of optical distortion were considered.

#### METHODS

Preparation of T7 DNA. T7 phage stocks were prepared as follows: Vigorously aerated cultures of E. coli B in a glycerol casamino acid medium\* were grown to  $10^9$ /ml at  $37^\circ$  and then inoculated with T7 phage\*\* to about  $10^8$  phage particles per ml. Aeration was continued for approximately two to four hours until lysis appeared complete. Foaming was controlled by Dow Antifoam A. The lysate was then brought to 60% in ammonium sulfate and the precipitate was allowed to settle in the cold. The bulk of the supernatant was siphoned off and the remaining suspension

---

\* A modification of the medium of Fraser and Jerrel (24) containing:

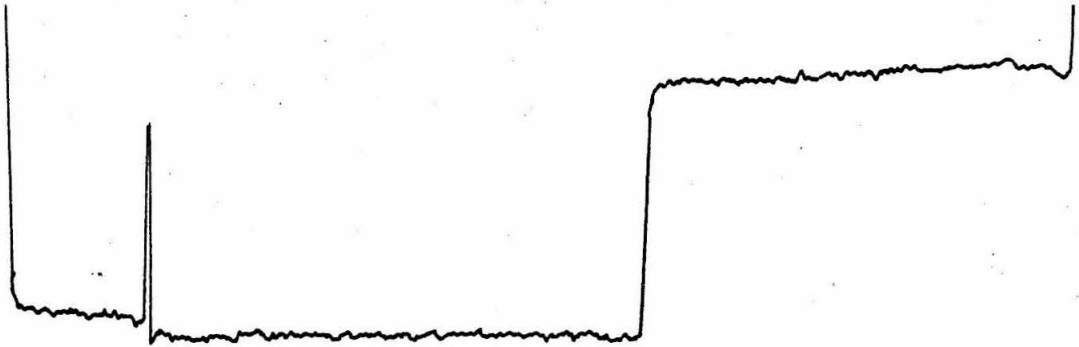
0.9 g	$\text{KH}_2\text{PO}_4$	} . . . made up in a portion of the $\text{H}_2\text{O}$ and added last
2.1 g	$\text{Na}_2\text{HPO}_4$	
3.0 g	$\text{NH}_4\text{Cl}$	
.3 g	$\text{MgSO}_4$	
.3 ml	1M $\text{CaCl}_2$	✓
3.0 ml	1% gelatin	✓
15.0 g	Casamino acids	✓
24.0 ml	glycerol	
1 liter	$\text{H}_2\text{O}$	✓

\*\* T7 phage stock was obtained from Prof. R. L. Sinsheimer.

passed through a Servall continuous flow centrifuge to collect the precipitate. The precipitate was then dissolved in 0.1 M NaCl, 0.01 M TRIS, pH 7.5, the phage were purified by several cycles of differential centrifugation and then treated with RNAase and DNAase to remove any cellular nucleic acid which may have remained. The phage were once more spun down and resuspended to form a phage stock which was stored in the refrigerator and used for preparation of DNA as needed. The phage stock sedimented with a single sharp boundary of about 480 s and banded as a single band in a CsCl density gradient at a density of approximately 1.52 g/ml. Phage suspensions which had stood for several months often contained aggregated material.

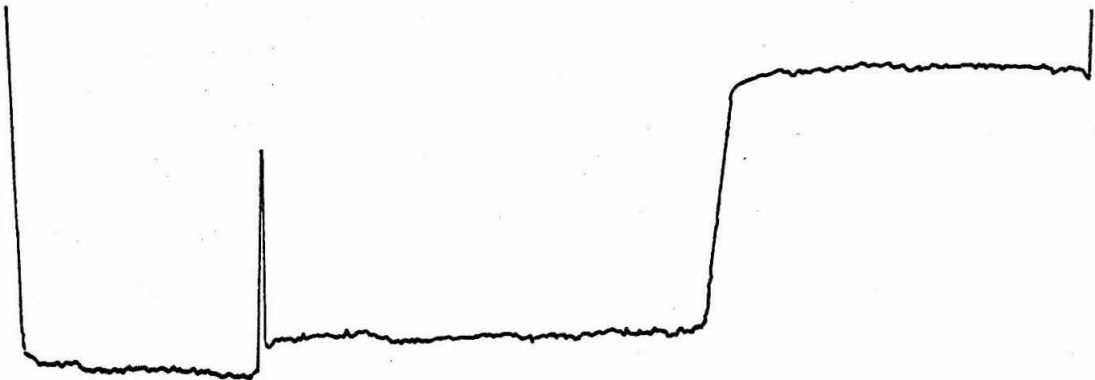
T7 DNA was prepared from purified phage stocks at a DNA concentration of about 1 mg/ml (an OD of about 20) by gentle shaking with water saturated phenol (25) at room temperature. Mallinckrodt analytical reagent grade liquified phenol (around 88% phenol) with no added preservative was used without further purification. Generally, after two or three phenol extractions the DNA solution was extracted several times with ether, aerated and dialyzed at least 12 hours in the cold against 0.1 M NaCl, 0.01 M TRIS, pH 7.5. Stock solutions for density gradient work were diluted to an optical density of approximately 1 and stored in solution in the refrigerator. One such DNA solution showed no change in banding molecular weight over a period of several months.

Velocity sedimentation patterns of native T7 DNA in solutions  $10^{-3}$  to 0.1 M in NaCl and denatured DNA in  $10^{-3}$  to  $10^{-2}$  M NaCl showed a single sharp boundary with no evidence of degraded material (Fig. 1).



Native T7 DNA at a concentration of 19  $\mu\text{g/ml}$

$$s_{20,w} = 21.7$$



Denatured T7 DNA at a concentration of 19  $\mu\text{g/ml}$

$$s_{20,w} = 16.4$$

Figure 1. Sedimentation velocity patterns of native and denatured T7 DNA run at 31,410 rpm in 0.01 M NaCl, 0.001 M TRIS, pH 7.4.

The extinction coefficient of the T7 DNA was measured and found to be, per mole of phosphorus,  $\epsilon (P) = 6,980$  at 258 m $\mu$ . Phosphorus was determined by the method of Allen (26).

Density Gradient Experiments. The density gradient experiments on T7 DNA were made in Spinco Model E #521 ultracentrifuge equipped with ultraviolet absorption optics using cells with quartz windows and 4° sector centerpieces. The 12 mm centerpieces were of Kel-F and the 3 mm centerpiece was of filled-Epon. The filling holes of these centerpieces were enlarged to a diameter of .05 inch. Cell assemblies were tightened with a torque wrench to 115-125 inch pounds.

Harshaw optically pure CsCl and Kawecki Chemical Co. CsCl were used for this work. The latter was heated to 500° for 24 hours and then a 60% aqueous solution was passed through a Norit column in order to reduce ultraviolet absorption to below .05 density units from 250 m $\mu$  through the visible (19). For individual experiments 0.6 ml of a CsCl stock solution of a density 1.80-1.88 g/ml, pH 7-8, was diluted with DNA solution and enough water to produce the desired density. When accurate knowledge of densities was required the solution was weighed in 300  $\lambda$  pipettes or the density determined from the refractive index by the relation

$$\rho^{25^\circ} = 10.8601 n_D^{25^\circ} - 13.4974$$
 (27). Some stock solutions were made by dissolving the CsCl in 0.01 M TRIS and 0.001 M EDTA.

On several occasions syringes appeared to give off ultraviolet absorbing material into the CsCl solutions, thus producing a sloping baseline in pictures of the density gradient run. Therefore 9 inch Pasteur pipettes which had been rinsed several hours in a pipette washer were used for filling cells.

Calculation of Molecular Weight. Molecular weights were calculated from density gradient band shapes using the procedures of Hearst, Ifft and Vinograd (3,4,5) and the hydration and compression parameters which they evaluated for T4 DNA. From Hearst and Vinograd (3)

$$M_{s,o} = \frac{RT}{\sigma^2 \bar{v}_{s,o} \left( \frac{d\rho}{dr} \right)_{\text{eff}} \omega^2 r}$$

- where  $M_{s,o}$  = the solvated molecular weight at band center  
 $R$  = gas constant =  $8.314 \times 10^7$  ergs deg<sup>-1</sup> mole<sup>-1</sup>  
 $T$  = temperature = 298°  
 $\sigma$  = standard deviation in cm of the gaussian concentration distribution at equilibrium  
 $\bar{v}_{s,o}$  = solvated partial specific volume of DNA at band center  
 $\left( \frac{d\rho}{dr} \right)_{\text{eff}}$  = the effective density gradient  
 $\omega$  = angular velocity  
 $r_o$  = centrifugal radius at band center

In order to evaluate  $M_{s,o}$  the values of  $\bar{v}_{s,o}$  and  $\left( \frac{d\rho}{dr} \right)_{\text{eff}}$  must be determined. From (3) and (5)

$$\frac{1}{\bar{v}_{s,o}} = \rho_o = \frac{\rho_o^o}{1 - k P_o}$$

- where  $\rho_o$  = density at band center in the spinning cell  
 $\rho_o^o$  = density at band center at atmospheric pressure  
 $k$  = isothermal compressibility coefficient of the solution =  $25.8 \times 10^{-6}$  atm<sup>-1</sup>  
 $P_o$  = pressure at band center.

$P_o$  could vary anywhere up to a maximum of 250 atmospheres under the conditions used here but in general would be considerably smaller than this. To avoid having to make pressure corrections for each experiment  $\frac{1}{v_{s,o}} = \rho_o^o = 1.708$  was used for all calculations. The maximum error

in  $M_{s,o}$  due to this approximation will be less than 1%.

From (3,4,5)

$$\left(\frac{d\rho}{dr}\right)_{\text{eff}} = \left[ \frac{1}{\beta_o} + \Psi \rho_o^{o^2} \right] (1 - \alpha) \omega^2 r$$

where  $\frac{1}{\beta_o} = 8.40 \times 10^{-10}$  (27,28)

$$\Psi = \frac{k - k_s}{1 - \alpha} = 2.30 \times 10^{-11} \text{ cm}^2 \text{ dyne}^{-1}$$

where  $k_s$  is the apparent compressibility of the solvated DNA and

$$\alpha = \left( \frac{\partial \rho_o^o}{\partial a_1^o} \right) \left( \frac{d a_1^o}{d \rho_o^o} \right) = 0.24$$

where  $a_1^o$  is the water activity at atmospheric pressure.

So  $\left(\frac{d\rho}{dr}\right)_{\text{eff}} = 6.89 \times 10^{-10} \omega^2 r$  and  $M_{s,o} = \frac{6.14 \times 10^{19}}{\sigma^2 (\omega^2 r_o)^2}$ .

The anhydrous molecular weight of the Cs salt of DNA,  $M_{Cs} = \frac{M_{s,o}}{1 + \Gamma'}$ .

From (4)  $\frac{1}{\rho_o} = \frac{v_3 + \Gamma' v_1}{1 + \Gamma'}$

where  $v_3$  = specific volume of anhydrous Cs DNA, taken as 2.12 (2,4)

$v_1$  = specific volume of the solvated  $H_2O$ , taken as 1.0

$\Gamma'$  = grams of  $H_2O$  per gram of Cs DNA

$\rho_o$  is taken as 1.708.

Thus  $\Gamma' = .27$  and  $M_{Cs} = \frac{4.83 \times 10^{19}}{\sigma^2(\omega^2 r_o)^2}$ . This is converted to the

anhydrous sodium molecular weight,  $M_{Na}$ , by the factor  $\frac{331}{441} = .751$ , the ratio of the average sodium and cesium monomer weights. Thus,

$$M_{Na} = \frac{3.63 \times 10^{19}}{\sigma^2(\omega^2 r_o)^2} . \text{ In this study the molecular weights were cal-}$$

culated from the relations  $M_{Na} = \frac{7.51 \times 10^4}{\sigma^2 r_o^2}$  for 44,770 rpm and

$$M_{Na} = \frac{6.63 \times 10^5}{\sigma^2 r_o^2} \text{ for 25,980 rpm.}$$

The value of  $\sigma^2 r_o^2$  for the individual experiments was determined from Joyce-Loebl densitometer traces of films exposed after equilibrium had been attained, generally 18-20 hours at 44,770 rpm and 5-6 days at 25,980 rpm. Since a gaussian follows the relation  $C = C_o e^{-\frac{x^2}{2\sigma^2}}$ , a plot of  $\log C$  vs  $x^2$  should produce a straight line with a slope of  $-\frac{1}{2\sigma^2}$ . Generally  $x$  was taken to be the total width of the curve,  $W$ , rather than the distance from the center of the curve. When  $\log C$  is plotted against  $W^2$  the slope is  $-\frac{1}{8\sigma^2}$ . This method eliminates errors due to placement of the center of the curve but it tends to obscure skewing when present.

For each density gradient experiment Joyce-Loebl densitometer traces of several exposures were analyzed to obtain an average  $\sigma$  as well as an idea of the scatter. A sloping baseline, which contributes to the uncertainty in  $\sigma$  was present in some pictures. The uncertainty in the molecular weight due to uncertainty in the traces was often as high as  $\pm 10\%$ .

## STUDIES ON THE OPTICAL SYSTEM

The ultraviolet absorption optical system supplied with the Spinco Model E ultracentrifuge, including an alternator attachment for running two cells simultaneously, was used for the work reported here. This system consists of light source, slit, filters, collimating lens, rotating centrifuge cell with quartz windows and  $4^\circ$  Kel-F centerpiece, condensing lens, mirror, camera lens, alternator, and Kodak Commercial film. For density gradient runs a Corning CS No. 7-54 corex glass filter was used in addition to the  $\text{Br}_2\text{-Cl}_2$  filters supplied with the machine. The positions of the optical components are shown schematically within the frame of the ultracentrifuge in Fig. 2. For simplicity the front to rear, side to side, and up and down directions as designated in Fig. 2 will be used in discussing the placement of the various components. In this system the axis of rotation is in the vertical direction and the radial axis of the cell in the optic system runs in the front to rear direction. The properties of various individual components of this optical system have been examined, particularly in their relation to the density gradient band shape registered on the film and general quality of the pictures obtained.

Light Source. The light source for this system is a GE H85A3/UV medium pressure mercury arc lamp. Although the emission spectrum from this lamp ranges from 230  $\mu$  through the visible wavelengths, spectrograph pictures show that the Corex- $\text{Br}_2\text{-Cl}_2$  filter system effectively isolates the 248-280  $\mu$  region (see Filters). As lamp age increases the intensity drops (fivefold in the one case measured), so exposure time is not a reliable measure of intensity from run to run.

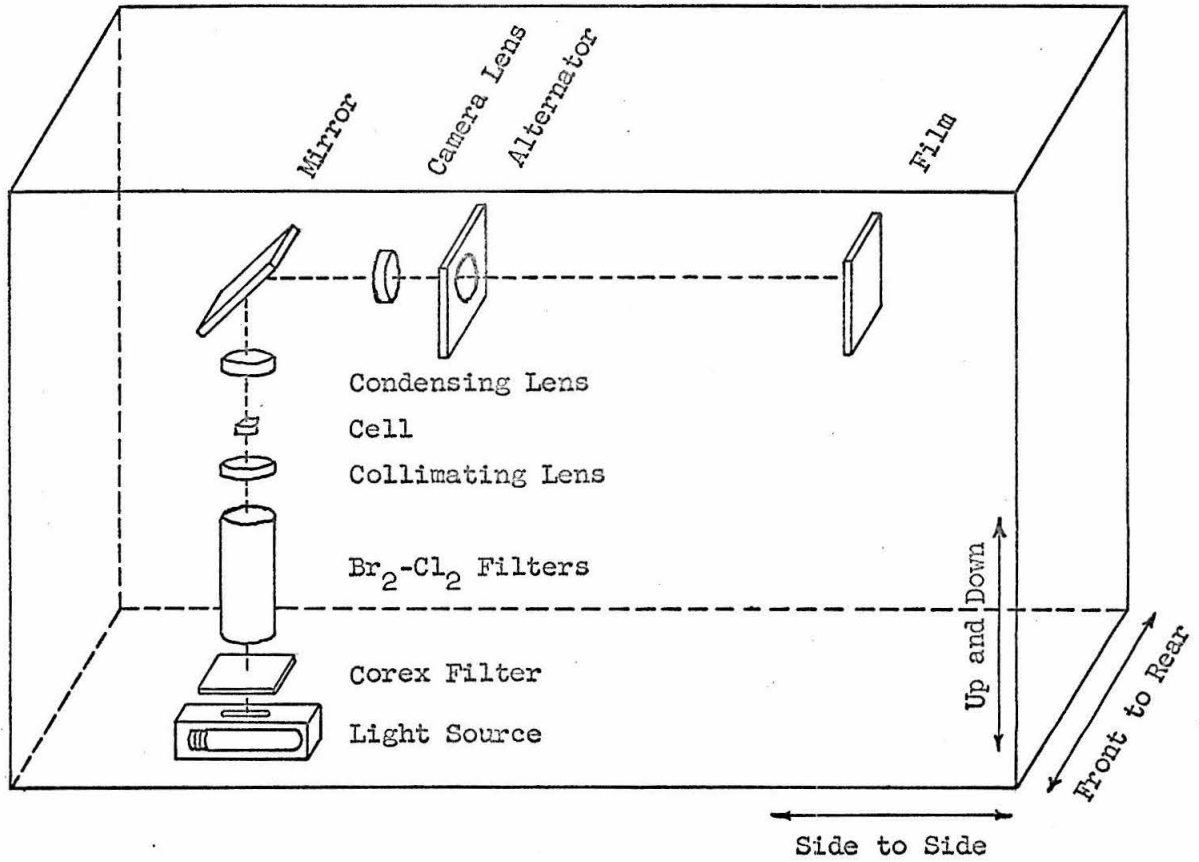


Figure 2. Ultraviolet absorption optical system of Spincro Model E Ultracentrifuge #521.

In order to obtain parallel, uniform illumination of the cell the light must come from a monochromatic point source at the focal point of the collimating lens. However, since the purpose of the optical system is to accurately reproduce the concentration distribution in the cell, light is required only to pass through the cell on isoconcentration surfaces and to be of uniform intensity down the length of the cell. Isoconcentration surfaces in the spinning cell are portions of concentric cylinders centered on the axis of rotation. In this system these surfaces are well represented by planes perpendicular to the radial axis of the cell, and light may traverse the cell on any path lying on one of these planes with a minimum of distortion in registering the concentration distribution in the cell.\* This means that the side to side position of the light source is not critical and therefore the arc of the lamp is placed parallel to the front of the machine. On the other hand vertical and front to rear positioning of the light source are quite critical since they affect both the evenness of illumination down the length of the cell and the angle between the entering light and the radial axis.

The vertical distance between the arc of the light source and the collimating lens was adjusted by direct measurement to equal the 257  $\mu$  focal length of the lens. If the source is vertically displaced very far from this position the illumination becomes uneven and the baseline

---

\* Actually, a light beam passing from wall to wall of a  $4^\circ$  sector cell in the plane perpendicular to the radial axis of the cell and 6.6 cm from the axis of rotation would cross isoconcentration cylindrical surfaces .004 cm apart. Using light displacement at the alternator as a rough measure of the angle of light entering the cell, it is estimated that the 1/2 inch long slit supplied with the machine would allow light passing through the cell to cross isoconcentration cylinders a maximum of .0015 cm apart due to the side to side displacement of the ends of the slit.

appears to bow. However pictures of an equilibrium band in a density gradient taken with the source vertically displaced as much as 1-2 inches showed little if any change in band shape.

The front to rear position of the light source was chosen so that the light enters the cell at  $90^\circ$  to the radial axis. When there is a density gradient in the cell the refractive index gradient will bend light across isoconcentration surfaces (29), and the most accurate reproduction of the concentration distribution would be given by light entering the cell at some angle other than  $90^\circ$ . However, the  $90^\circ$  position for the light source was chosen because it is correct for sedimentation velocity runs, the reference lines are sharp, and the angle at which light enters the cell can be adjusted by bottom wedge windows more easily than by changing light source position every run. The problem of light bending across isoconcentration surfaces is treated more fully in the appendix.

The shadow method (30) was used to determine the  $90^\circ$  front to rear position of the light source. This method depends on the reflection of light off the air-water interface in the cell when light which is not parallel to the interface passes through the cell. This reflection would normally be focused on the film at the position of the meniscus but if the camera lens is displaced about an inch from its proper position the reflection will not be correctly focused and will appear as a dark line or shadow to the side of the meniscus.

To position the source on this machine the slit was removed and the camera lens was displaced about an inch from its proper position. A cell partially filled with water was spun at 44,770 rpm and a series of pictures were taken at different front to rear positions of the light source.

With the light in the correct position the shadow disappeared (or was evenly distributed on both sides of the meniscus). Less than 1/8 inch displacement of the light source from the correct front to rear position caused the shadow to appear to the side of the meniscus. The correctness of the front to rear light source position can be verified by checking to see that the reference edges and top and bottom edges of the cell all appear sharp.

Front to rear misalignment of the light source will produce sloping baselines, blurring of certain cell and reference edges and changes in density gradient band shapes. Blurring of edges resulting from front to rear misalignment is apparently caused by reflections off surfaces of the cell assembly or counterbalance, for as the source is moved rearward from its correct position the cell bottom edge and top reference edge become blurred in the picture while the cell top edge and bottom reference edge remain sharp; the opposite occurs upon moving the light source forward. When wedge windows or refractive index gradients are used it is often impossible to obtain pictures in which both cell edges appear sharp. This blurring is presumably caused at least in part by reflections off the cell assembly, but the possibility of refractive index dispersion effects for light of different wavelengths has not been excluded (see Filters).

Slit. The slit used for this work has been 1/8" x 1/8", which allows the use of an alternator for running two cells simultaneously. This slit assembly consists of a 1/2" x 1/8" slit which lies along the arc of the light source and is positioned prior to placing another 1/2" x 1/8" slit across the arc to define the 1/8" x 1/8" aperture. After the arc of the lamp has been correctly positioned beneath the

collimating lens (see Light Source) the slit has only to be placed over it so that the lens sees the arc symmetrically. The image of the arc which is seen by the optical system is focused behind the camera lens, and this image as well as the edges of the slit may be readily seen on a card placed at this position. Viewing the image of the arc through an empty, evacuated chamber the  $1/2''$  x  $1/8''$  slit which runs along the arc should be positioned so that the arc is seen on the card to be centered between the edges of the slit. The slit which lies across the arc affects the vertical position of the beam at the camera lens and should be placed so that the beam is at a convenient height for use of the alternator. Once the slit is positioned a slight side to side movement of the light source serves as a good fine adjustment for the final placement of the images at the alternator.

It is possible that changing light sources may slightly alter the front to rear position of the arc. When a slit is used this possible displacement can be readily checked by examination of the image of the arc focused behind the camera lens to see if the arc is still centered between the edges of the slit. If the arc position has indeed changed it may be that a slight rotation of the source may remedy the situation without the necessity of repositioning the source by the shadow method.

Theoretically the narrower the slit the more parallel the light and hence the truer the film reproduction. In practice, however, pictures taken with no slit, a  $.005''$  x  $1/2''$  slit or a  $1/8''$  x  $1/8''$  slit showed no appreciable differences in band shape. However, if the slit is not placed symmetrically over the arc of the lamp uneven illumination of the cell and sloping baselines may result.

Filters. A combination of a  $\text{Br}_2$  gas filter, a  $\text{Cl}_2$  gas filter and a purple corex glass filter was used for all density gradient runs, but omission of the corex filter in velocity runs allowed an approximately twofold increase in intensity. Figures 3 and 4 give the absorption spectra of the filters and tracings of spectrograph pictures taken on Kodak Commercial film through the two filter combinations used, by placing a spectrograph at the mirror position. The addition of the corex filter to the  $\text{Br}_2$ - $\text{Cl}_2$  combination appreciably improves spectral purity by eliminating light below the 244 line as well as a very small amount of visible light.

The addition of the corex filter to the  $\text{Br}_2$ - $\text{Cl}_2$  combination in banding runs increased the height and sharpness of the bands and reduced the blurring of the bottom edge of the cell. Some blurring of the cell edge might be expected from reflection of the light deflected by the density gradient off surfaces of the cell assembly (see Light Source) but it is unlikely that addition of a corex filter would reduce blurring from this cause. It seems more likely that, due to the high refractive index dispersion in the ultraviolet, light of the various wavelengths from 230-280  $\mu$  is bent to different degrees through the refractive index gradient and focused at slightly different positions on the film to produce the observed effects. The marked increase in spectral purity obtained by use of the corex apparently improves the situation but it is impossible to estimate how important the remaining dispersion problem may be. Obviously the lower the density gradient the smaller these effects would be.

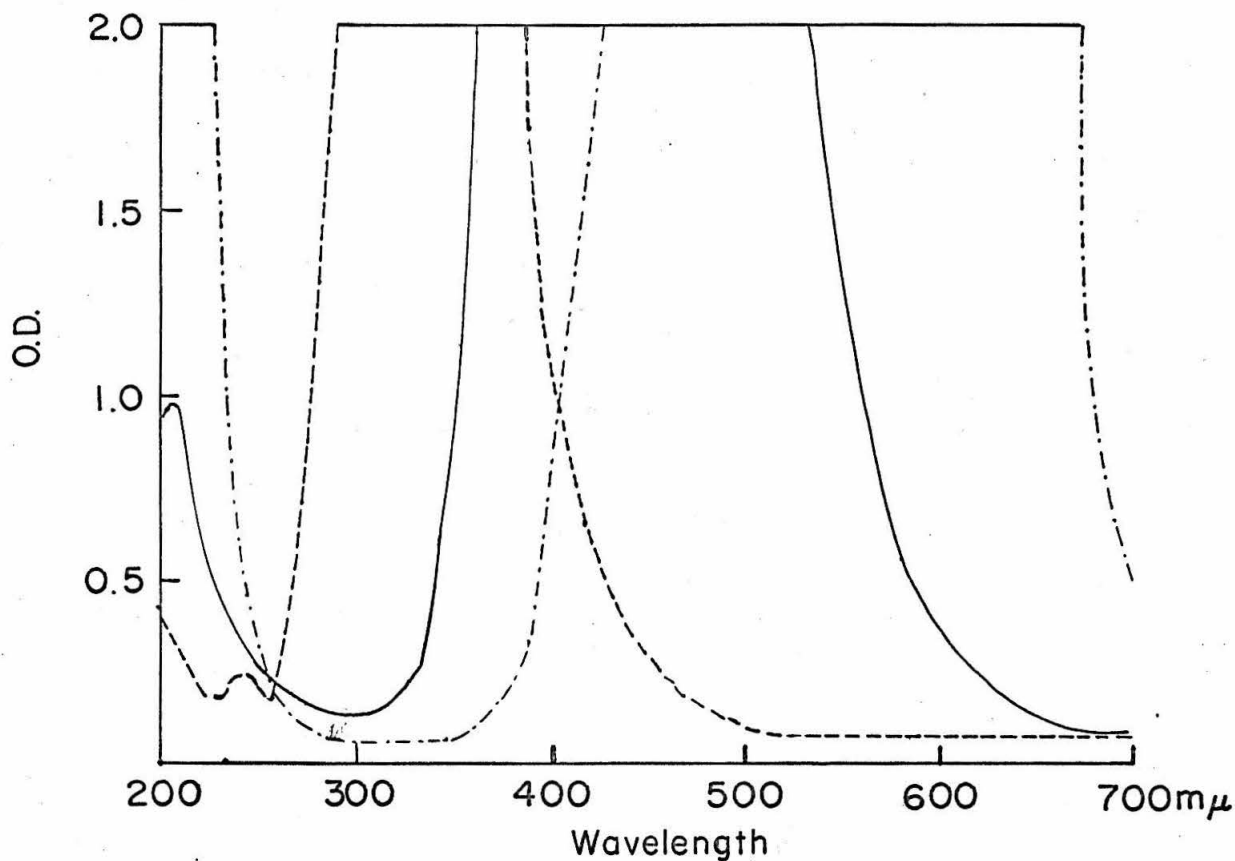
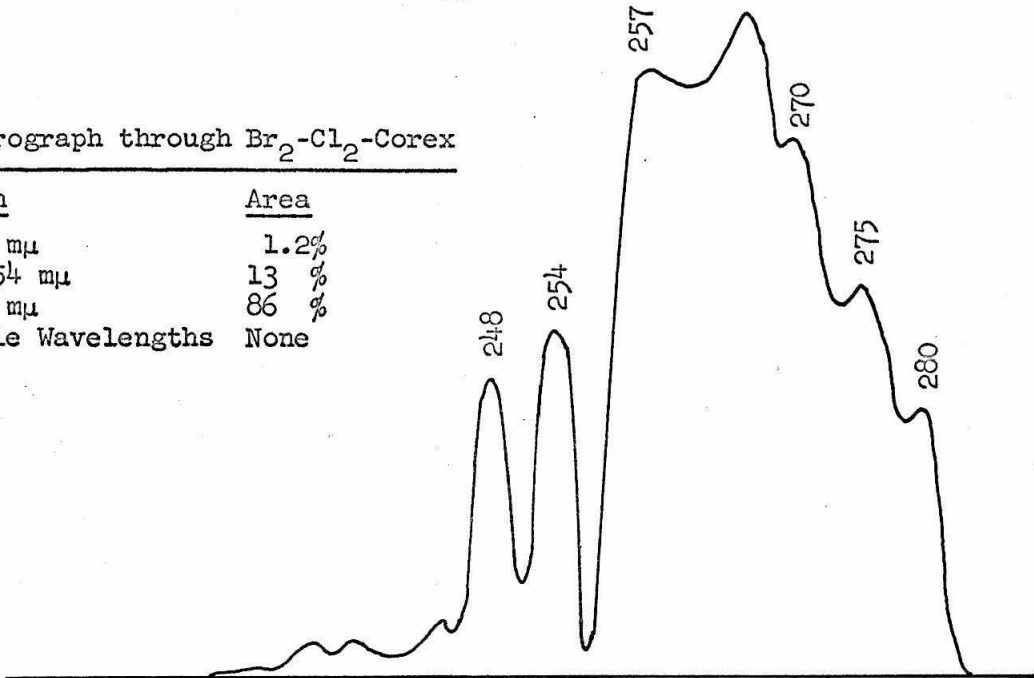


Figure 3. Absorbancies of filters used in the optical system of ultracentrifuge #521 as read in a Cary Model 11 Recording Spectrophotometer: — Br<sub>2</sub>; ---- Cl<sub>2</sub>; -.-.- Corex.

Spectrograph through Br<sub>2</sub>-Cl<sub>2</sub>-Corex

<u>Region</u>	<u>Area</u>
< 244 mμ	1.2%
244-254 mμ	13 %
> 254 mμ	86 %
Visible Wavelengths	None



Spectrograph through Br<sub>2</sub>-Cl<sub>2</sub>

<u>Region</u>	<u>Area</u>
< 244 mμ	19%
244-254 mμ	20%
> 254 mμ	61%
Visible Wavelengths	0.25%

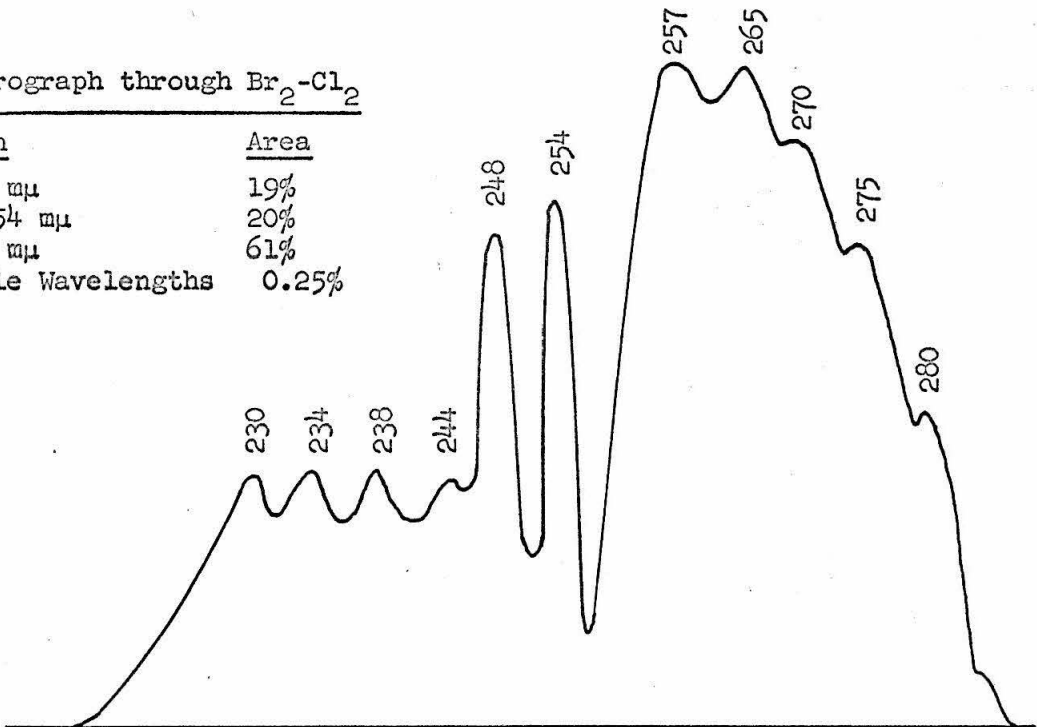


Figure 4. Spectrograms of GE H85A3/UV light source taken through different filter combinations with an Adam Hilger Quartz Spectrograph on Kodak Commercial film.

The assistance of Mr. Robert Stewart in taking the spectrographs and identifying wavelengths is gratefully acknowledged.

Qualitative support for the notion that dispersion effects are involved in the blurring of the bottom cell edge comes from pictures of a density gradient taken through a  $\text{Cl}_2$ -corex combination, which transmits light in the 260  $\mu$  and 400  $\mu$  regions. As shown in Fig. 5, the 400  $\mu$  image of the cell bottom falls inside the 260  $\mu$  image of the cell in a position which would suggest that dispersion between 265 and 230 could account for the additional blurring of the bottom edge which is seen without the corex.

Camera Lens. The position of the camera lens determines the focal plane in the cell as well as the magnification from cell to film. Although the magnification changes with camera lens position it is interesting that there is essentially no loss of sharpness in the film image of cell boundaries, reference edges, or scribe lines on windows and no change in the normalized shape of a density gradient band upon changing the camera lens position as much as two inches. This is an indication that the cell is illuminated by light that is essentially parallel.

However, although the light may be parallel upon entering the cell, the refractive index gradient in the solution due to the compression gradient (or to the density gradient, if present) bends the light passing through the solution away from that passing through the air bubble. The light beams in each group remain internally parallel, and thus both images remain sharply focused, but the two groups diverge through the lens system, only to be focused adjacent to each other again on the film. If focus is incorrect the images of the air bubble and solution on the film will be either too widely spread or overlapped.

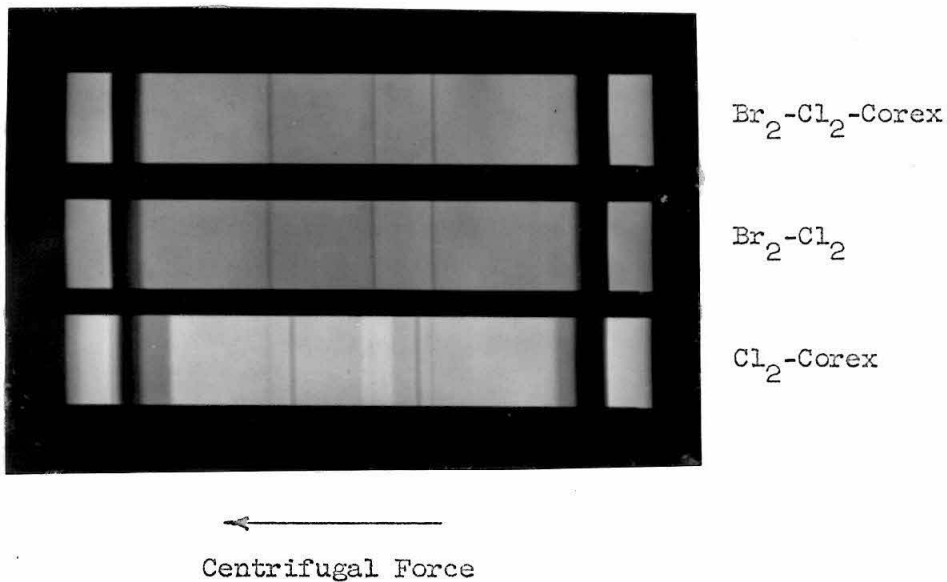


Figure 5. Pictures, taken through different filter combinations, of a cell spinning at 44,770 rpm and containing a CsCl solution of density approximately 1.7 g/ml. The center line inside the cells is the meniscus and the two outer lines are scribe lines on the bottom window. The top window was a negative 1° wedge window.

Two methods were used to position the camera lens. The shadow method (see Light Source) is to be preferred, but its accuracy was checked by focusing scribe lines on the windows when diffused light was passed through the cell. The shadow method is again based on the use of the reflection of light off the air-water interface which occurs when the light source is out of position. If the camera lens is correctly focused this reflection will be focused back at the meniscus, but if not it will appear as a dark line or shadow to the side of the meniscus on the film. To position the camera lens by the shadow method the light source is moved toward the front of the machine from its correct position, a cell partially filled with water is spun at the desired speed (44,770 rpm in this machine) and a series of pictures is taken at different camera lens positions. The picture in which the shadow disappears into (or is evenly distributed around) the meniscus determines the correct camera lens position. For this machine the correct camera lens position was determined by the shadow method to be 8-1/4".

In the second method of focusing a ground quartz diffuser was placed over the collimating lens inside the chamber and a cell with scribe lines on top and bottom windows was partially filled with water and spun at 44,770 rpm. Pictures were taken with the camera lens at different positions to determine the positions where various lines and edges appeared most sharply focused. (If a diffuser is not used all lines remain sharp at all camera lens positions.)

The results are as follows:

<u>Object focused</u>	<u>Camera lens position at best focus</u>
Scribe line on bottom window (through H <sub>2</sub> O)	8-3/8
Scribe line on bottom window (through air)	8-3/4
Scribe line on top window	7-7/8
Meniscus - never sharp but best at	7-7/8
Aperture edge - a reference knife edge at midplane of cell	8-1/4

It can be seen from these results that for water in the cell the shadow method positions the camera lens so that the focal plane falls near the midplane of the cell.

The degree of divergence between light passing through air bubble and solution will be a function of the refractive index gradient present in the solution. For this reason the camera lens position which gives the sharpest meniscus will be slightly different for different runs, depending on the gradient present. However, in order to keep the magnification factor constant for all runs the camera lens position was determined for water, and once determined was not changed.

Alternator. The alternator is an attachment used in conjunction with a 1/8" x 1/8" slit and a side wedge window to allow automatic photography of two cells run simultaneously. The alternator itself is a horizontal bar which automatically assumes one of two positions every time the film shift motor operates. It is placed between the camera lens and film at the position where the image of the 1/8" x 1/8" slit is most sharply focused. In a double cell run the focused image of the slit as

seen through the cell containing the side wedge is displaced vertically from the undeviated image of the slit thus producing a clear separation of the light passing through the two cells. The alternator bar is placed so that in each position it blocks out the light from one cell but allows light from the other to proceed to the film. Since no counterbalance is used in double cell runs the only reference line present on the film will be that of the rotor, and since the light through it is undeviated this line will appear only in pictures of the cell which has no side wedge.

Placing the side wedge at the bottom of the cell assembly deviates light upward at the camera lens whereas light is deviated downward if the side wedge is at the top of the cell assembly. The alternator on this machine was aligned so that the side wedge must be placed at the bottom of the cell assembly. The alternator bar can be placed at approximately the right height for double cell operation by an adjustment on the alternator itself. Since movement of the light source in the side to side direction shifts the images at the alternator vertically, fine adjustment is readily achieved by this means. The regions above and below the slit images at the alternator can be blocked out to keep any unwanted reflections in these regions from reaching the film. Once the alternator and slit were positioned on this machine they were not changed or removed and velocity runs as well as density gradient runs were made through this system. If one cell only is to be run the power to the alternator can be disconnected and the bar will not shift between pictures.

It should be possible to make density gradient runs with three cells and a counterbalance by using a side wedge at the top of the third cell

assembly and a negative wedge in the cell which has no side wedge. If the alternator assembly is removed from behind the camera lens, pictures of each cell including counterbalance reference lines could be taken by blocking out the unwanted images manually.

Film and Densitometer. The ultraviolet picture of the centrifuge cell was recorded on Kodak Commercial Sheet Film and the film record was translated to a plot of film OD against distance in the cell by Joyce-Loebl double beam recording microdensitometers. If the densitometer trace is to be an accurate representation of the concentration distribution in the cell, the OD on the film must be a linear function of DNA concentration in the cell and the pen displacement of the densitometer must be a linear function of film OD.

The film was developed by the following standard procedure: 5 minutes in D-11 developer, 30 seconds in stop bath, 5-10 minutes in fixer, an hour in running water rinse, dip in Photo-flo and dry. Occasionally 2 minutes in hypo clearing agent and a 5 minute running water rinse were substituted for the one hour rinse. The slope of the plot of film OD against the log of the incident intensity was of the order of 0.75-0.90 for films treated in this manner.

To examine the range of intensities over which film response is linear an exposure series of a density gradient run was taken using a fresh lamp. As can be seen in Fig. 6 the film OD was a linear function of the log of the exposure time for times between about 15 seconds and 10 minutes. Since lamp intensity varies widely with lamp age exposure time is not a reliable measure of intensity from one experiment to the next, but if a standard developing procedure is used the OD of an exposed portion

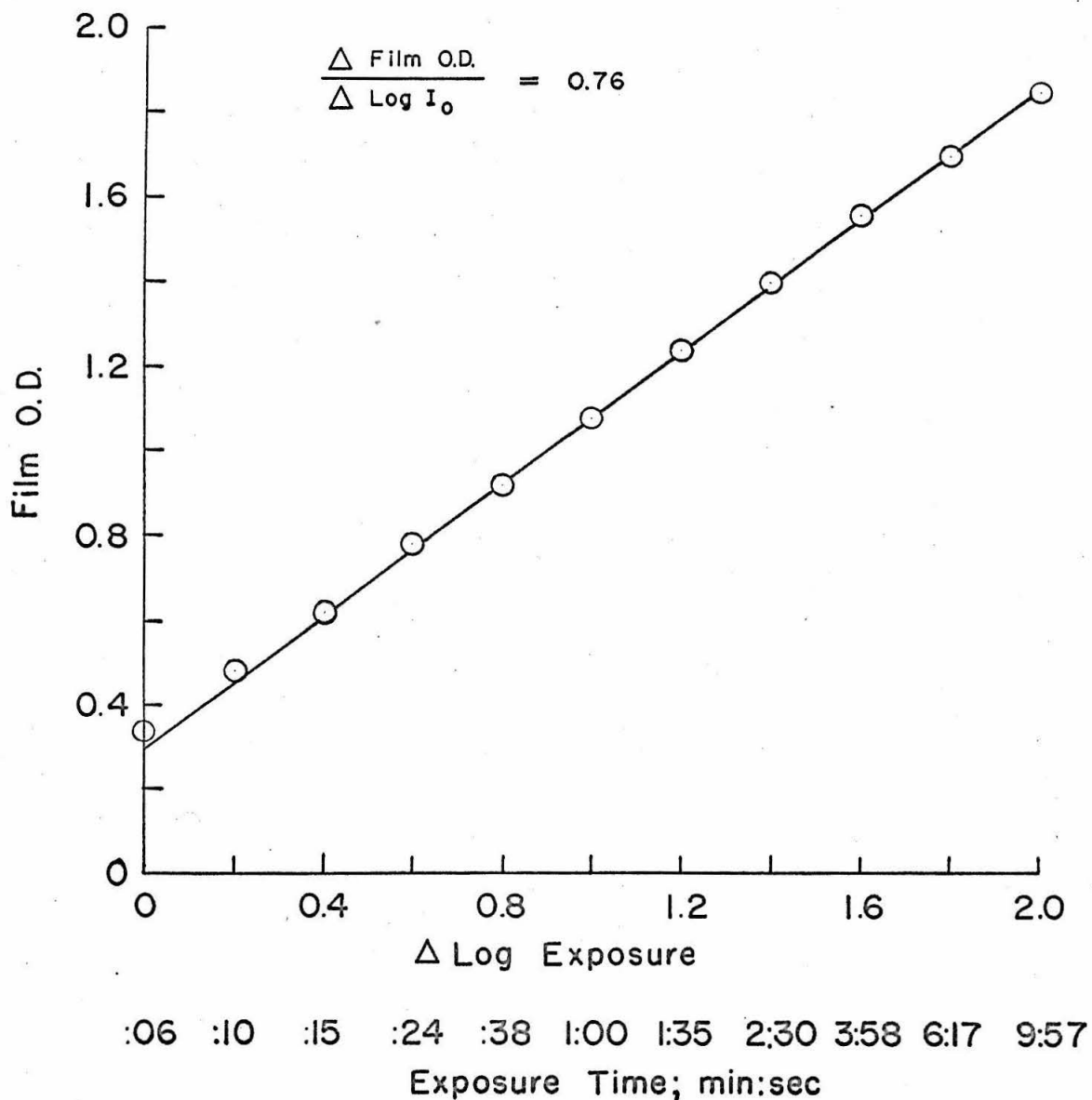


Figure 6. Response of Kodak Commercial film under standard developing procedure as a function of exposure time in an ultracentrifuge run.

of the film relative to an unexposed portion should be a reliable exposure index. Thus, in this work any film OD lying between 0.6 and 2 was assumed to be in the linear range of film response. The linear range may extend beyond an OD of 2 but this was not investigated because the densitometers used did not respond linearly to film OD much beyond this range.

Linearity of film response to DNA concentration was checked by taking a series of 6 minute exposures of a density gradient run placing DNA solutions of known ODs between the light source and the collimating lens. As shown in Fig. 7 the film OD was found to be a linear function of DNA OD at 258  $\mu$  up to a DNA OD of at least 1.1. No trace of blackening could be detected on a film exposed for 6 minutes through a DNA solution of an OD around 3, demonstrating the absence of light of wavelengths not absorbed by DNA or of light leaks in the system. Thus, in this system the DNA concentration distribution in the cell will be accurately represented on film if the maximum DNA concentration does not exceed an OD of 1.1 over the path length of the cell and if the film OD is in the range of 0.6 to 2.

In velocity sedimentation experiments the corex filter was removed in order to obtain an approximately twofold increase in intensity, and one minute exposures were generally used.

During the course of this work films were traced on three different Joyce-Loebl and Co. Ltd. double beam recording microdensitometers, a fact which reflects the difficulties encountered in obtaining reliable tracings. The machines used were: MK III Serial No. 35 and MK III B Serial No. 118 at the California Institute of Technology and MK III B Serial No. 238 at

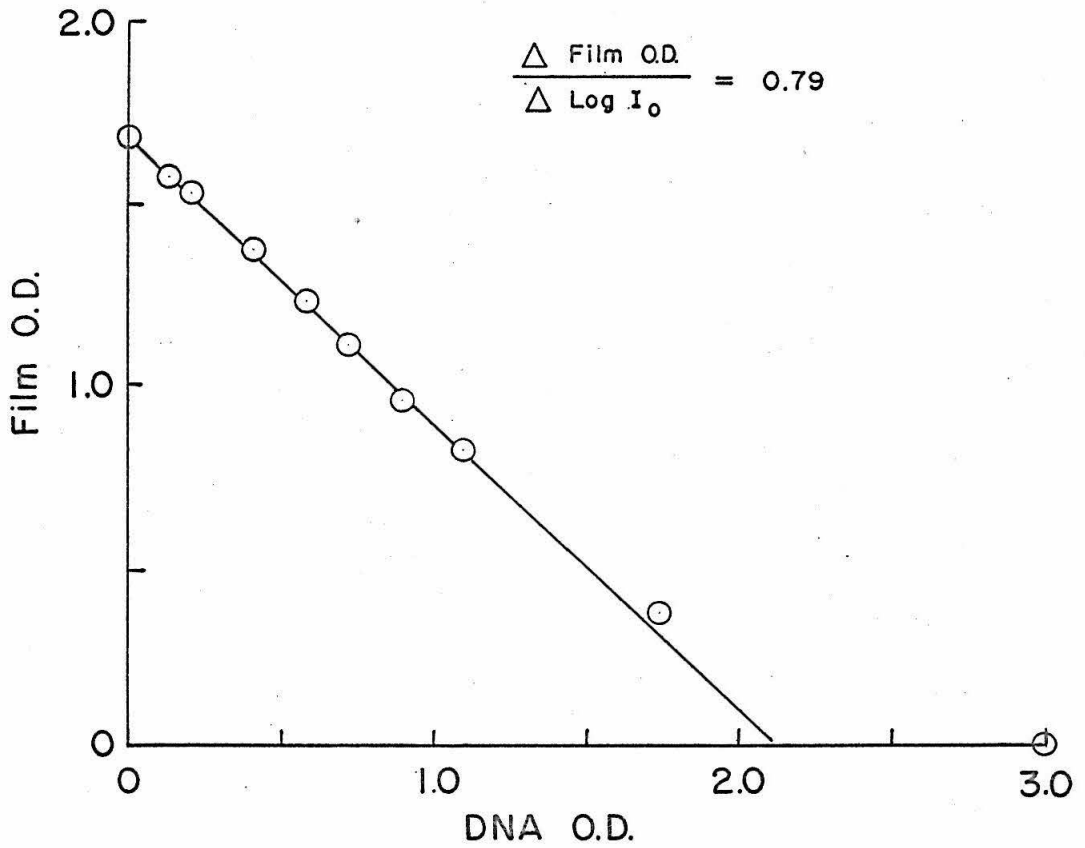


Figure 7. Linearity of film response to the optical density of DNA solutions placed in the light path of the ultracentrifuge optical system.

the University of California at San Diego. The latter was made available through the kindness of Professors John Singer and Bruno Zimm and the helpfulness of Mr. Neville Kallenbach.

Several difficulties were encountered at various times in using machines 35 and 118, the main ones being lack of pen sensitivity, lack of reproduceability, and non-linearity of pen response to film OD. Machine 238, which was only a few months old, behaved perfectly when checked by the following criteria:

- 1) The pen response was very active for specimens of OD up to around 2.3 using travelling wedges of total range 2.4, 0.79 or 0.5 density units.
- 2) Retraces were perfect for specimens of all optical densities in this range using any of the travelling wedges.
- 3) Pen response to sample density was linear up to at least 2 OD as checked by tracing a step wedge through different neutral density filters.
- 4) The same film when placed in a forward or backward orientation on the specimen stage gave traces which were identical when superimposed in the proper sense.
- 5) Traces of the same specimen using travelling wedges of different range gave identical values for the variance of the gaussian.

The film to trace magnification was checked for the 20x and 50x lever arm settings and found to be 20.2 and 50.6. These 1% corrections were not included in calculating variances of the gaussians traced on this machine. The effective slit width used in tracing the films was 0.002 cm, about one tenth the value of  $\sigma$  for the narrowest film gaussians traced.

Molecular weights calculated from traces made by machines 35 and 118 were in quite good agreement with each other but in several instances were  $1-2 \times 10^6$  higher than those calculated from traces on machine 238. The molecular weights reported in Fig. 8 were calculated from traces on machine 238 unless otherwise noted.

Effect of Bent Light. In density gradient work the refractive index gradient bends light across isoconcentration surfaces as it passes through the cell, and this may lead to considerable error in the concentration distribution recorded on film. Hearst and Vinograd (29) recognized this problem and derived an analytical expression for the concentration distribution which would be registered on film by light which was bent across a gaussian distribution in the cell. They concluded that the film record would be accurate within 1% between  $\pm 2 \sigma$  if the light is deflected through  $0.25 \sigma$  or less in passing through the cell. However, since their analytical expression becomes unwieldy at higher light deflections the error due to banding light across a gaussian distribution has been evaluated here by straight numerical integration. The procedure used is outlined in the appendix and only the results will be quoted here.

The variance of the gaussian band formed by T7 DNA in a CsCl density gradient at equilibrium is around .03 cm at 25,980 rpm and around .01 cm at 44,770 rpm. As shown in the appendix light is bent through the gradient in a 12 mm cell at 25,980 a maximum of around .003 cm or  $0.1 \sigma$  and even less than  $0.1 \sigma$  in 3 mm cells at 25,980 or 44,770, so under these conditions the error in the film record should be negligible. However, at 44,770 in a 12 mm cell the light is bent through .007-.009 cm, or  $0.7-0.9 \sigma$ , and the error in film reproduction in this case would lead

to an apparent 4-8% lowering of the molecular weight of the material in the cell. Since the experimental uncertainty in molecular weight is around  $\pm 10\%$  this lowering of the molecular weight would be all but undetectable. Thus in the work to be reported here errors from this source should have little or no influence on the molecular weights found.

#### MOLECULAR WEIGHT OF T7 DNA

The results of several CsCl banding molecular weight determinations on two different preparations of T7 DNA are presented in Fig. 8. The error flags, where present, indicate the extremes of the spread in molecular weights calculated from different exposures, or in some cases different baselines. Figs. 9 and 10 show some densitometer traces and their accompanying  $\log C$  vs  $W^2$  plots. Many, if not most, of the curves from which the molecular weights were calculated showed slight skewing toward heavier densities, but the  $\log C$  vs  $W^2$  plots were generally linear down to 10-20% of C max.

The decrease in banding molecular weight in 12 mm cells at 44,770 rpm would appear to be due to some optical effect rather than a physical spreading of the band, since the molecular weight determined in 3 mm cells at this speed does not decrease at the same DNA concentrations. The most obvious optical difference between gradient runs at the same speed in 3 mm and 12 mm cells is that the bending of light upon passing through the cell is 16 times greater in the 12 mm cell. As shown in the previous section and the appendix the decrease in molecular weight due to the bending of light across isoconcentration surfaces in the cell should be less than 10% under these conditions and in any case should not be concentration dependent. However, the lowering in molecular weight

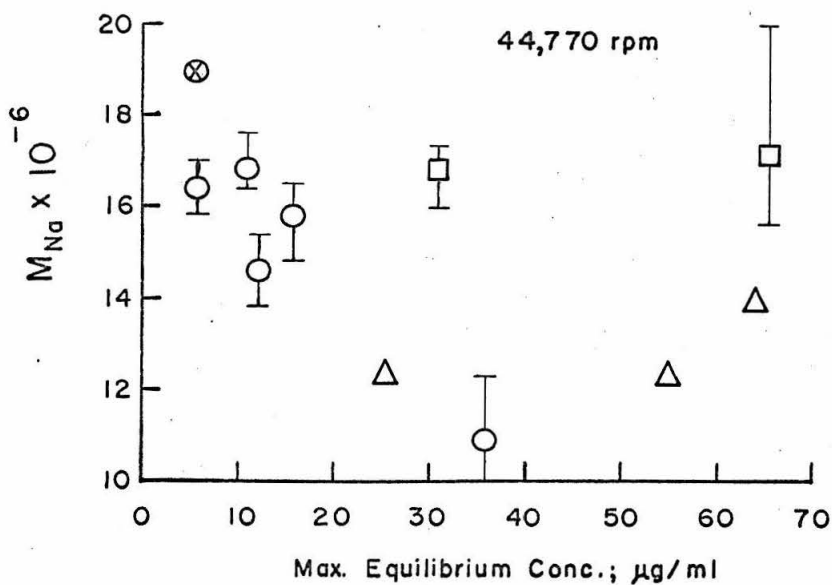
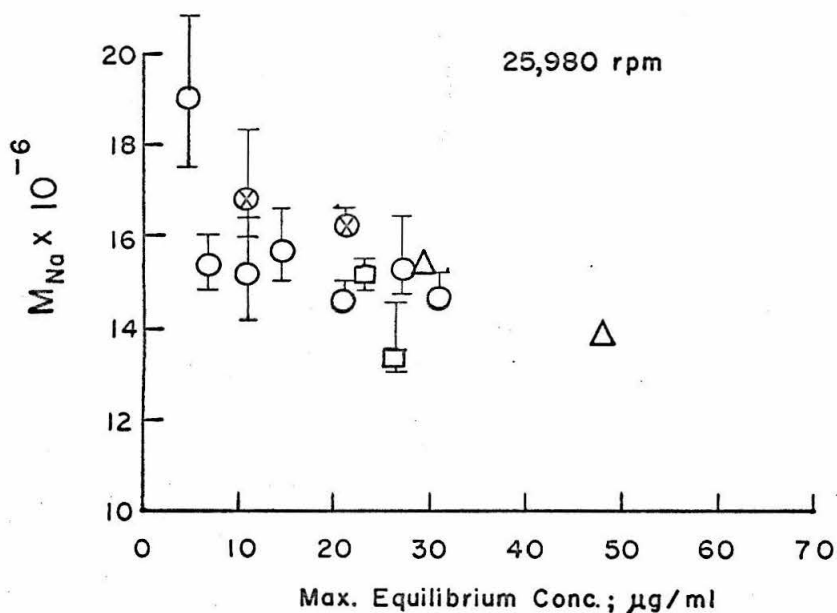


Figure 8.  $M_{Na}$  as a function of DNA concentration at 25,980 and 44,770 rpm.

- Run in 12 mm cell, traced on densitometer #238
- ⊗ Significantly different duplicates of above points (○) from densitometer #118
- △ Run in 12 mm cell, traced on densitometer #118
- Run in 3 mm cell, traced on densitometer #238

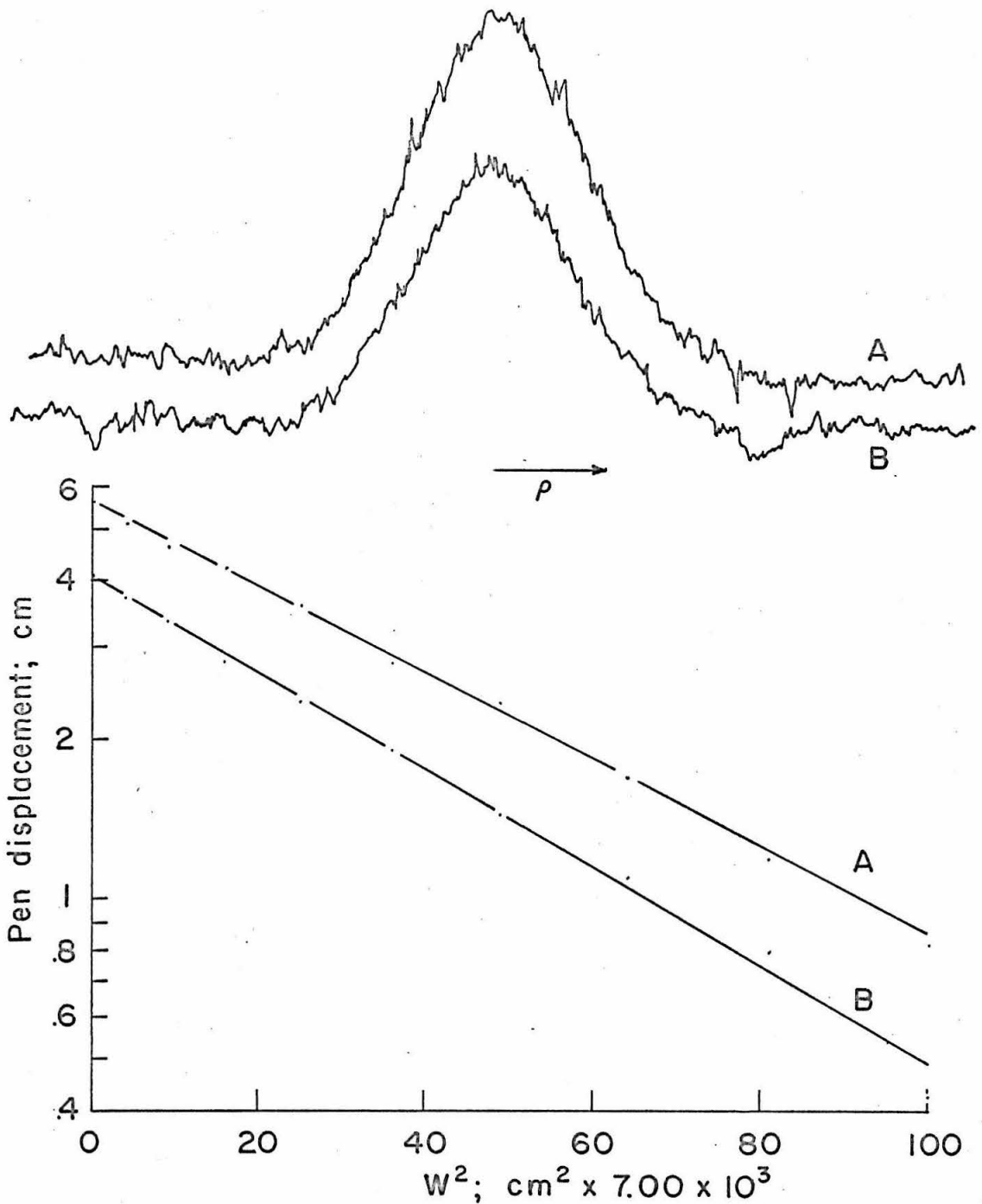


Figure 9. Densitometer traces and  $\log C$  vs  $W^2$  plots for two density gradient runs at 25,980 rpm in 12 mm cells. Traces were made on densitometer #238 using a travelling wedge which produced pen deflections of 1 cm per .026 optical density units on film. A. Maximum DNA concentration 5  $\mu\text{g}/\text{ml}$ ,  $M_{\text{Na}} = 18.8 \times 10^6$ ; B. Maximum DNA concentration 7  $\mu\text{g}/\text{ml}$ ,  $M_{\text{Na}} = 15.6 \times 10^6$ .

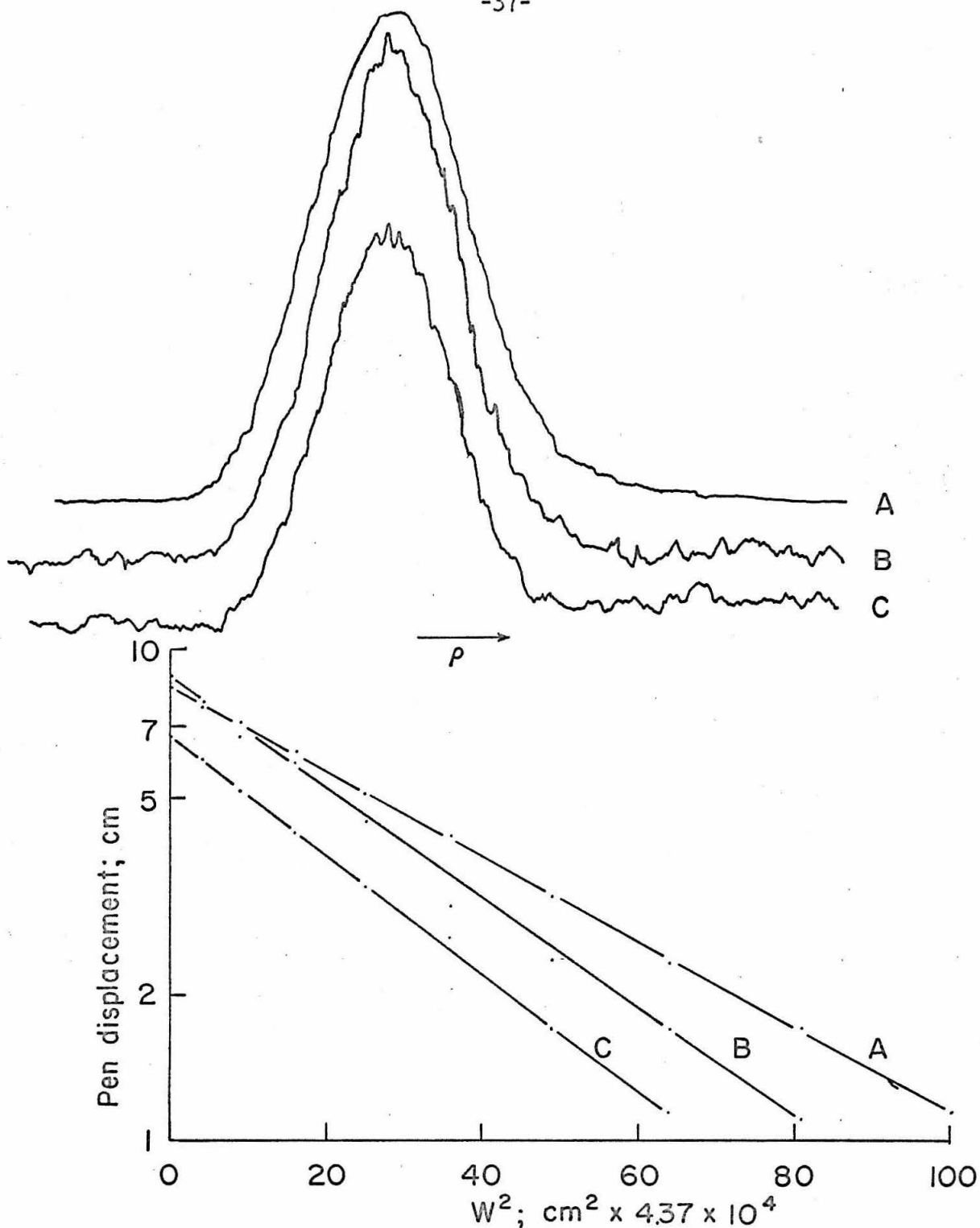


Figure 10. Densitometer traces and  $\log C$  vs  $W^2$  plots for three density gradient runs at 44,770 rpm. A. Max DNA conc.  $55 \mu\text{g/ml}$ ;  $M_{Na} = 12.2 \times 10^6$ ; 12 mm cell; densitometer #118; wedge 0.13 OD/cm. B. Max DNA conc.  $11 \mu\text{g/ml}$ ;  $M_{Na} = 16.4 \times 10^6$ ; 12 mm cell; densitometer #238; wedge 0.026 OD/cm. C. Max DNA conc.  $32 \mu\text{g/ml}$ ;  $M_{Na} = 17.3 \times 10^6$ ; 3 mm cell; densitometer #238; wedge 0.026 OD/cm.

observed might be due to dispersion in the bending of the light of different wavelengths upon passing through the gradient, with consequent displacement of the images made by the different wavelengths at the film. This idea is supported by the fact that addition of a corex filter to the  $\text{Br}_2\text{-Cl}_2$  combination improves band shape. This problem could be explored more thoroughly with the help of a monochromator.

#### DISCUSSION

The anhydrous molecular weight of T7 DNA as the sodium salt was found by the CsCl density gradient method to be  $15\text{-}17 \times 10^6$ . Molecular weights were calculated using the procedures of Hearst, Ifft and Vinograd (3,4,5) and using the hydration and compression parameters which they evaluated for T4 DNA. The fact that these parameters were not directly determined for T7 DNA might introduce slight error into these calculations, especially since T4 DNA is glucosylated. Molecular weights have commonly been calculated without regard for hydration and pressure effects; the molecular weights so calculated are about 4-5% higher than those calculated by the procedures used here.

A systematic examination of the optical system for possible sources of error in reproduction of band shape did not turn up any likely suspects, except for the possibility of dispersion effects at high gradients. The tracing of films appeared to be the least reliable element of the system and in fact the use of different densitometers led to differences in molecular weights of 5-10%. Only the molecular weights calculated from the tracings considered to be the most reliable were given here, and these were generally among the lowest values obtained.

The banding molecular weight determined here is in fairly good agreement with that determined by Davison and Freifelder,  $15 \times 10^6$  (22) and also that determined by Meselson,  $18 \times 10^6$  (21), but it is distinctly higher than that determined by Thomas and Pinkerton,  $10 \times 10^6$  (20) on a sample of T7 DNA prepared here. Unfortunately we have no molecular weight determination on the sample on which Thomas and Pinkerton determined their molecular weight because our centrifuge was inoperative at that time. Although three separate preparations measured here all had banding molecular weights in the  $15-17 \times 10^6$  range, it is possible that the sample which they received was slightly degraded, either here or in transit.

Davison and Freifelder (22) have determined the total DNA content of the T7 bacteriophage to be  $19 \times 10^6$  grams per mole of phage by sedimentation-diffusion and light scattering on whole phage. The T7 phage used for the studies reported here was found by Davison to be essentially identical to their material (31). Thus the molecular weight of  $15-17 \times 10^6$  found for T7 DNA by the density gradient method is about 80-90% of the total DNA content of a single phage. The sharpness of the velocity sedimentation boundary suggests that if more than one molecule of DNA is liberated per phage particle all such molecules must be of essentially identical molecular weight. Since almost any error in the density gradient method tends to lower the observed molecular weight the banding result appears to exclude the possibility of half molecules of molecular weight  $9.5 \times 10^6$ . Thus when taken together the density gradient and sedimentation velocity results argue strongly that the preparations of T7 DNA are homogeneous populations, each molecule of which contains the entire DNA content of a single phage.

These results do not support the contention of Thomas and Pinkerton that the banding molecular weight of homogeneous DNA preparations is a factor of two below the true molecular weight, and indeed suggest that the banding method may be quite accurate for T7 DNA. This conclusion would be strengthened by an independent determination of the molecular weight of the isolated T7 DNA. If we may disregard the T7 DNA molecular weight determined by Thomas and Pinkerton the discrepancy in results might possibly be due to length dependent non ideality factors which might broaden the equilibrium bands observed for very high molecular weight DNAs but which might be all but inconsequential for molecules the size of T7 DNA.

SECTION II. DENATURATION AND RENATURATION OF T7 DNA

REVIEW . . . . .	42
Denaturation . . . . .	42
Renaturation . . . . .	45
DENATURATION . . . . .	47
METHODS . . . . .	47
Determination of Percentage of Native Material . . . . .	47
Melting . . . . .	48
Banding . . . . .	51
Sedimentation velocity . . . . .	53
Formamide as Denaturant . . . . .	55
RESULTS . . . . .	60
Composition of Partly Denatured Samples . . . . .	60
Hyperchromicity and Banding Behavior . . . . .	62
Kinetics of Denaturation . . . . .	66
The formamide system . . . . .	69
Aqueous solutions . . . . .	71
Approach to equilibrium . . . . .	73
Effect of denatured DNA . . . . .	73
Concentration dependence . . . . .	75
Divalent metal ions . . . . .	75
Effect of Stirring on Denaturation . . . . .	78
DISCUSSION . . . . .	82
RENATURATION . . . . .	88
METHODS . . . . .	88
RESULTS . . . . .	89
Optimal Conditions for Renaturation . . . . .	89
Properties of Renatured DNA . . . . .	92
Renaturation Kinetics . . . . .	92
DISCUSSION . . . . .	100

## REVIEW

The Watson-Crick hypothesis for the structure of DNA (32) provides a model for interpretation of phenomena observed during denaturation and renaturation, and thus has stimulated a great deal of work in this field in the past ten years. Denaturation, a highly cooperative phenomenon, has been interpreted as the collapse of the well ordered Watson-Crick structure into a more random configuration (33). The recovery of native properties by denatured DNA has been called renaturation (34). At present there is some disagreement as to whether or not the individual complementary strands of the double helix actually separate and recombine during denaturation and renaturation (35,36).

### Denaturation

Denaturation of DNA has been induced by agents such as heat (33,37, 38,39), acid (37,38,40,41), alkali (42), low ionic strength (40), and high concentrations of certain salts (43) and organic compounds (33,44, 45,46); it is accompanied by changes in such properties of DNA as ultra-violet absorption (39,40), viscosity (33,40), optical rotation (40,44), radius of gyration (33,40), banding density in a CsCl density gradient (9,11), morphology in electron micrographs (47), chemical reactivity of the bases (48), and biological activity (45,49). Although denaturation is often accompanied by complicating side effects such as aggregation of denatured material (33,42) or degradation of the covalent DNA structure (34,50,51,52), much has nevertheless been learned about the denaturation process.

The cooperative collapse of the ordered native DNA structure in response to heat has been called melting by analogy to melting of a one

dimensional crystal (39). A plot of ultraviolet absorbancy of a DNA solution against temperature is called a melting profile and the temperature at which the increase in OD is half maximal is called the melting temperature,  $T_m$ . It has been pointed out that  $T_m$  is not necessarily the temperature at which the native structure is half collapsed (53); nevertheless, the  $T_m$  of a DNA solution is a measure of the stability of the native structure and depends on ionic strength, pH, solvent composition, and the composition of the DNA itself. The stability of the native DNA structure, as measured by  $T_m$ , increases with increasing ratio of GC to AT in the sample (54,55). This, coupled with the fact that nucleotides appear to be distributed in a non-regular sequence along the DNA chain (56), suggests that in the course of denaturation, regions of the helix rich in A-T pairs may collapse before G-C rich regions do so.

Although the entire transition from the native to the denatured state of DNA occurs over only a few degrees change in temperature, the collapse process has been studied in considerable detail. The early part of the collapse process has been shown to be reversible as evidenced by the recovery of native optical density upon rapid cooling of DNA solutions from a partially hyperchromic state (57), the recovery of native viscosity and hypochromicity after partial acid denaturation (37,58,59), the recovery of native characteristics after partial denaturation in organic solvents (46), and the fact that prolonged heating of *E. coli* DNA density hybrids at  $T_m$  does not produce separation of the subunits in a CsCl density gradient (60).

Addition of formaldehyde to DNA solutions prevents the reversal of the early stages of denaturation as shown by the fact that such solutions do not recover any hypochromicity upon cooling (61). Intermediate molecular states of denaturation have been demonstrated for T<sup>4</sup> DNA which has been denatured to an intermediate hyperchromicity in formaldehyde solution by 1) the observation of partially denatured molecules in electron micrographs of such DNA (62) and 2) the fact that in a CsCl density gradient such DNA forms a single band of density intermediate between the densities of native and denatured DNA (61). The subunits of density hybrids of E. coli DNA heated in formaldehyde do not separate until the increase in absorbance is about 75% completed (63).

If denaturation is taken beyond the point of maximum ultraviolet absorption for any length of time the DNA becomes irreversibly denatured; that is, native properties are not recovered upon rapid cooling of the solution (34,57). The fact that both reversible and irreversible denaturation may be observed has been interpreted in terms of the intramolecular heterogeneity of DNA (57). Since the linear sequence of bases in a DNA chain is essentially random and the two strands of the double helix are perfectly complementary, presumably only one of the multitude of possible pairings between complementary strands will allow the perfect base pairing along the full length of the molecule necessary to produce the native structure. If a molecule is only partially denatured a few small native (GC rich?) sequences may remain which can hold the strands in register and serve as nuclei for the rapid reconstitution of the native structure upon removal of the denaturant. But if the collapse process is carried to the point where the native register is lost, the few random

pairing attempts possible upon rapid removal of the denaturant have a very low probability of establishing the unique base pairing necessary to form the native structure. If the double stranded structure is chemically cross linked and thus permanently held in register it cannot be irreversibly denatured (64,65).

### Renaturation

It has been found that certain completely denatured DNAs can recover their native properties, at least to some extent, if the denaturing conditions are withdrawn very slowly or if the material is held for some time under conditions slightly milder than those which initiate denaturation (34,60,66,67). The term renaturation has been applied to this process and will be here restricted to cover reconstitution of the native structure of irreversibly denatured DNA and not applied to reversal of the early stages of the collapse process.

Renaturation has been measured by the extent to which a denatured DNA sample recovers the native condition of such properties as ultra-violet absorption (34), biological activity (66), banding position in a CsCl density gradient (34,60), and appearance in electron micrographs (34,68). The degree to which a denatured DNA sample will renature is dependent upon the source of the DNA (34). Bacteriophage DNA renatures extensively (68) and bacterial DNA partially (34), but DNA from higher organisms has not been shown to renature at all (34). Renaturation is strongly dependent on the ionic strength of the renaturation medium as well as on temperature and DNA concentration (66,67). An excess of non-homologous DNA can inhibit renaturation (66).

Most studies of renaturation have been done on bacterial DNA, which is known to be heterogeneous. Generally renaturation of bacterial DNA proceeds to a maximum of 50-60% recovery of the native condition as measured by biological activity or ultraviolet absorption (67,69). Renaturation is generally accompanied by non-specific aggregation, especially at high DNA concentrations (60,68). Such non-specific aggregates have been dispersed by the use of a diesterase which attacks denatured DNA (60). Mixed renaturation between homologous DNA samples bearing different markers has been shown to produce biological and density hybrids (60,66,70), but renaturation of mixtures of non-homologous DNA samples does not produce such hybrids (60,66).

Renaturation has been interpreted as a bimolecular reaction between separated complementary strands of the DNA double helix (34,36). Conditions slightly milder than those which denature presumably allow complementary strands to try a great number of possible pairings until long stable sequences of perfect base pairing are found. Only complementary strands should be able to find long sequences of complementary pairing and the possibility of a given strand finding a complement would be less the more heterogeneous the DNA sample. This may explain why DNA of higher organisms does not renature and why the presence of non-homologous DNA inhibits renaturation. However, Cavalieri, Sarkar and Small (35,69), on the basis of renaturation kinetics of *E. coli* DNA, feel that renaturation is not bimolecular and that the above data can be explained equally well without the assumption that the complementary strands ever separate.

## DENATURATION

### METHODS

The work to be reported here attempts to study the mechanism of denaturation and renaturation of a homogeneous DNA using methods which do not degrade its primary structure. The DNA of bacteriophage T7 was chosen for this work because it should be essentially homogeneous, it contains only the four "normal" DNA bases--adenine, thymine, guanine, and cytosine (71), it contains no extra attached sugars (71), and its small size renders it relatively insusceptible to hydrodynamic shearing forces (22). The details of preparation of this DNA are given in Section I.

### Determination of Percentage of Native Material

One of the aims of this work has been to examine the kinetics of irreversible denaturation. In order to do this it is necessary to have methods which can accurately assess the degree to which a given sample is native. Three methods were used to examine the composition of DNA samples irreversibly denatured to various degrees: melting procedures give information about the percentage of total bases in the native configuration, whereas density gradient banding and sedimentation velocity experiments give information on the molecular composition of the sample. These methods have been tested for their ability to resolve mixtures of native and fully denatured DNA and this information is used to interpret the results obtained on partly denatured samples.

For convenience the percentage of native material in a sample will be designated  $\%N$  and subscripts will be used to identify the method by which  $\%N$  was determined, such as  $\%N_m$  when determined by melting techniques and  $\%N_D$  when determined by banding in a CsCl density gradient.

Melting. A sharp increase in ultraviolet absorption over a narrow range of temperature is a characteristic of native DNA which is attributed to the cooperative melting out of stacked sequences of base pairs (72). Since denatured DNA exhibits almost no change in optical density through the characteristic melting range of native DNA, the percentage increase in OD over this temperature range is a possible measure of the proportion of bases in a sample which are involved in native sequences. However, since T7 DNA renatures with great facility under a variety of conditions the melting assay will be inaccurate unless the possibility of renaturation under the assay conditions is excluded.

Melting profiles were measured in a Beckman DK-2 ratio recording spectrophotometer equipped with a Beckman temperature-regulated cell holder. Temperature measurements were made by means of a thermometer in the blank solution and the OD measured was that at maximum absorption. For accurate temperature profiles the optical densities in the sharply melting region were measured after both temperature and OD had stabilized, but when only the total hyperchromic change was desired readings were taken as fast as the heating block would heat.

An easy way to see if renaturation occurs in a given solvent is to melt a DNA sample in that solvent two times in succession. If the second melting profile shows any sharply melting component at the characteristic native melting temperature renaturation has occurred during the cooling and reheating cycle. The results of such double melting profiles on native T7 DNA at 28  $\mu\text{g/ml}$  in solvents containing different concentrations of NaCl are shown in Fig. 11. The cooling period was 45-60 minutes. Renaturation occurred in solutions containing NaCl at a concentration of

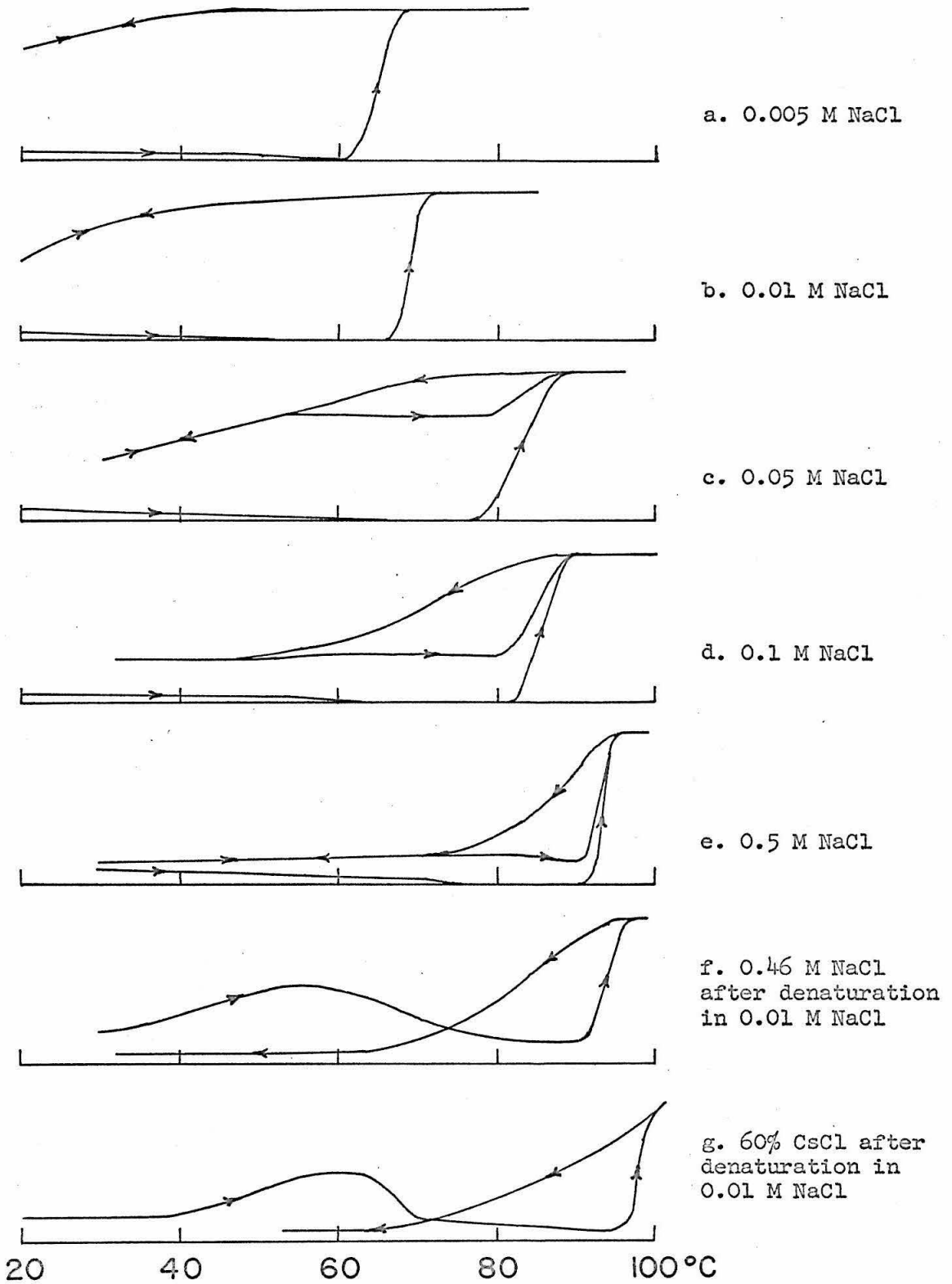


Figure 11. Melting profiles of T7 DNA at different NaCl concentrations.

.05 M or higher, but did not occur in solutions .005 M or .01 M in NaCl. The percentage increase in OD due to the melting of native DNA is essentially independent of both ionic strength and DNA concentration (not shown).

Differences in the extent of renaturation among samples denatured at different salt concentrations could be due either to differences in the nature of the material formed upon denaturation or to differences in the ease of renaturation in the different solvents. To demonstrate that the latter is the case a solution of T7 DNA which had been melted and cooled in .01 M NaCl was brought to 0.46 M NaCl by addition of a tenth volume of 5 M NaCl and then melted again. The melting profile of the DNA in 0.46 M NaCl (Fig. 11f) shows that extensive renaturation occurred during the heating and thus demonstrates that high ionic strength solvents are unsuitable for determination of  $\%N_m$ .

No renaturation of T7 DNA in 0.01 M NaCl,  $10^{-3}$  M TRIS, pH 7.5 was ever detected during the cooling and heating cycle nor after storage in the refrigerator at ca. 4°. DNA samples were therefore melted in this solvent for determination of  $\%N_m$ . Since all T7 DNA samples at temperatures above the melting range have the same extinction coefficient, all OD measurements were put on a common base by expressing OD as the ratio of the given OD to that of the completely melted sample. The value of  $\%N_m$  for a given sample in .01 M NaCl can then be calculated:

$$\%N_m = 100 \times \frac{\left(\frac{OD_{65}}{OD_{85}}\right)_{\text{denat}} - \left(\frac{OD_{65}}{OD_{85}}\right)_{\text{sample}}}{\left(\frac{OD_{65}}{OD_{85}}\right)_{\text{denat}} - \left(\frac{OD_{65}}{OD_{85}}\right)_{\text{native}}}$$

where  $OD_{65}$  and  $OD_{85}$  refer to optical density measurements made at temperatures just below and just above the melting range, and the subscripts native and denatured refer to fully native and fully denatured samples.

In .01 M NaCl the ratio  $\left( \frac{OD_{65}}{OD_{85}} \right)$  was taken to be .735 for native and .986

for denatured DNA, and thus in this solvent

$$\%N_m = 100 \times \frac{.986 - \left( \frac{OD_{65}}{OD_{85}} \right)_{\text{sample}}}{.251}$$

Table 1, page 52, compares  $\%N_m$  for mixtures of native and denatured DNA with  $\%N_p$ , the percentage of native material determined from CsCl density gradient banding experiments.

Banding. The second method used to estimate the percentage of native material in a sample was that of banding in a CsCl density gradient. Mixtures of native and denatured T7 DNA banded in CsCl at 44,770 rpm are resolved into two peaks about .014 density units apart. These have little or no overlap, and thus the percentage of native material can be estimated from the relative amounts of material in the native and denatured bands. T4 DNA, which bands at a position about .010 density units lighter than native T7 DNA, was used as a density marker.

Since the amount of material in such bands is measured by the ultraviolet absorption optics of the ultracentrifuge, the relative extinction coefficients of native and denatured DNA in CsCl through this optical system must be known in order to determine their relative concentrations. The extinction coefficient at 258 m $\mu$  of denatured DNA

relative to that of native DNA (both in 60% CsCl at 25°) is estimated to be roughly 1.08. This figure was obtained from the melting profile of denatured DNA in 60% CsCl shown in Fig. 11g by comparing the OD of denatured DNA at 25° with that of renatured DNA. This correction was disregarded because: 1) the error introduced by neglecting this factor is generally within experimental error, 2) the precise correction for the ultracentrifugal wavelengths is not known, and 3) in experiments involving partially denatured or partially renatured samples DNA banding about certain densities might possess hyperchromicities intermediate between those of native and denatured DNA.

Mixtures of native and denatured DNA were both melted and banded to determine whether the two methods yield similar and accurate measures of the proportion of native material in a sample. Table 1 shows the results of four such experiments:

Table 1

% Native calculated from amounts added to mixture	$\%N_m$ % Native calculated from melting data	$\%N_D$ % Native calculated from banding data
25	28	29
55	52	59
67	61	69
75	79	81

Thus these methods appear to agree fairly well and to approximate the actual percentage of native material in a mixture of native and denatured DNA to within ca.  $\pm 10\%$ .

Sedimentation Velocity. Sedimentation velocity is a poor method for quantitative estimation of the proportion of native material in a sample because of the pronounced Johnston-Ogston effect (73). It is however useful as a qualitative test for the number of components present at low salt concentration and also as a test for the presence of small quantities of denatured material in a sample.

Preliminary experiments on sedimentation of mixtures of native and denatured DNA gave very erratic results, probably due to poor control of pH. Boundary instability was also noticed in several early experiments but this problem was eliminated after servicing of the rotor temperature indicator and control system of the ultracentrifuge. Runs were made in cells with 12 mm 4° Kel-F centerpieces and conditions were standardized to 44,770 rpm in  $10^{-3}$  M NaCl containing 1 or  $2 \times 10^{-4}$  M TRIS. Both native and denatured T7 DNA sedimented with sharp boundaries under these conditions. At 44,770 rpm the sedimentation pattern of native DNA exhibited the sloping plateau noted by others (20,74,75) in presumably homogeneous samples of native DNA, but this effect was absent, or very slight, at 25,980 or 31,410 rpm.

As would be expected from charge effects in such dilute salt, sedimentation coefficients were strongly dependent on DNA concentration and pH. Fig. 12 shows the variation of sedimentation coefficient with concentration for native and denatured DNA in the  $10^{-3}$  M NaCl,  $10^{-4}$  M TRIS solvent, which generally had a pH around 8.3, although measurements of pH after runs varied between 7.5 and 8.85. Lowering the pH of a denatured sample from 8.85 to 5.3 raised the sedimentation coefficient from 10.0 to 15.4 s.

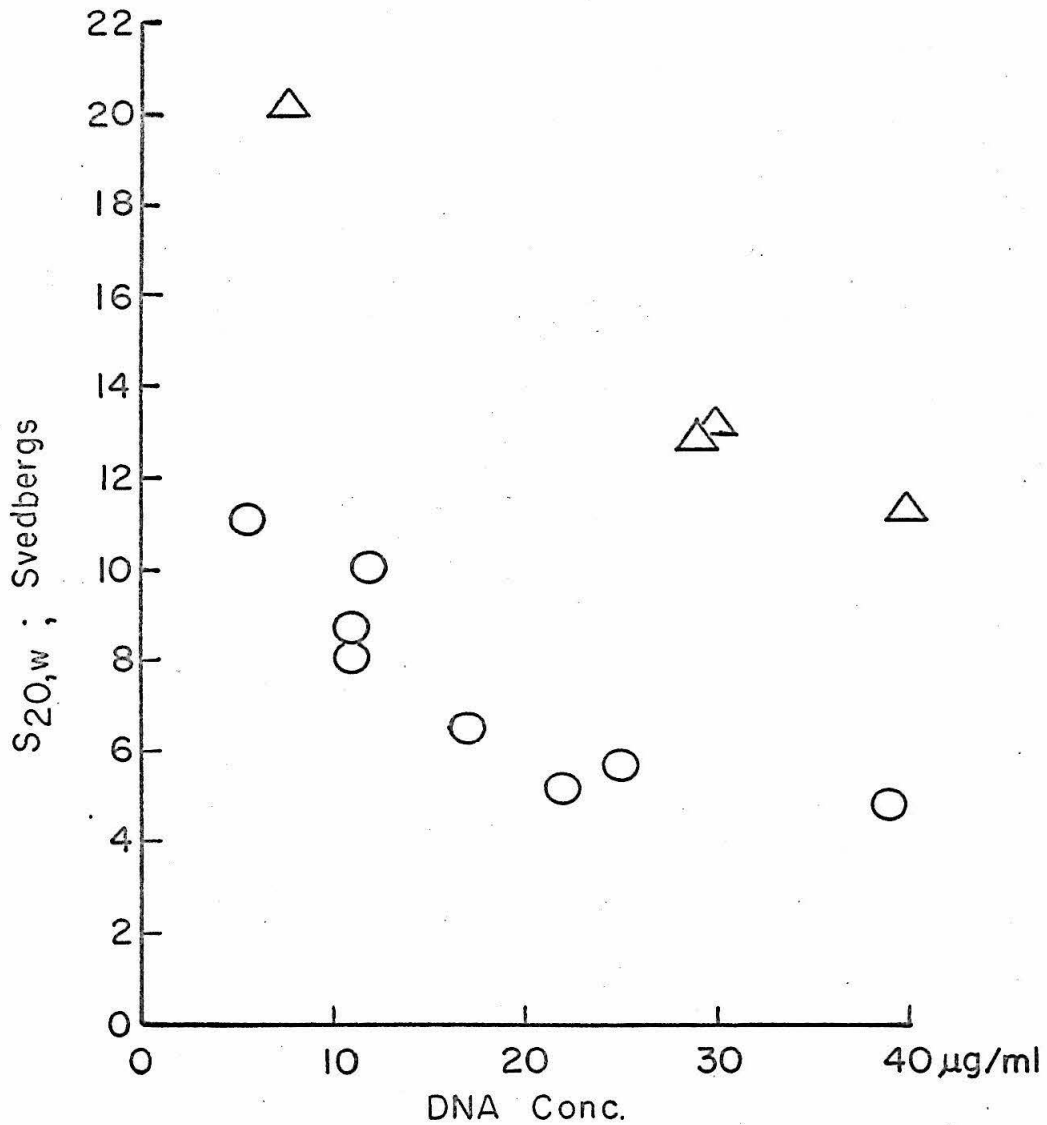


Figure 12. Sedimentation coefficient of native and denatured T7 DNA in  $10^{-3}$  M NaCl,  $10^{-4}$  M TRIS at 44,770 rpm.

△ Native DNA: 48 µg/ml = 1 OD

○ Denatured DNA: 36 µg/ml = 1 OD

The separation of mixtures of native and denatured DNA in  $10^{-3}$  M NaCl depended strongly on pH. A 1:1 mixture of native and denatured DNA gave two sharp boundaries of 9.0 and 14.8 s when sedimented at pH 9 whereas the same mixture at pH 6 was all but unresolvable, exhibiting sedimentation coefficients of 13.2 and 15.4 s. Thus the sedimentation coefficient of denatured DNA is apparently more strongly affected by pH changes in this range than is that of native DNA, as might be expected from the difference in their titration properties (37,40,41).

The Johnston-Ogston effect varied with conditions but generally the relative concentration of the denatured component was enhanced at least 50%. The sedimentation pattern of a mixture containing about 93% native material showed a sharp denatured component with about 20% of the total absorption.

#### Formamide as Denaturant

In order to get away from the degradative effects of the high temperatures needed for denaturation in aqueous solution, formamide was used as the denaturing agent in most of the work reported here. It has been shown that DNA dissolved in formamide at room temperature loses its secondary structure and that it behaves as completely denatured material when returned to aqueous solution (44). In the early stages of this work it was discovered that the presence of a moderate amount of salt in the formamide solution apparently stabilizes the native structure of DNA in formamide. Thus it seemed likely that conditions could be established for the complete cycle of denaturation and renaturation at room temperature under conditions in which there is no degradation of the primary DNA structure.

In order to establish that formamide does not degrade the primary structure of nucleic acids TMV RNA was dissolved in formamide and tested for change in infectivity and sedimentation pattern. The TMV RNA was prepared by phenol extraction of TMV prepared by the method of Simmonds (76), alcohol precipitated, washed with alcohol followed by ether and dried. Samples were dissolved in formamide at 1 mg/ml and allowed to stand at room temperature for periods of 1-24 hours before precipitation in the cold by addition of an equal volume of cold aqueous buffer followed by alcohol to 75%. The precipitates were redissolved in aqueous 0.02 M phosphate buffer, pH 7.3, and tested for changes in infectivity and sharpness of the ultracentrifuge boundary. Generally the infectivity and sedimentation characteristics of the TMV RNA indicated a 10-40% degradation of formamide-treated RNA as compared with untreated control RNA. It is assumed that this degradation was due to the precipitation and solution procedures since the infectivity and sedimentation properties of the RNA remained constant with times of storage up to 24 hours in formamide at room temperature. The fact that the infectivity and sedimentation patterns of the RNA are stable for long periods of solution in formamide strongly indicates that the formamide itself does not degrade the primary structure of TMV RNA. It has subsequently been found that the infectivity of  $\phi$ X174 DNA is also stable in formamide (77). Thus it is concluded that formamide does not chemically degrade RNA or DNA.

Although the use of formamide for denaturation and renaturation studies has the advantage of not degrading DNA it does have disadvantages as compared to aqueous solutions. Formamide is not transparent to ultraviolet light so observations involving ultraviolet absorption of DNA can only be made in 1 mm cells and at high DNA concentrations. Under these

conditions spectra can be obtained down to 250-260  $\mu$  (78). Upon exposure to water, formamide slowly hydrolyzes to formic acid and ammonia and the solution gradually becomes acid (79). Matheson, Coleman and Bell 99% formamide was used for this work. The formamide was tested periodically with brom thymol blue and was discarded if not green to this indicator. Conductivity measurements showed that some commercial bottles of formamide contained appreciable quantities of salt. Such formamide was not used.

The standard procedure for denaturation of DNA by formamide was as follows: A small volume of DNA in concentrated aqueous solution was diluted about twentyfold into an appropriate amount of a formamide, water, salt, and buffer mixture to give the desired final solvent composition for denaturation. The aqueous DNA stock solutions were generally about 1 mg/ml in 0.1 M NaCl, 0.01 M TRIS, pH 7.5 and were diluted with the denaturing solvent to a DNA concentration of ca. 35-50  $\mu$ g/ml, a concentration convenient for determination of melting profile after transfer to 0.01 M NaCl. The DNA was quickly dispersed in the denaturing solvent by gentle inversion of the tube or by gentle stirring for about 15 seconds. The temperature of the denaturing mixture was controlled to within 0.1° by a water bath. At an appropriate time the denaturation reaction was stopped by addition of an equal volume of water and the diluted mixture was dialyzed, with rapid stirring, a minimum of three hours at room temperature against three or four 500 ml changes of 0.01 M NaCl,  $10^{-3}$  M TRIS, pH 7.5, a procedure which effects an essentially complete change of solvents. Visking Company #8 dialysis tubing which had been boiled in sodium bicarbonate and stored in 50% ETOH was used.

To determine solvent compositions convenient for kinetic study of irreversible denaturation the value of  $\%N_m$  was determined for samples of T7 DNA which had been subjected for 30 minutes at 25° to 90 volume % formamide of various NaCl concentrations. The results shown in Fig. 13 indicate that the rate of denaturation decreases with increasing salt concentration and that no denaturation is detectable at NaCl concentrations greater than 0.14 M or so under these conditions. Almost all studies on denaturation kinetics were done at 25° in 90% formamide at NaCl concentrations between .060 and .085 M.

In order to study denaturation kinetics of DNA in the above system it is necessary that dilution of the denaturing mixture with an equal volume of water actually stop the denaturation reaction and prevent further denaturation or renaturation. The composition of the diluted mixture was generally 45% formamide, 0.030-0.040 M NaCl. This percentage of formamide is too low to denature native DNA and the salt concentration is too low to support renaturation of fully denatured DNA (as shown in the section on renaturation). Furthermore, the following experiment suggests that no denaturation or renaturation of partly denatured samples occurs after dilution: A sample of DNA was denatured 15 minutes at 25° in 90% formamide, 0.082 M NaCl and then diluted with an equal volume of 0.01 M NaCl to produce a solution of 45% formamide, 0.046 M NaCl. A portion of the diluted DNA sample was immediately dialyzed into 0.01 M aqueous NaCl and a second portion was allowed to stand for 60 minutes at room temperature in the 45% formamide solution before dialysis. The two samples gave values of  $\%N_m$  of 74.6 and 74.2% respectively. Such partly denatured samples in 0.01 M aqueous NaCl could be stored at least five days in the refrigerator without change in  $\%N_m$ .

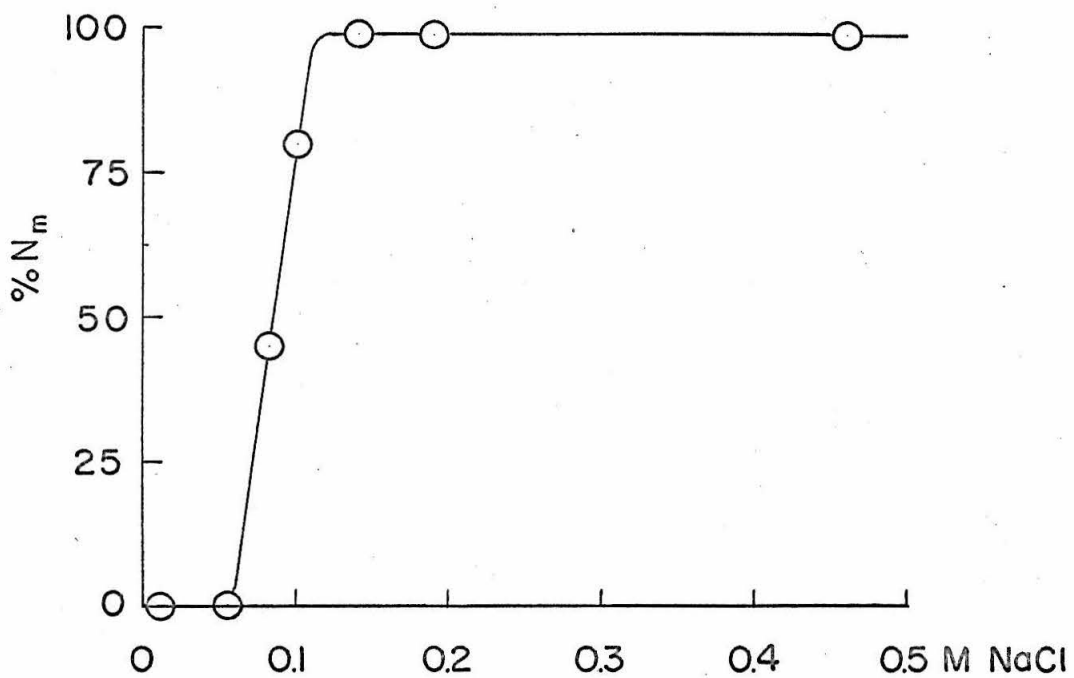


Figure 13. Denaturation of T7 DNA. %N<sub>m</sub> of native T7 DNA samples after 30 minutes at 25° in 90% formamide<sup>u</sup> at various NaCl concentrations.

## RESULTS

### Composition of Partly Denatured Samples

Samples of T7 DNA which had been partly denatured were compared to mixtures of native and fully denatured DNA by melting, banding, and sedimentation velocity procedures to learn something of the distribution of molecules in the population among possible states of denaturation.

CsCl density gradient banding patterns of partly denatured samples were similar but not identical to banding patterns of native-denatured mixtures. As shown in Fig. 14 the DNA of partly denatured samples bands in two peaks centered approximately on the native and denatured densities, but the peak near the native density is somewhat broader and shifted slightly toward heavier densities from the position of a fully native peak. The height of the minimum was somewhat variable but the two peaks were never as well separated as those of a comparable mixture of native and denatured DNA.

For partly denatured samples  $\%N_D$  was calculated from the relative amounts of material under the two peaks by arbitrarily assuming that the material in the less dense peak is native and that in the more dense peak denatured.

Melting profiles of partly denatured samples were indistinguishable from those of mixtures of native and denatured DNA. However for a given partly denatured sample the ratio  $\frac{\%N_m}{\%N_D}$  was found to vary between .70 and .96 whereas this same ratio for native-denatured mixtures varied between .88 and .98. It appears that some of the material in the "native" band of partly denatured samples melts as though it is not totally native.

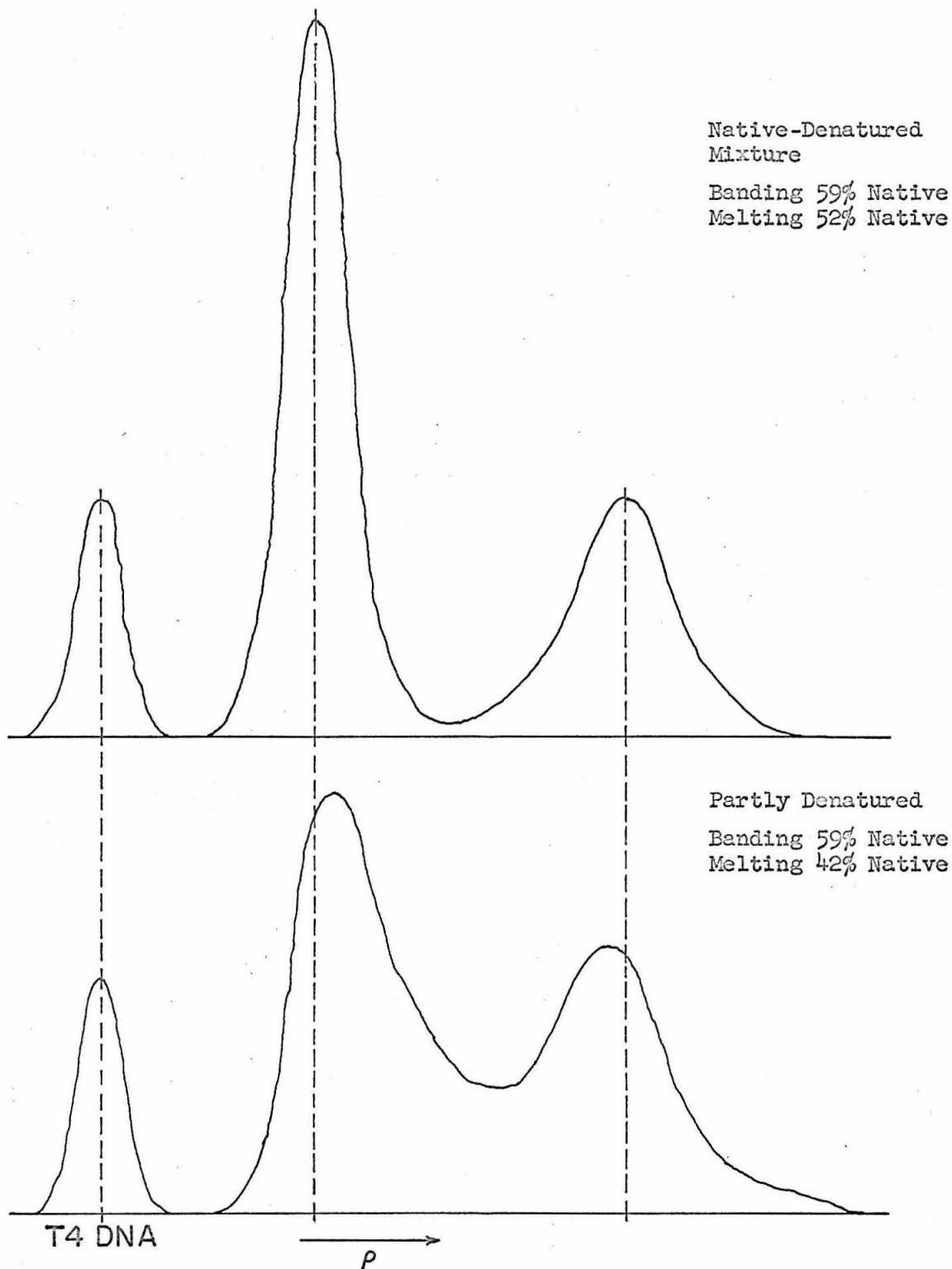


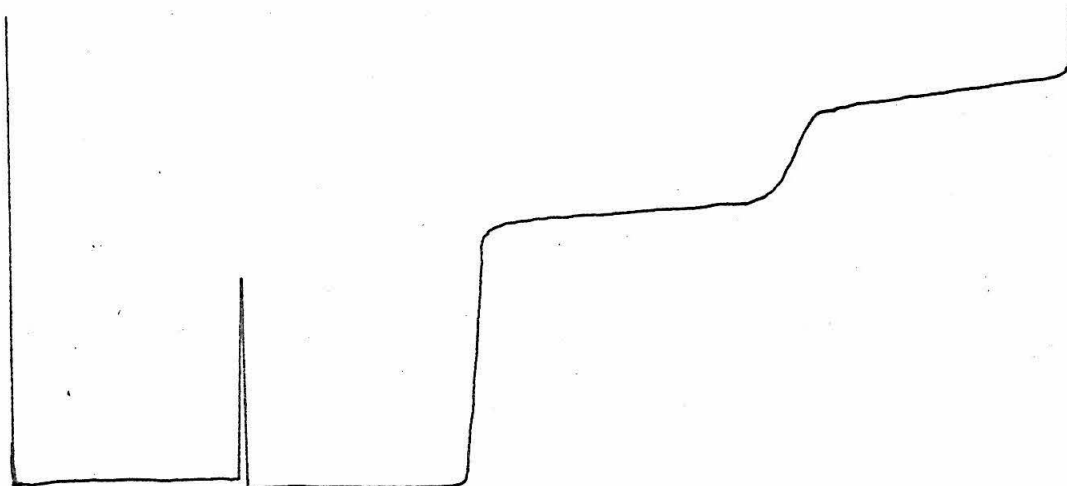
Figure 14. Equilibrium distribution in a CsCl density gradient at 44,770 rpm of a native-denatured mixture of T7 DNA and a sample denatured 15 min at 25° in 50% formamide, 0.082 M NaCl, unbuffered.

It was thought that perhaps sedimentation velocity runs on partly denatured samples might show a third component corresponding to partly denatured material. Aside from possible spreading of the boundaries, however, little difference from sedimentation patterns of mixtures of native and denatured material was noted (see Fig. 15). Due to the problems associated with the use of the sedimentation velocity system subtle differences would be hard to detect. The presence of two boundaries does suggest, however, that the two peaks noted in the CsCl density gradient are not an artifact produced by the action of high salt on a partially denatured molecular species isolated from the denaturation mixture.

#### The Relationship between Hyperchromicity and Banding Behavior

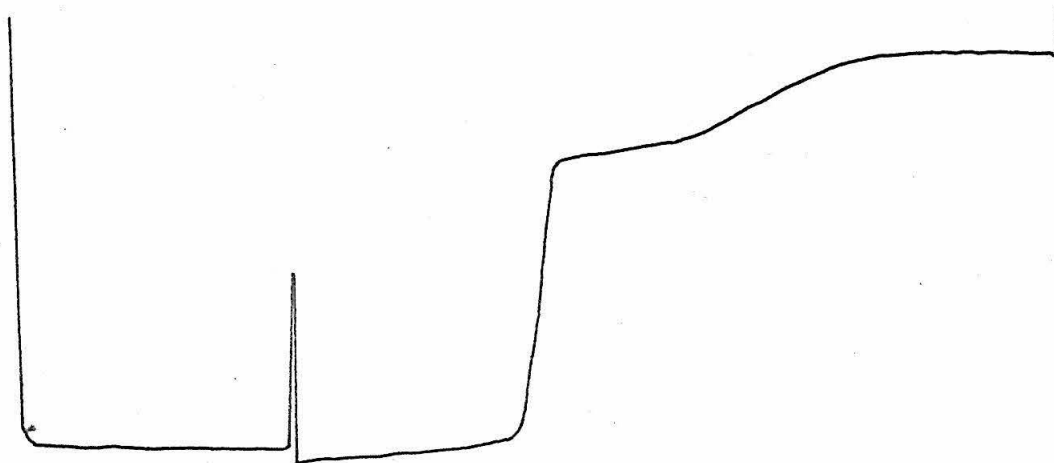
To examine the relationship between the hyperchromicity of a sample and its irreversible denaturation a sample of T7 DNA was melted in formamide and samples taken at various hyperchromicities were banded. The melting was done at a DNA concentration of 300  $\mu\text{g/ml}$  in 90% formamide, 0.5 M NaCl in a 1 mm path length cell against an appropriate blank. Water from an external water bath was circulated through the block of the cell holder to maintain the desired temperature. At various hyperchromicities approximately 5  $\lambda$  of DNA solution were diluted into 0.14 ml  $\text{H}_2\text{O}$  and then 0.6 ml CsCl stock solution at 44,770 rpm. The ODs were not corrected for expansion of the formamide solution during heating.

Fig. 16 shows a melting profile for T7 DNA in 90% formamide, 0.5 M NaCl heated at the rate of  $1^\circ$  per 3-5 minutes by gradually raising the temperature of the circulating water bath. Since 1 mm cells are too small for measurement of solution temperature by a thermometer the



Native-denatured DNA mixture, 62% native by banding.

$s_{20,w} = 13.6$  for native and 6.1 for denatured



Partly denatured DNA sample, 59% native by banding.

$s_{20,w} = 13.5$  for native (midpoint) and 6.3 for denatured

Figure 15. Sedimentation velocity patterns for a native-denatured mixture and a sample denatured 20 minutes at 25° in 90% formamide, 0.070 M NaCl, 0.005 M TRIS, pH 8.05. Run at 44,770 rpm in 10<sup>-3</sup> M NaCl, 2 x 10<sup>-4</sup> M TRIS.

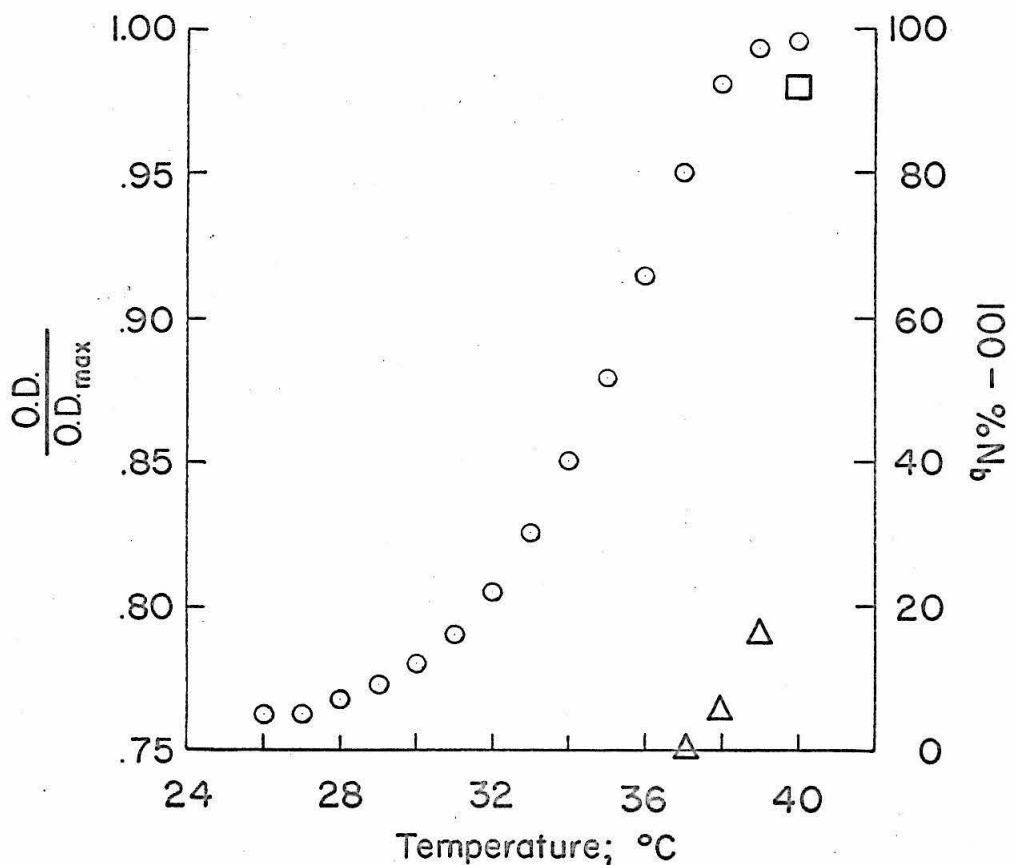


Figure 16. Melting profile of DNA in 90% formamide, 0.5 M NaCl and associated appearance of material banding at the density of denatured DNA in CsCl. The DNA solution was heated at a rate of approximately 1° per 3-5 minutes.

- OD as a function of temperature
- △ (100 - %N<sub>b</sub>), the percentage of material which bands at the density of denatured DNA. Samples for banding were removed at the temperatures indicated by their positions on the graph.
- (100 - %N<sub>b</sub>) after 15 min. at 40°

temperatures given are those of the heating block, which would lead the actual temperature of the sample. The extinction coefficient of the DNA and the hyperchromicity upon melting in the formamide solution were roughly the same as those for DNA in aqueous 0.5 M NaCl solution. Samples for banding were taken at the temperatures noted in Fig. 16. The banding patterns in this experiment showed no material banding at the denatured density until 80-90% of the total increase in OD was complete. Slight skewing of the bands toward heavier densities was however noted at lower hyperchromicities. The shape of the melting transition in this experiment appears unsymmetric and slightly broader than in aqueous solution but the exact shape is uncertain due to uncertainty in the actual temperature of the sample, as well as possible kinetic effects in the denaturation itself.

It is possible that fully denatured material is formed at hyperchromicities lower than 80% but at a rate too slow to be noticeable in this experiment. To rule out such kinetic effects a sample of T7 DNA in 90% formamide, 0.5 M NaCl was held at a temperature of 34-34.2° and a measured hyperchromicity of 60-65% for seven hours before a sample was taken for banding. All of the material banded around the native density, and although there appeared to be slight skewing toward heavier densities there was no evidence of any material of the fully denatured density.

Although the conditions of the above melting experiments were not identical to those used in kinetic studies of irreversible denaturation, it seems reasonable to assume that the molecular details of the denaturation process will be the same. These experiments suggest that under conditions of irreversible denaturation every molecule in the population

must be highly hyperchromic. Hyperchromic molecules which are not fully denatured apparently recover their native structure to different extents upon removal from denaturing conditions since the "native" band of partly denatured samples covers a wider range of densities than does that of native DNA and appears to melt as though it were not fully native. Since a DNA sample may be held for hours at an intermediate hyperchromicity without proceeding to the fully denatured condition, metastable states of intermediate hyperchromicity must be possible under these conditions.

#### Kinetics of Denaturation

The kinetics of the irreversible denaturation of T7 DNA in 90% formamide were followed by the procedures outlined in Methods. Figs. 17 and 18 show the decrease in  $\%N$  of solutions isolated after various times in denaturing conditions. The pH's given in Fig. 18 are those of the aqueous buffers which were diluted to 0.01 M in the denaturation mixture. The hydrogen ion activity in formamide is not known but pH measurements of buffers 0.01 M in 90% formamide (made with a Beckman pH meter with glass and calomel electrodes) gave a reading of 6.8 for pH 4.55 aqueous acetate buffer and 8.5 for pH 8.05 aqueous TRIS buffer.

Denaturation follows similar kinetics whether measured by melting or banding methods but generally  $\%N_D$  is somewhat greater than  $\%N_m$  (Fig. 17, 24), perhaps an indication that some of the material which bands in the native peak is partially denatured as suggested above. Although  $\%N$  can be approximated only very roughly by sedimentation velocity, results with this method agree qualitatively with those of melting and banding.

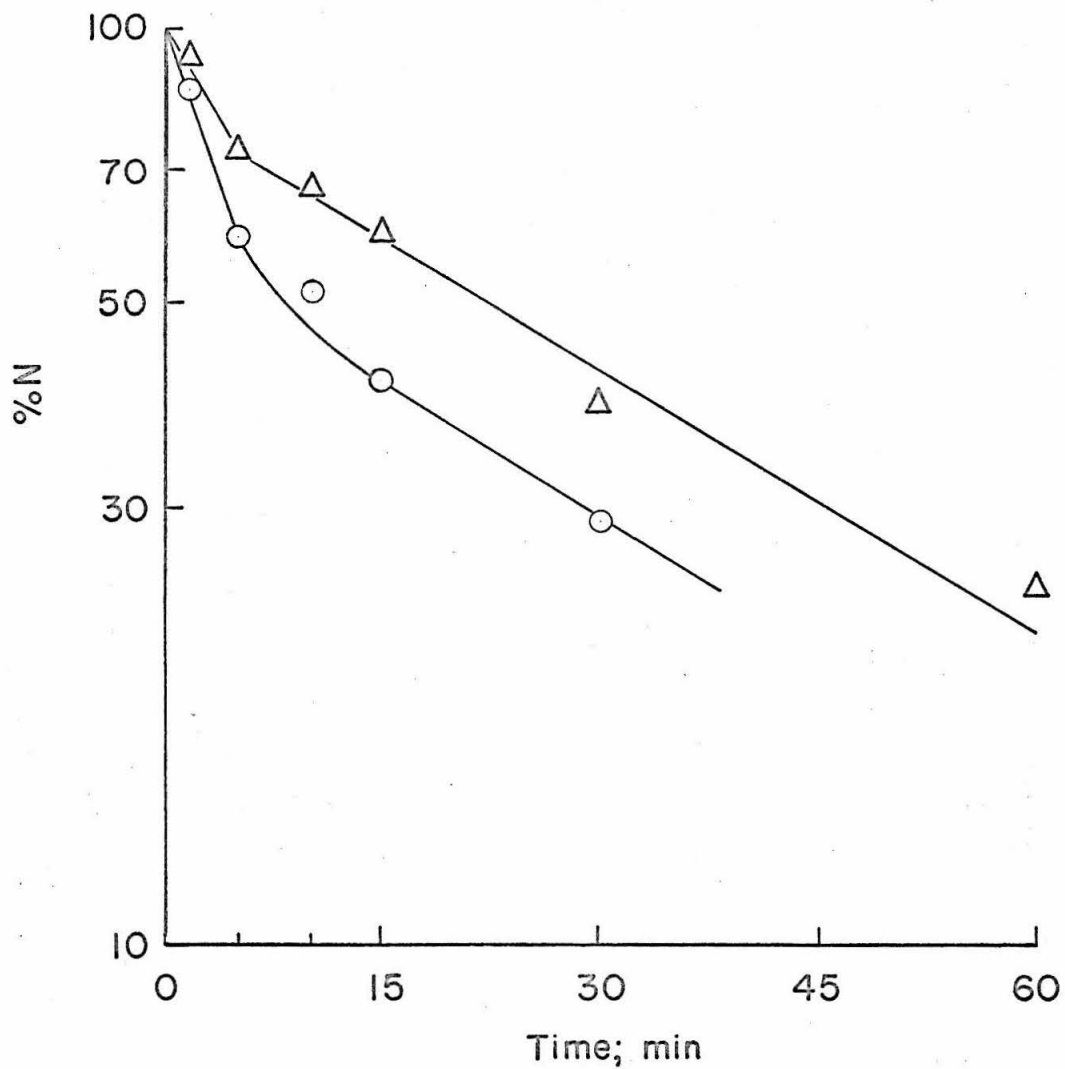


Figure 17. Denaturation kinetics of DNA.

System: 25°, 90% formamide, 0.082 M NaCl, unbuffered

Δ %N measured by banding

○ %N measured by melting

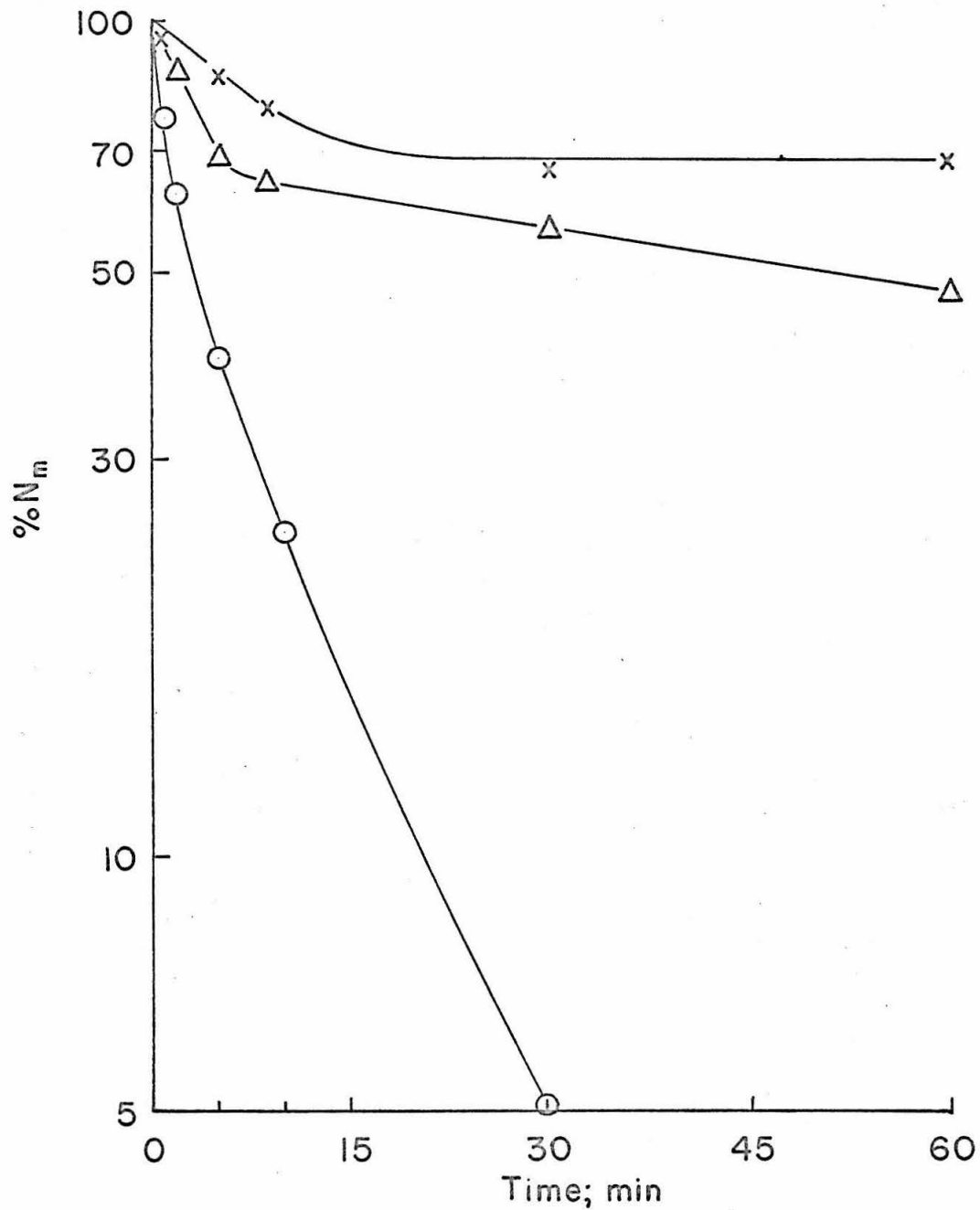


Figure 18. Denaturation kinetics of DNA as a function of the aqueous pH of added buffers.

System: 25°, 90% formamide, 0.0725 M NaCl, 0.01 M buffer

X TRIS, pH 8.05

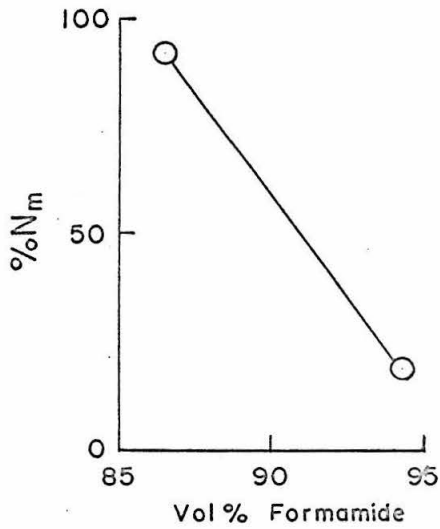
Δ Phosphate, pH 5.64

O Acetate, pH 4.9

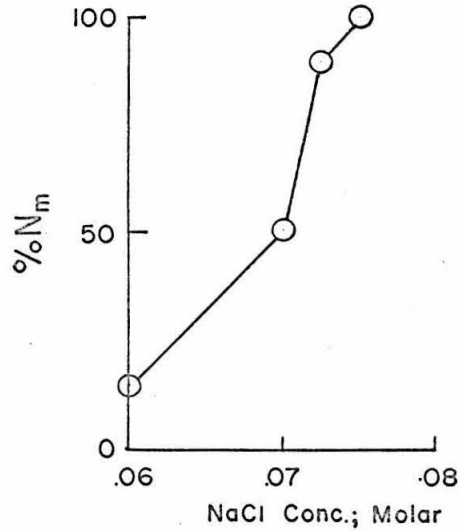
Contrary to what one would expect for a homogeneous DNA the denaturation kinetics are not first order. Several possible explanations for this situation suggest themselves:

The formamide system. As mentioned above, formamide in contact with water is known to undergo slow hydrolysis to formic acid and ammonia (79). It is possible that some such subtle change in the composition of the denaturing formamide solution might alter the rate of denaturation to a significant degree during the course of the denaturation reaction. The sensitivity of the initial rate of denaturation to slight changes in the denaturation medium was tested by measuring the melting per cent native of DNA after five minutes in denaturing solution in which one parameter at a time was varied. The results, given in Fig. 19, show that this rate is quite sensitive to small changes in salt concentration, temperature, formamide concentration and pH.

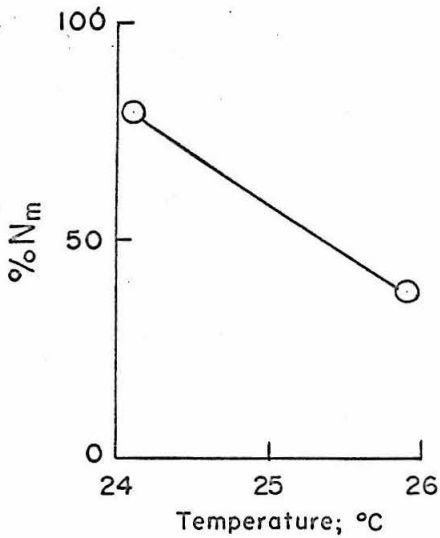
The following experiment suggests that it is unlikely that hydrolysis of formamide during the course of the experiment produces changes in the composition of denaturing solution large enough to affect denaturation kinetics. A solution of T7 DNA in 90% formamide at twice the NaCl concentration of an appropriate denaturing mixture did not show detectable denaturation over the course of an hour at 25°. Such a solution was placed at 25° together with a separate solution of 90% formamide. Equal volumes of the two were mixed to produce a denaturing mixture. This was done at times separated by fifty minutes to see if hydrolysis or any other reaction of the 90% formamide solution over this period of time might affect the denaturation kinetics. The denaturation kinetics of the two mixtures were found to be essentially identical, demonstrating the lack of such effects.



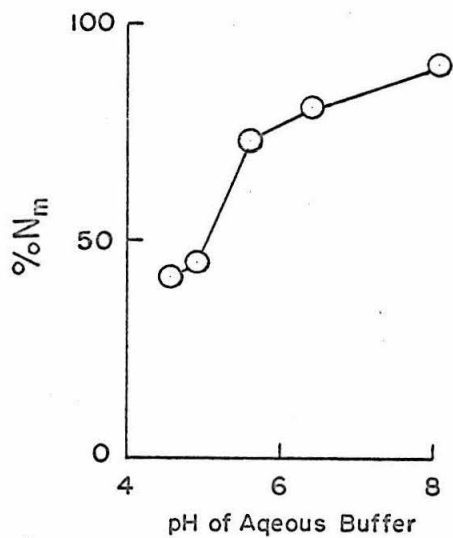
System: 25°, 0.0673 M NaCl  
0.01 M TRIS, pH 8.05



System: 25°, 90% Formamide  
0.01 M TRIS, pH 8.05



System: 90% Formamide  
0.07 M NaCl  
0.01 M TRIS, pH 8.05



System: 25°, 90% Formamide  
0.0725 M NaCl  
0.01 M Buffer

Figure 19. Effect of environmental changes on the initial rate of denaturation of T7 DNA. All points taken after five minutes in the denaturing solvent.

One might suspect that the heat of mixing of water and formamide could raise the temperature of the solution upon addition of the aqueous DNA solution and thus produce the observed kinetics. It was found however that addition of the DNA solution to the formamide mixture lowered the temperature  $0.2^{\circ}$  and that the equilibrium temperature was restored within three minutes. If this factor were important it should produce effects opposite to those observed.

Denaturation kinetics in aqueous solutions. Since no factor in the formamide system could be found which might account for the observed kinetics it was of interest to know whether the same denaturation kinetics would be observed in aqueous solutions. Denaturation of T7 DNA in aqueous salt solutions at elevated temperatures was followed in much the same way as in the formamide system. A concentrated DNA solution was diluted about twentyfold into a temperature equilibrated salt solution and the denaturation reaction stopped at various times by diluting 1 ml of sample into an equal volume of buffer at  $0^{\circ}$ . The denaturing solutions were heated in capped tubes to minimize losses of  $H_2O$  by evaporation and consequent alteration of solvent composition. The two examples given in Fig. 20 show that the denaturation kinetics in aqueous solution are essentially identical to those obtained in the formamide system, again suggesting that they are a property of the DNA itself and are not due to peculiarities of the denaturing system.

Although pH is difficult to measure and to control under the conditions of low salt and elevated temperatures used in the aqueous system it is quite evident from many experiments, including the one shown in Fig. 20, that there is a rapid change in denaturation kinetics at

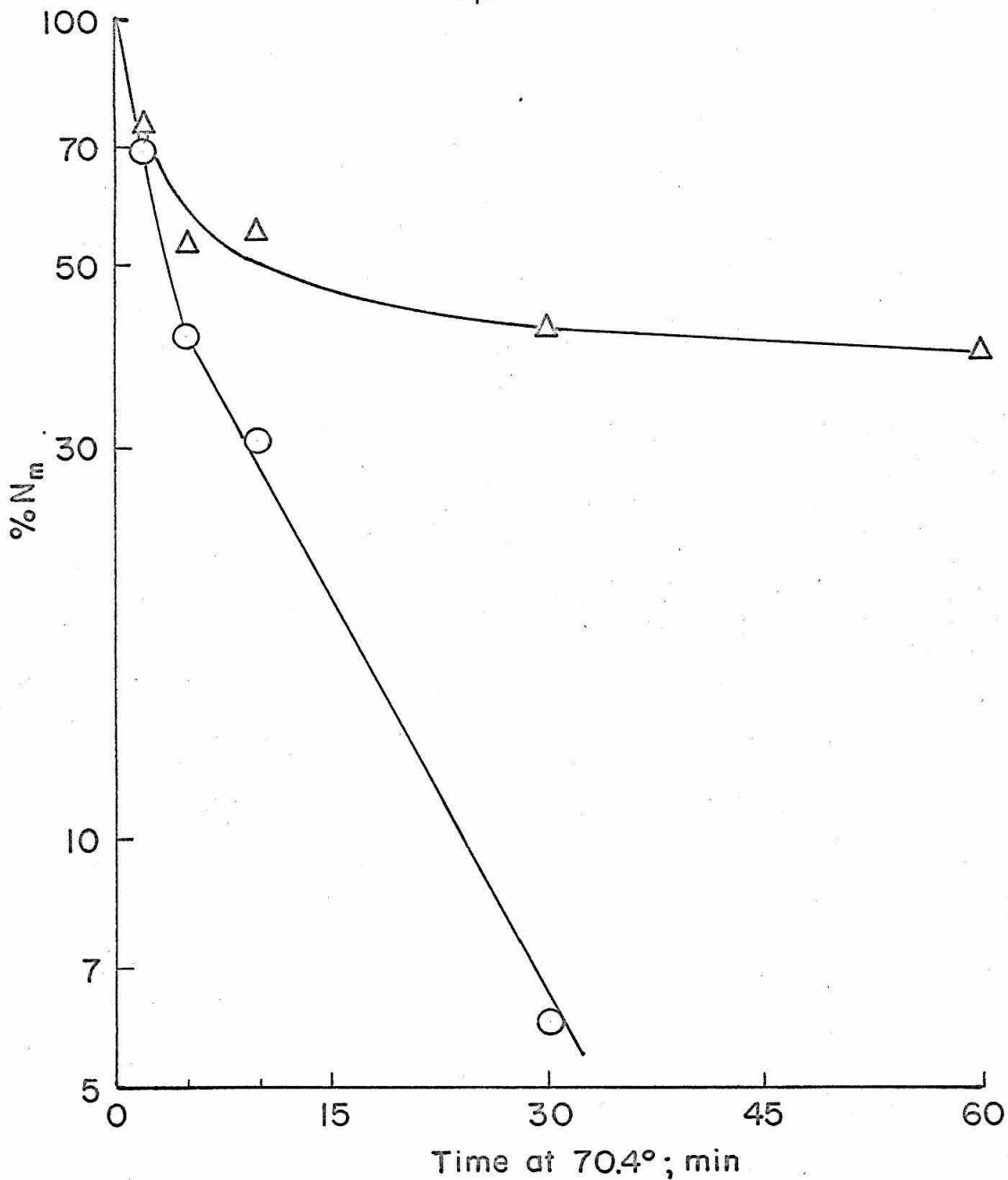


Figure 20. Denaturation kinetics of DNA in aqueous solution at 70.4°. DNA stock in 0.1 M NaCl, 0.01 M TRIS, pH 7.4.

- Diluted twentyfold in H<sub>2</sub>O
- △ Diluted twentyfold in H<sub>2</sub>O previously titrated to pH 9.3 with NaOH

approximately pH 7. The DNA is considerably more stable to denaturation if a small amount of base is added to bring the pH to the range of 7-9 than if no base is added, leaving a pH around 6-7. This is true in the presence or absence of the small amounts of TRIS buffer used in the DNA stock solutions.

Approach to equilibrium. The nature of the denaturation kinetics described above suggests an approach to equilibrium. If this were indeed the case the data of Fig. 18 suggest that in 90% formamide the equilibrium should be on the side of native DNA at high pH but on the side of denatured DNA at low pH. Thus DNA denatured extensively at low pH would be expected to revert substantially to native DNA if the pH is raised. The following experiment was designed to test this possibility: A solution of T7 DNA in 90% formamide, .0725 M NaCl, 0.01 M TRIS, pH 7.4 and green to bromthymol blue was allowed to denature for 60 min. At that time a small amount of glacial acetic acid was added to make the solution orange to methyl red and denaturation was allowed to continue another 60 min. Triethylamine was then added to make the solution again green to bromthymol blue. After a further 60 min. the DNA showed no reversal of denaturation, as shown in Fig. 21. This indicates that the observed kinetics are not the result of an approach to equilibrium between native and fully denatured DNA.

Effect of denatured DNA. Another possible basis for the observed denaturation kinetics of T7 DNA might be that denatured DNA or other substances accumulated during denaturation can somehow inhibit the remaining partially denatured DNA from further denaturation. That this is not the case is shown by the following experiment: A sample of T7 DNA

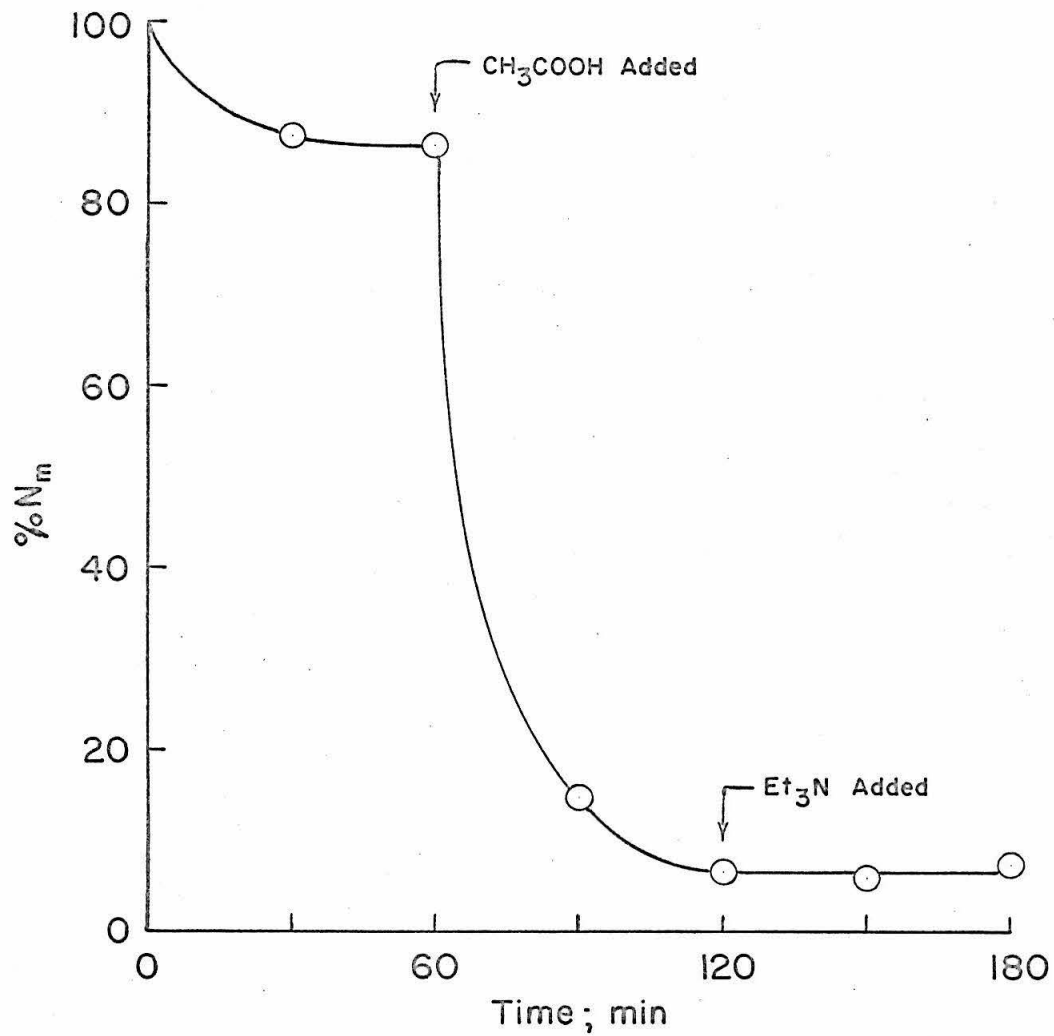


Figure 21. Non-reversibility of denaturation.

System: 25°, 90% formamide, 0.0725 M NaCl, 0.01 M TRIS

was completely denatured in about 97% formamide. Water, salt, buffer, and an equal quantity of native DNA were added to bring the solution to 90% formamide, .0725 M NaCl, and 0.01 M phosphate buffer (aqueous pH 5.6). The kinetics of denaturation of the native T7 DNA were unaffected by the presence of the equal quantity of denatured DNA (Fig. 22).

Concentration dependence. The rate of denaturation of T7 DNA at 40  $\mu\text{g/ml}$  as measured from melting data was compared with the rate of denaturation under identical conditions but at 4  $\mu\text{g/ml}$  and as measured from banding data. The results, shown in Fig. 23, show no difference between the denaturation kinetics of the two samples, although it is likely that the more dilute DNA denatured slightly farther since  $\%N_p$  is usually 1.1 to 1.2 times the value of  $\%N_m$ . Although this slight difference in degree of denaturation may be due to experimental error, it may also be due to the viscosity effect noted by Schildkraut et al. (60). The fact that a tenfold difference in concentration affects the denaturation rate only slightly argues strongly that the denaturation reaction is basically unimolecular. It also excludes interaction hypotheses such as those mentioned in the preceding section.

Divalent metal ions. The kinetics of denaturation of T7 DNA in the presence of .004 M EDTA are similar to those in the absence of EDTA. This indicates that the presence of small quantities of divalent metal ions is probably not an important factor in producing the observed kinetics.

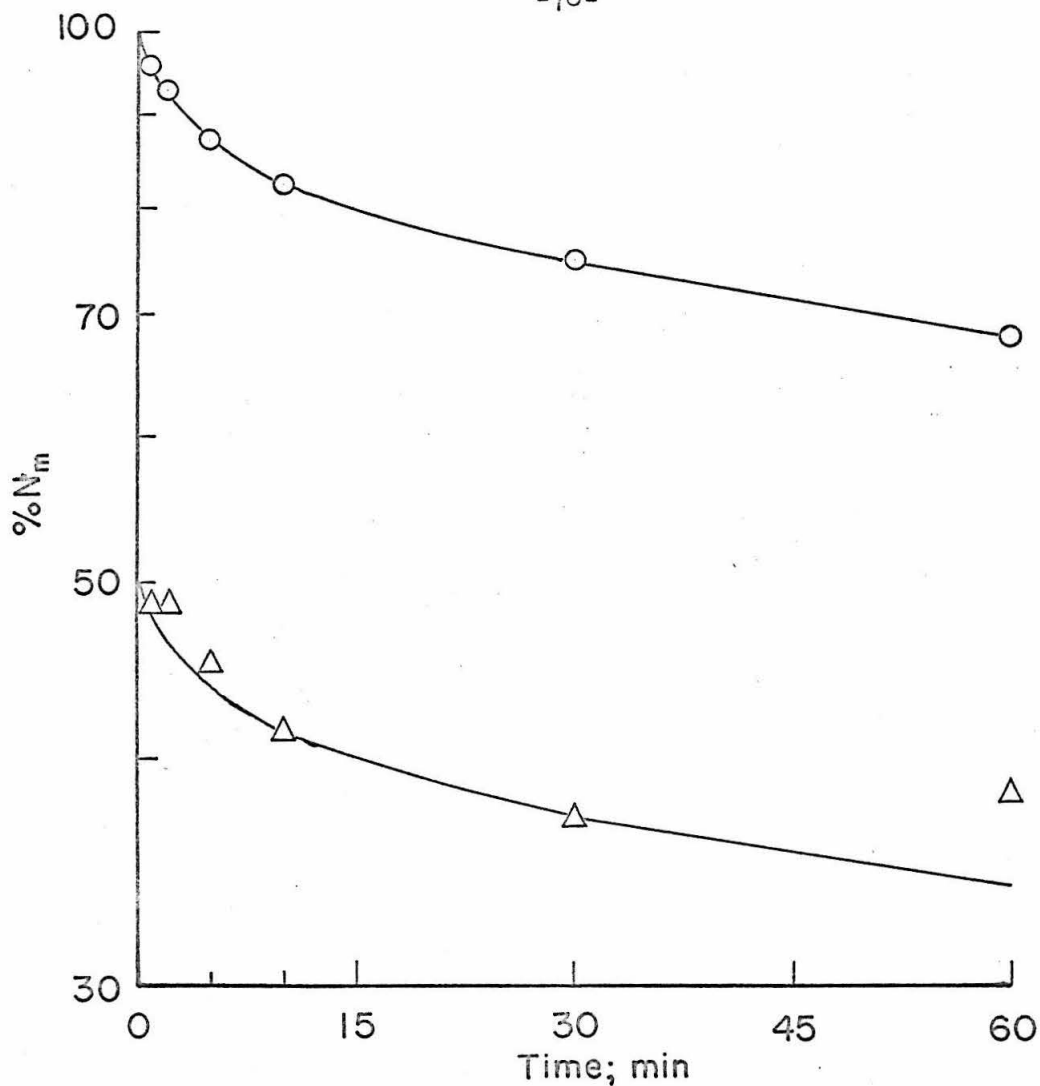


Figure 22. Effect of added fully denatured DNA on denaturation kinetics.

System: 25°, 90% formamide, 0.0725 M NaCl, 0.01 M phosphate, pH 5.6

- No denatured DNA added.
- △ Denaturation in presence of an equal quantity of fully denatured DNA. Line shows kinetics expected from points taken without added denatured DNA.

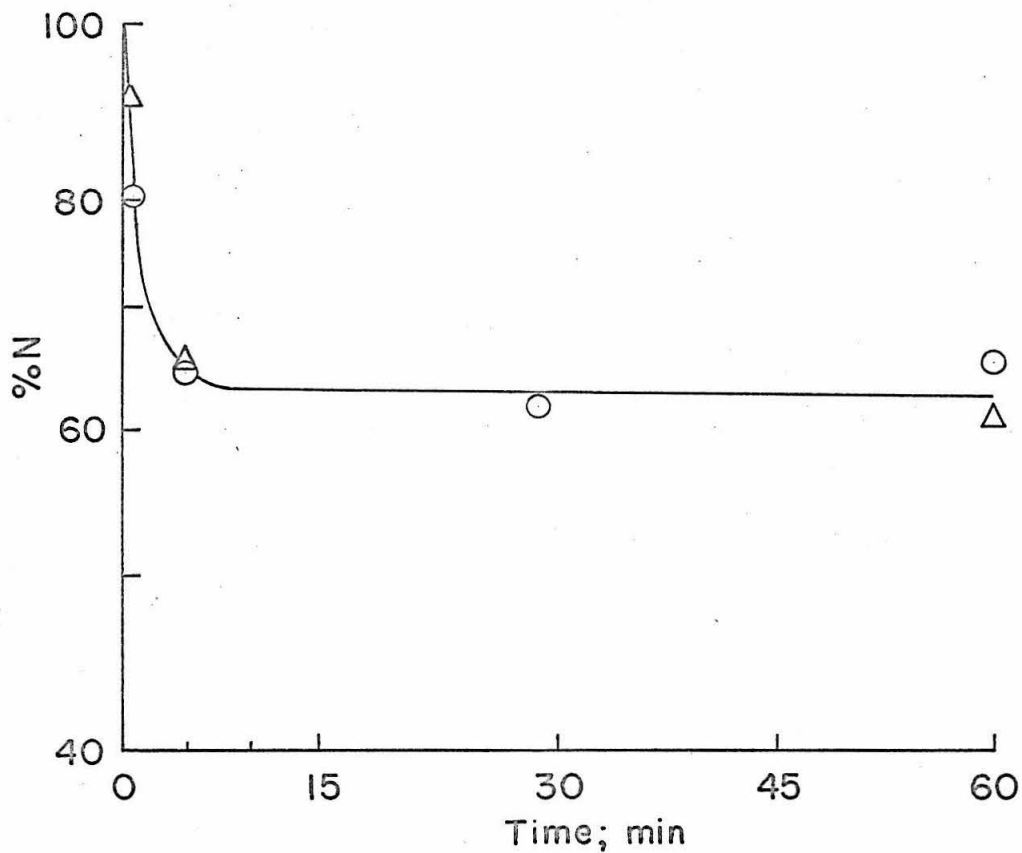


Figure 23. Effect of DNA concentration on denaturation kinetics.

System: 25°, 90% formamide, 0.075 M NaCl,  
0.005 M TRIS, pH 8.05

- DNA at 40 µg/ml; %N measured by melting.
- △ DNA at 4 µg/ml; %N measured by banding.

### The Effect of Stirring on Denaturation

All of the above results were obtained on solutions which were not stirred or shaken during denaturation except briefly and gently during the initial dilution of DNA in the denaturing mixture. It has been found that stirring or shaking a denaturing DNA solution markedly accelerates the rate of denaturation. Stirring experiments were done in a water jacketed tube using a teflon covered magnetic stirring bar 1.2 cm long and 0.9 cm in diameter to provide the stirring. Comparisons of the kinetics of denaturation of stirred and unstirred samples under otherwise identical conditions are shown in Figs. 24 and 25. The kinetics of denaturation of the stirred samples approach first order. The rate of stirring was not measured but was non-turbulent and approximately constant throughout the experiment. Strong indications have been obtained that rate of denaturation increases with rate of stirring but this awaits study with more quantitative methods for producing and estimating shear.

It does not matter when during the process of denaturation stirring is begun; it always increases the rate. Thus a sample denatured without stirring to the point where denaturation appears to cease denatures rapidly and completely upon initiation of stirring (Fig. 26). The denaturation rates of DNA samples at concentrations of 40  $\mu\text{g}/\text{ml}$  and 4  $\mu\text{g}/\text{ml}$  are both accelerated by stirring.

Stirring apparently does not in itself produce denaturation in a sample which is not already denaturing. Vigorous stirring does not induce denaturation in DNA samples in conditions of formamide and salt which are not quite sufficient in themselves to initiate denaturation. The relationship between hyperchromicity of a sample and stirring effect

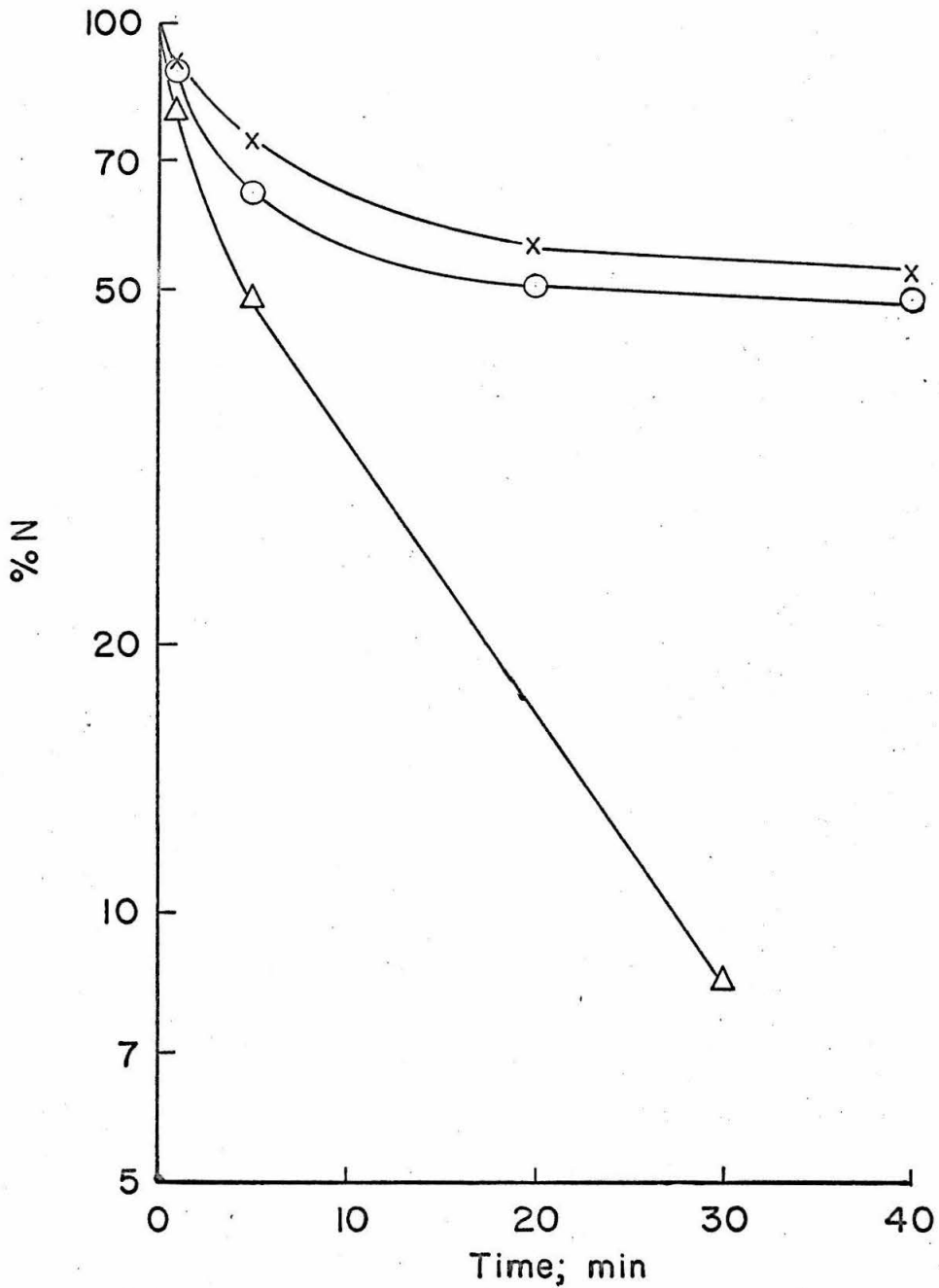


Figure 24. Effect of stirring on denaturation.

System: 25°, 90% formamide, 0.070 M NaCl,  
0.005 M TRIS, pH 8.05

- X unstirred, %N measured by banding.
- O unstirred, %N measured by melting.
- Δ stirred throughout, %N measured by melting.

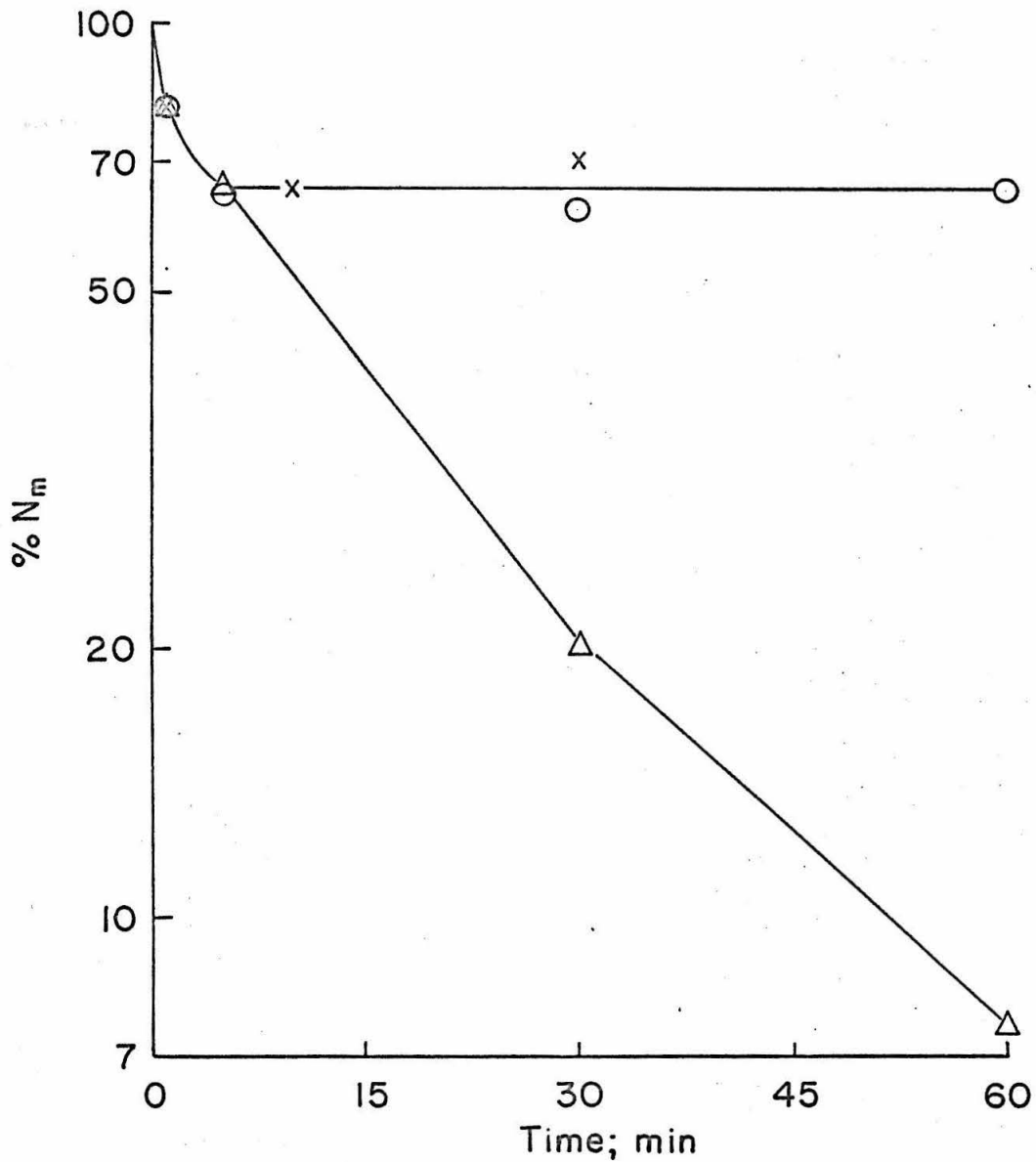


Figure 25. Effect of stirring on denaturation.

System: 25°, 90% formamide, 0.075 M NaCl,  
0.005 M TRIS, pH 8.05

- No stirring after first minute (40 μg/ml data of Fig. 22).
- △ Stirred throughout.
- × Stirred for 5 min at 80% formamide, 0.15 M NaCl prior to 0 time above.

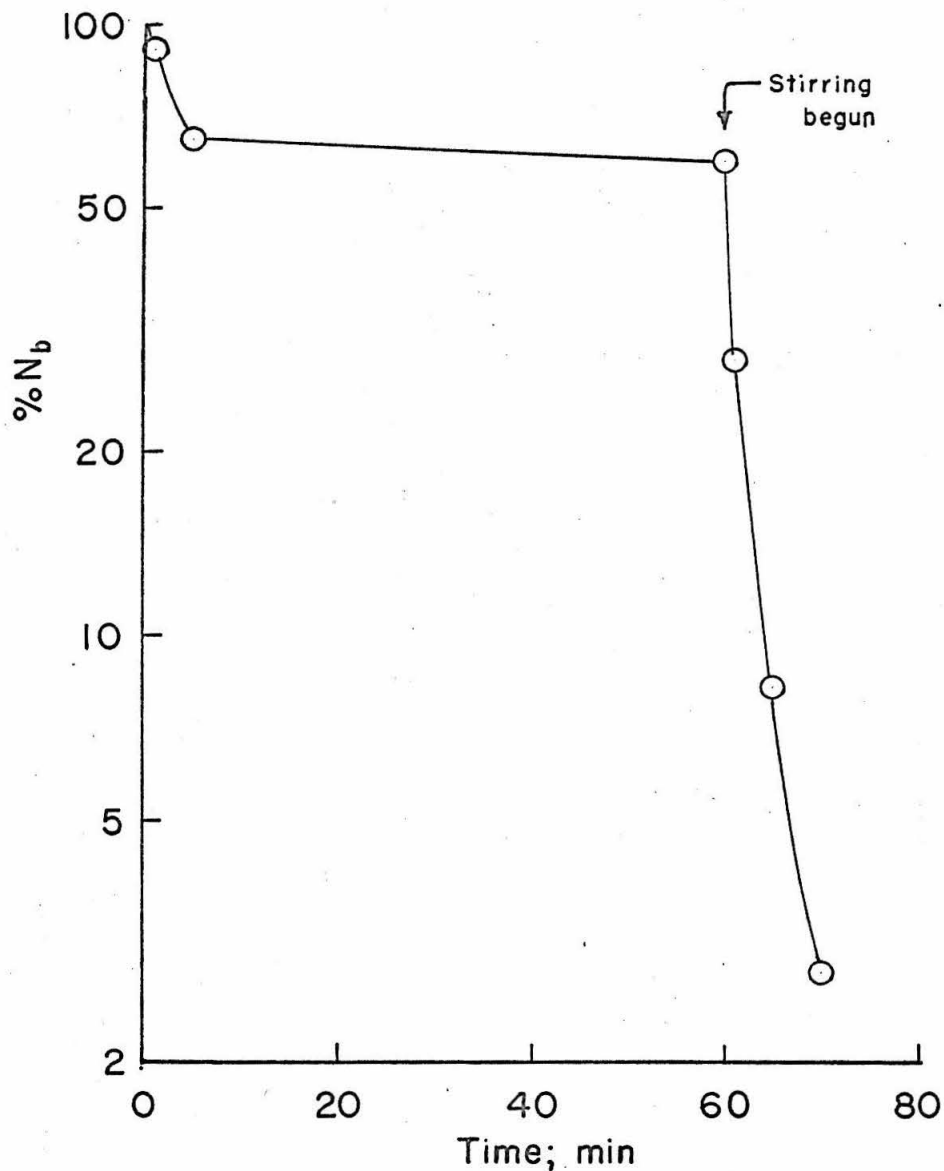


Figure 26. Effect of stirring on denaturation.

System: 25°, 90% formamide, 0.075 M NaCl,  
0.005 M TRIS, pH 8.05

DNA at 4 µg/ml; data taken from same experiment shown in Fig. 22.

has not been examined to see if partially hyperchromic samples can be denatured by stirring.

A previous history of stirring under non-denaturing conditions does not affect denaturation kinetics. If a DNA sample is stirred vigorously in 80% formamide, 0.15 M NaCl no denaturation occurs. After addition of an equal volume of pure formamide the denaturation kinetics without stirring are indistinguishable from those of a sample in 90% formamide, .075 M NaCl which has never been stirred (Fig. 25).

#### DISCUSSION

To summarize the above data on the mechanism and kinetics of denaturation of T7 DNA:

1) Irreversible denaturation of T7 DNA does not occur until the DNA is highly hyperchromic. Thus, under conditions in which irreversible denaturation is observed, virtually every molecule in the population must be in some intermediate state of denaturation. These intermediate states of denaturation appear to be stable indefinitely under conditions in which the DNA is hyperchromic but is not irreversibly denaturing.

2) Samples of DNA isolated from denaturing conditions are mixtures of fully denatured molecules and molecules which appear to be native to varying degrees. It appears that upon removal of the DNA from denaturing conditions those DNA molecules in intermediate states of denaturation recover their native structure at least partially.

3) The rate of denaturation of T7 DNA falls off rapidly with time but appears to be almost independent of DNA concentration. The rate of denaturation is very sensitive to slight changes in the environment produced by reactions of the formamide-water solvent mixture. The

denaturation reaction is not reversible, is not inhibited by the presence of denatured DNA, and is not affected by presence or absence of EDTA.

4) Stirring during the denaturation reaction accelerates the rate of denaturation.

The data summarized in points 1) and 2) above agree well with the picture of DNA denaturation presented in the introduction. The kinetics of denaturation of T7 DNA summarized in point 3) are, however, not in accord with what might be predicted from this theory. If the stability of molecular regions is governed by their base composition, then for a homogeneous population of molecules one would expect the most stable region to be the same for each molecule. If one assumes that all native sequences in a molecule must be melted out to produce irreversible denaturation, the collapse of the most stable sequence will be the rate limiting step and the population should denature with first order kinetics. An initial lag in denaturation rate might be expected if appreciable time is consumed in reaching the rate limiting step or if there are two or more regions of comparable high stability which must collapse to produce complete denaturation. Far from having an initial lag the denaturation rate of T7 DNA is most rapid at early times.

The possibility that the observed denaturation kinetics are being influenced by renaturation of irreversibly denatured molecules during isolation of DNA from denaturing mixtures can be ruled out by data from several sources:

1) The most obvious demonstration comes from stirring experiments, p. 78. Since fully denatured stirred samples and partly denatured unstirred samples are isolated under identical conditions, the failure

of the latter to fully denature cannot be attributed to renaturation of fully denatured DNA during isolation.

2) The experiment under Approach to equilibrium, p. 73, Fig. 21, demonstrates that raising the pH of a largely denatured sample to the condition where the DNA previously would not denature below about 80% N does not result in any renaturation upon isolation.

3) The experiment under Effect of denatured DNA, p. 73, Fig. 22, demonstrates that fully denatured DNA added to a denaturing mixture does not renature at all, even though denaturation of the native DNA has decidedly non first order kinetics in which denaturation levels off around 70% N.

4) Aqueous denaturation experiments at low salt concentration, p. 71, Fig. 20, also demonstrate that non first order kinetics are obtained under conditions where renaturation effects are impossible.

An explanation for the observed denaturation kinetics of T7 DNA which immediately suggests itself is that the DNA is not molecularly homogeneous and that some molecules are less stable to irreversible denaturation than others. Although T7 DNA was chosen for this work because of its relative homogeneity it is of course impossible to state with certainty that a DNA sample is molecularly homogeneous. However, let us briefly consider the evidence concerning various possible sources of heterogeneity in T7 DNA:

1) One might hope that the fact that this DNA was isolated from material presumed to be biologically homogeneous might assure homogeneity of the product. However there is no certainty that the biological material is homogeneous. It has, in fact, been postulated on the basis

of genetic evidence that the base sequences of DNA molecules from different T<sub>4</sub> phages may be circularly permuted (80). However, such a population of molecules might still be expected to denature with a first order rate if stability to denaturation is dependent solely on the base sequence of the most stable region.

2) The phage population as a whole might contain small amounts of other strains or mutants having DNAs with different stabilities to denaturation. However, the phage preparation sediments as a single sharp boundary and yields a single band in a CsCl density gradient. Differences in DNA molecules might be expected to alter per cent GC content slightly thus changing both stability to denaturation and molecular weight determined by the CsCl density gradient banding method. Since the banding molecular weight is very close to that expected for the total amount of DNA in the phage such compositional heterogeneity must necessarily be very small indeed.

3) It is possible that during isolation the DNA might have been partially degraded or suffered single chain scissions. Since sedimentation patterns of both native and fully denatured DNA yielded sharp boundaries with no evidence of trailing material this possibility appears to be an unlikely one.

4) The kinetic data suggest that if the DNA consists of a mixture of molecules possessing different denaturation rates it must contain a large number of different molecular species. Thus, for a single DNA sample denatured under different conditions, extrapolations of the final rates to zero time gave widely different values for the proportion of material possessing the slowest rate of denaturation.

5) The fact that stirring samples under denaturing conditions can produce kinetics approaching first order also argues against intermolecular heterogeneity.

The above comments on possible sources of heterogeneity in the T7 DNA samples used here certainly do not exclude the possibility that the samples were intermolecularly heterogeneous. However, intermolecular heterogeneity is not required to explain the observed denaturation kinetics.

The observed kinetics can be explained if one assumes that the stability of a native region in a partially denatured molecule depends not only on its base composition and sequence but on other molecular factors as well. For example one might expect that the stability of a particular native region might depend on its position in the molecule and on the number and locations of other native regions in the same molecule. Under these circumstances the stability of a particular native region would change as the molecule progressively denatures, and the order in which various regions of the molecule denature would be important in determining what the rate limiting step toward denaturation will be. Since the T7 DNA molecule possesses 30,000 base pairs it is quite probable that at many points during the denaturation process several native regions in a molecule may have roughly equal probabilities of collapse. Under denaturing conditions the collapse of each region would be irreversible and the denaturation might therefore proceed by random processes down mutually exclusive paths, each with its own characteristic rate determining step. Thus intermolecular heterogeneity could be generated from a homogeneous population of molecules by the process of

denaturation itself. The differences in activation energies between the different paths of denaturation would necessarily be small since a slight increase in temperature is enough to denature the whole sample rapidly and completely.

The idea that molecular heterogeneity can be generated by denaturation is supported by the fact that different partially denatured molecules apparently do not recover their native structure to the same degree upon removal from denaturing conditions, as evidenced by banding and melting properties of partly denatured samples.

The fact that stirring during denaturation produces kinetics which approach first order may be an indication that stirring minimizes the effects of position and total molecular configuration on the rate of denaturation of the individual native regions. This could conceivably be accomplished by reducing molecular hindrances to unwinding or untangling of the two strands by tumbling the molecule. It is also possible that stirring, by giving kinetic energy to partly unwound strands, may aid in denaturing native segments.

Although these experiments cannot exclude intermolecular heterogeneity as the source of the observed results they do suggest that the configuration of the partially denatured molecule may contribute to its stability to irreversible denaturation.

## RENATURATION

The following studies show that T7 DNA can be renatured very extensively in a formamide-water-salt medium at 25°, thus making it possible to denature and renature DNA under conditions which do not degrade its primary structure.

### METHODS

These renaturation studies were principally aimed at establishing optimal renaturation conditions and procedures for accurate kinetic work. Therefore, DNA concentrations of 30-75 µg/ml in the renaturing solvent were used for convenience in the melting assay, even though aggregation is known to occur during renaturation at these DNA concentrations in other systems (67). In most cases the extent of renaturation was measured by the melting procedure described above although many partially renatured samples were also banded in a CsCl density gradient.

The procedure followed in most renaturation experiments was as follows: A sample of T7 DNA was denatured in 90% formamide, 0.01 M NaCl at 25° for thirty minutes. After removal of a control sample to demonstrate that denaturation was in fact complete, the solution was brought to the composition desired for renaturation by addition of an appropriate amount of aqueous salt solution. Renaturation occurred equally well if the denatured DNA was first dialyzed into aqueous solution and then renatured in a formamide-water-salt solvent.

## RESULTS

### Optimal Condition for Renaturation

The range of solvent compositions which support renaturation at 25° was studied by varying the salt and formamide content of the renaturing mixtures. Figures 27 and 28 show this range to be very broad.

In Fig. 27 the extent of renaturation of T7 DNA over a period of 30 minutes at 25° in 75% formamide is shown as a function of salt concentration. These results show that rate of renaturation increases with salt concentration and that no renaturation occurs in 75% formamide at salt concentrations of 0.05 M NaCl or lower. It is interesting to note that denaturation of T7 DNA also does not occur in 75% formamide at 0.05 M NaCl, and since rate of denaturation decreases with increasing salt concentration it would appear that the solvent conditions for denaturation and renaturation are mutually exclusive. This implies that renaturation is not a direct equilibrium reversal of denaturation.

In Fig. 28 the renaturation of T7 DNA over a period of 60 minutes at 25° in 0.25 M NaCl is shown as a function of formamide concentration. In these experiments the renatured solutions were dialyzed directly into 0.01 M NaCl, a procedure which doubtless led to some renaturation during dialysis for samples renatured at high formamide concentrations. These results show that renaturation occurs over a wide range of formamide concentrations with an optimum around 50 volume % formamide, but that no renaturation occurs in solutions containing less than 20% formamide at this salt concentration. The fact that T7 DNA can renature so readily over such a wide range of formamide concentrations means that special care must be taken in kinetic experiments to dilute samples directly to a solvent composition which will not support further renaturation. For example

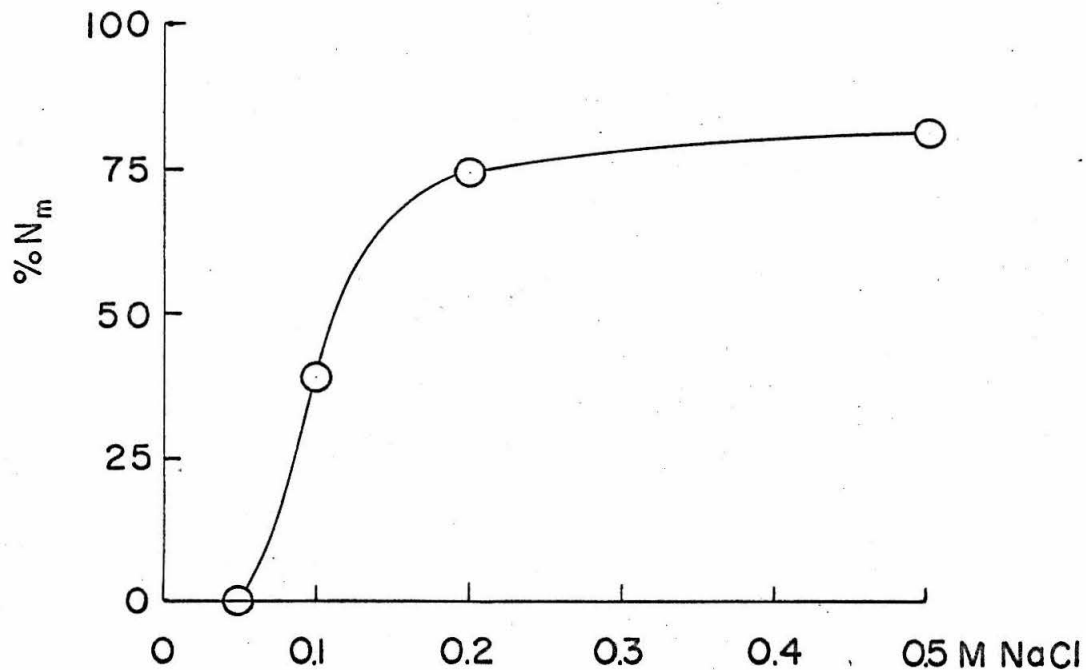


Figure 27. Renaturation of T7 DNA. %N<sub>m</sub> of denatured T7 DNA samples after 30 minutes at 25° in 75% formamide at various NaCl concentrations. DNA concentration during renaturation was 120 µg/ml.

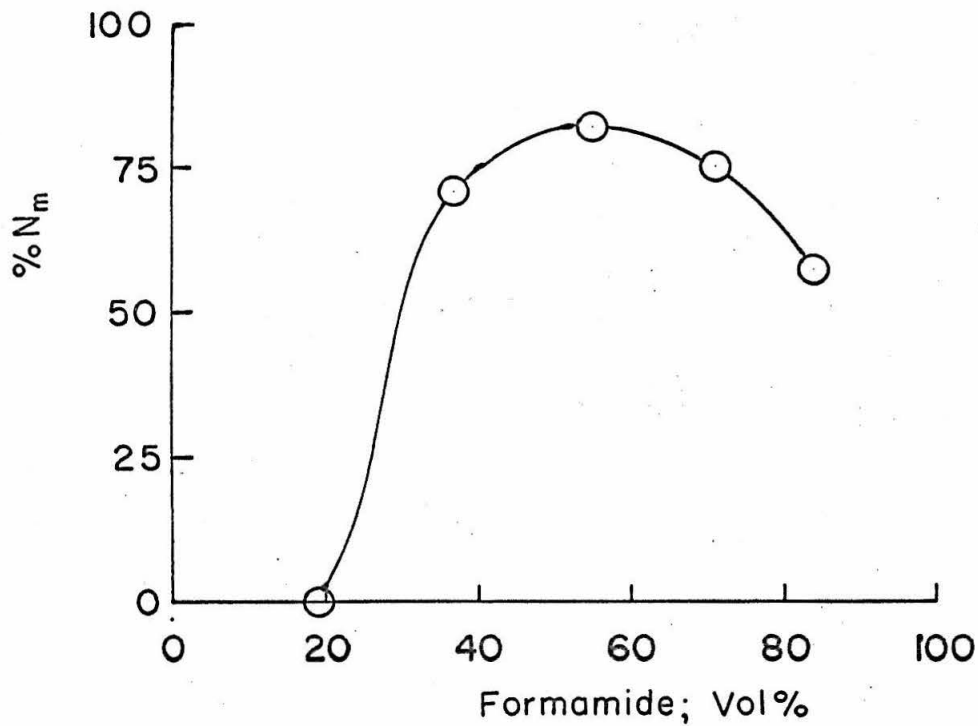


Figure 28. Renaturation of T7 DNA. %N<sub>m</sub> of denatured T7 DNA samples after 60 minutes at 25° in 0.25 M NaCl<sup>m</sup> at various formamide concentrations. Samples were dialyzed without dilution. DNA concentration during renaturation was 18 µg/ml.

samples renatured in 0.5 M NaCl, 75% formamide would require about a fourfold dilution into water to effectively stop the reaction.

#### Properties of Renatured DNA

Renatured T7 DNA melts sharply at the characteristic native melting temperature but the percentage increase in OD upon melting depends upon the degree of renaturation of the sample. The maximum hyperchromic effect obtained for renatured DNA was approximately 85-90% of that characteristic of native DNA. Such maximally renatured T7 DNA forms a single band in a CsCl density gradient at a position .001-.002 density units heavier than native T7 DNA. A banding pattern at 44,770 rpm together with a  $\log C$  vs  $W^2$  plot of the pattern are shown in Fig. 29 for a renatured sample which had about 82% of the native hyperchromic effect. The band is slightly skewed toward heavier densities in the lower third of the curve. The banding molecular weight calculated for this sample is approximately  $14 \times 10^6$ .

#### Renaturation Kinetics

Two preliminary experiments were done on the kinetics of renaturation of T7 DNA in formamide. In experiment I the DNA was renatured at a concentration of 40  $\mu\text{g}/\text{ml}$  in 50% formamide, 0.25 M NaCl and in experiment II the DNA concentration was 75  $\mu\text{g}/\text{ml}$  while the solvent was 75% formamide, 0.25 M NaCl. Samples were diluted at various times to solvent composition containing less than 20% formamide and dialyzed into aqueous 0.01 M NaCl. Both melting and banding profiles were obtained on samples from experiment I but only melting profiles were obtained for samples from experiment II.

Fig. 30 shows banding profiles for samples from experiment I and Table 2 gives melting data for the two experiments.

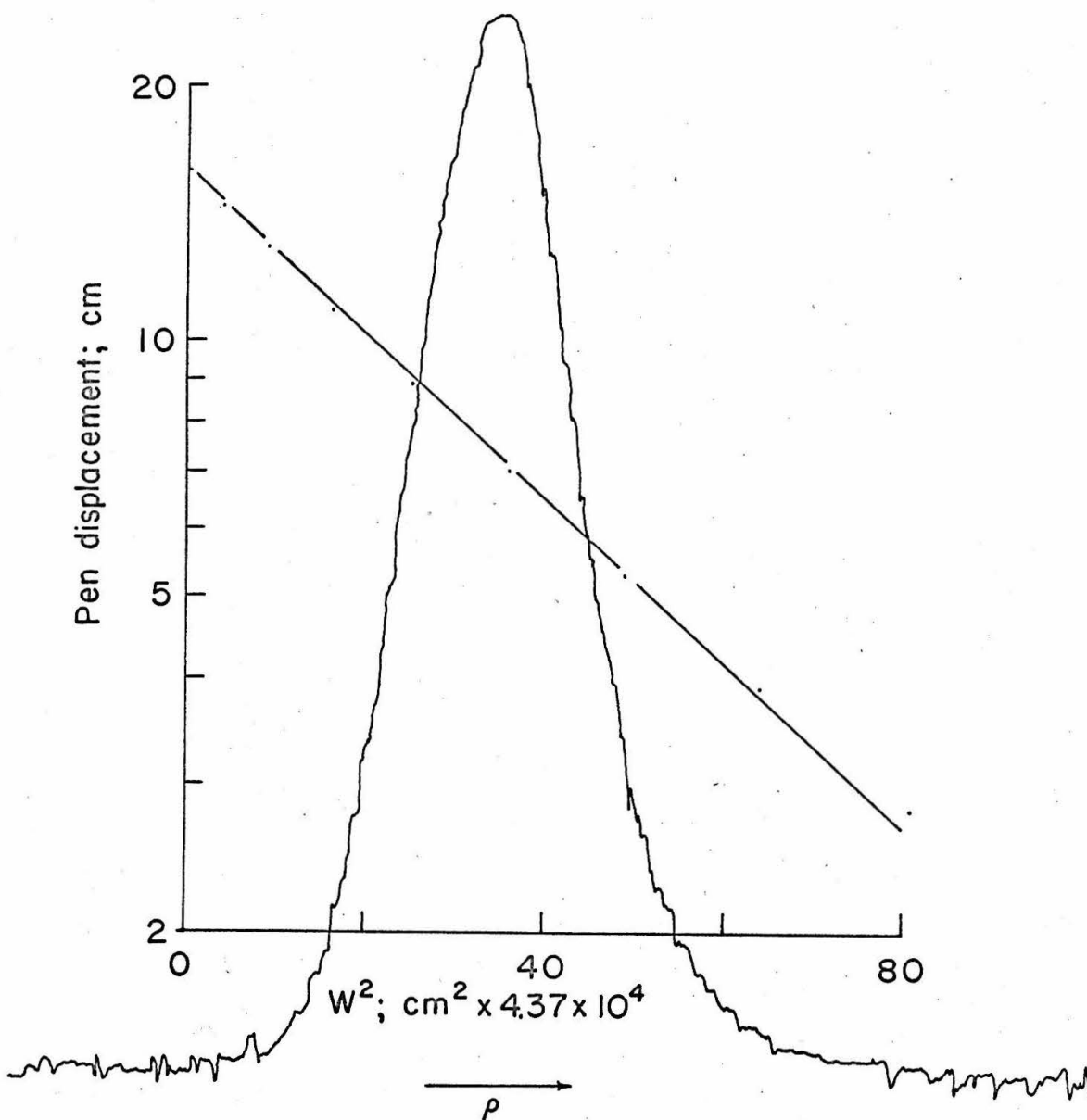
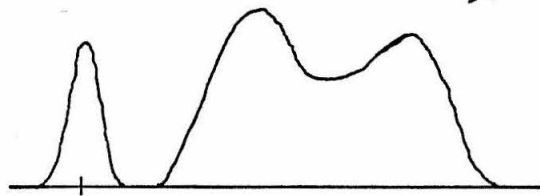
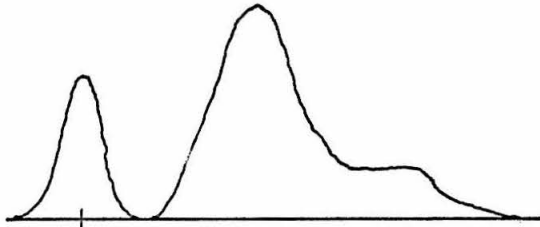


Figure 29. Equilibrium distribution of renatured T7 DNA<sub>2</sub> in a CsCl density gradient at 44,770 rpm and associated log C vs W<sup>2</sup> plot. Max DNA conc. 38 μg/ml; M<sub>Na</sub> = 14 x 10<sup>6</sup>; run in 12 mm cell; traced on densitometer #118 with a <sup>Na</sup>0.05 OD/cm wedge.

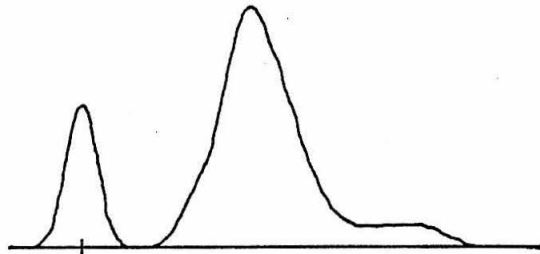
DNA was renatured 23 hrs in 75% formamide, 0.2 M NaCl at a DNA concentration of 40 μg/ml; %N<sub>m</sub> = 82.



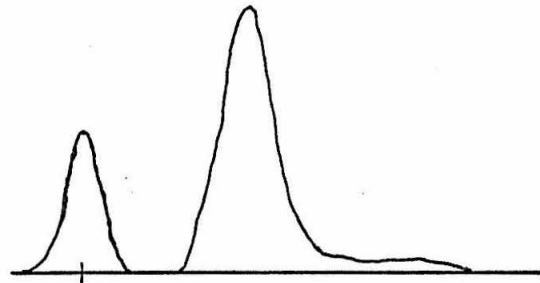
2 min  
%N<sub>b</sub> = 56  
%N<sub>m</sub> = 37



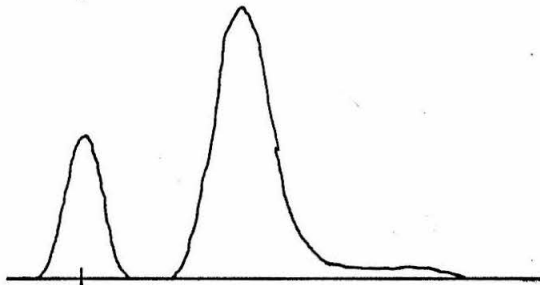
5 min  
%N<sub>b</sub> = 75  
%N<sub>m</sub> = 55



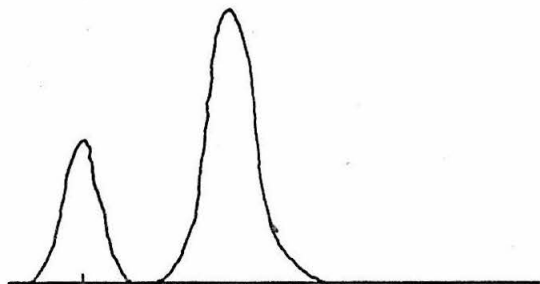
10 min  
%N<sub>b</sub> = 83  
%N<sub>m</sub> = 66



15 min  
%N<sub>b</sub> = 91  
%N<sub>m</sub> = 71



30 min  
%N<sub>b</sub> = 95  
%N<sub>m</sub> = 79



60 min  
%N<sub>b</sub> = 100  
%N<sub>m</sub> = 83

T4 DNA       $\rho \rightarrow$

Figure 30. Kinetics of renaturation. Banding profiles (Expt. I, text).

Table 2

Time	Expt. I		Expt. II	
	$\frac{*OD_{65}}{OD_{85}}$	%N <sub>m</sub>	$\frac{*OD_{65}}{OD_{85}}$	%N <sub>m</sub>
2 minutes	.894	36.7	.885	40.2
5 "	.847	55.4	.843	57.4
10 "	.820	66.1	.810	70.1
15 "	.809	70.5	.798	74.9
30 "	.787	79.3	.785	80.1
60 "	.777	83.3	.770	86.1
6 hours			.775	84.1

$\frac{*OD_{65}}{OD_{85}}$  = ratio of OD just previous to sharp melting  
to OD of fully melted material

The CsCl density gradient patterns of the partially renatured samples from experiment I show two bands, one at the denatured density and one at a density between .001 and .003 density units heavier than the native position. There appears to be a considerable amount of material banding in the region between the two bands in the early samples but as renaturation proceeds the denatured band disappears and the lighter band sharpens and approaches the native position more closely. The molecular weight calculated from the band width of the one hour sample of Fig. 30 was  $12 \times 10^6$ .

Preliminary kinetic data have been obtained from these two experiments. A fairly good approximation to the percentage of total material which bands at the denatured position can be made from the banding profiles of experiment I. From these data the rate of transfer of this material to lighter densities can be calculated. Although there may be substantial error in these approximations, the rate of disappearance of the denatured peak appears to follow second order kinetics quite closely as is shown in Fig. 31. On the other hand the kinetics of disappearance of material which melts as native material can also be plotted for various kinetic models. Melting data from experiments I and II do not fit first, second, third or fourth order plots (assuming equal concentrations of all initial reactants) if 100% native is taken as completion of the reaction. However, examination of the melting data of Table 1 shows that the reaction appears complete in the neighborhood of 86% native in both experiments. If 86% native is taken as the point at which the reaction is complete, the melting data from both experiments fit second order plots quite nicely as shown in Figs. 32 and 33. The fact that both melting and banding data from these experiments can be fitted to second order kinetics should be taken as more suggestive than conclusive due to the approximations and assumptions involved.

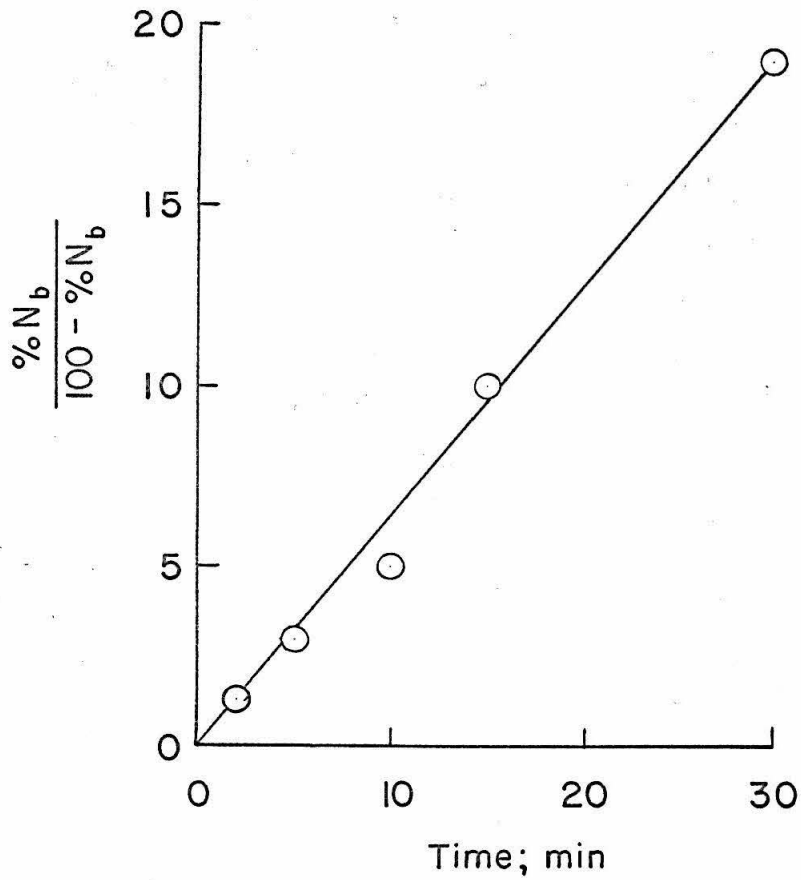


Figure 31. Second order kinetics of transfer of material from denatured to native density gradient band in renaturation. Experiment I in text.

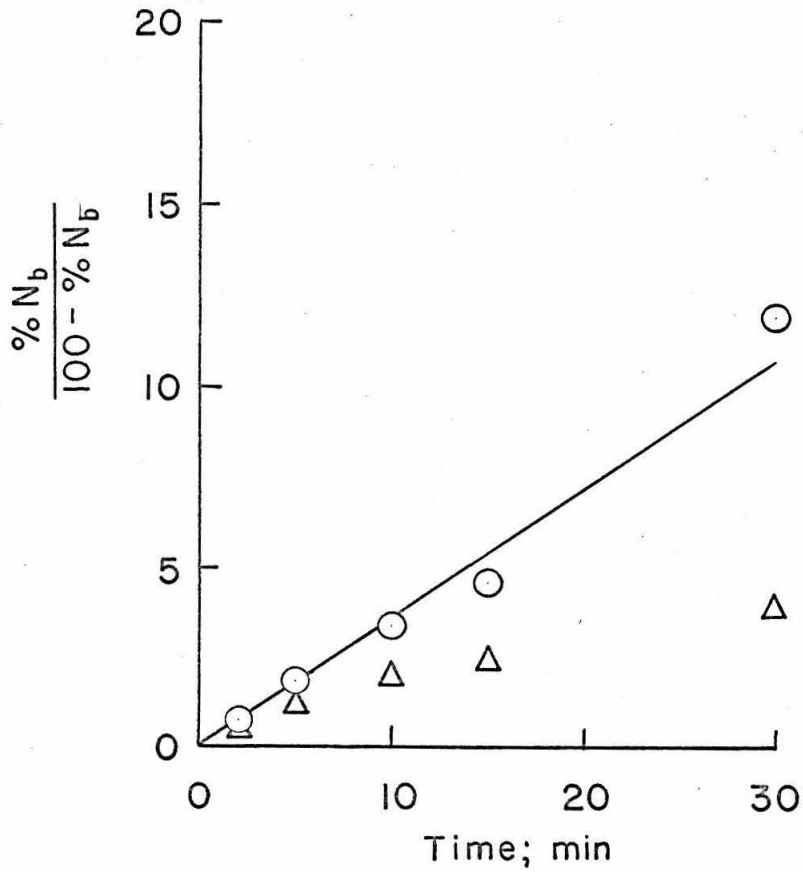


Figure 32. Renaturation kinetics. Second order plot of melting data of Experiment I in text.

- 86% Native as completion
- △ 100% Native as completion

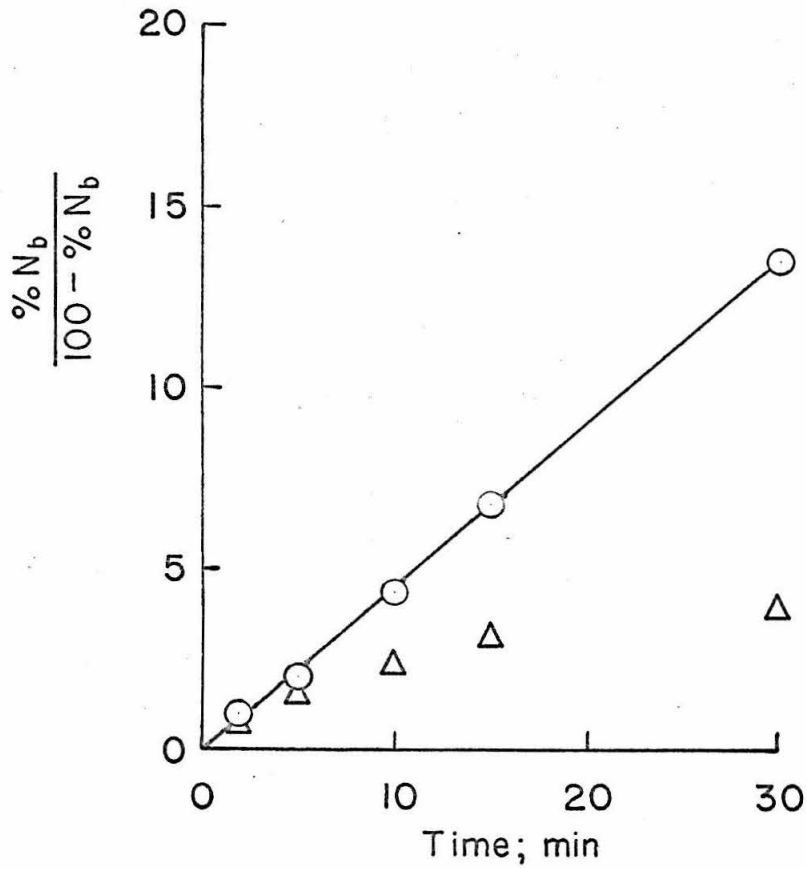


Figure 33. Renaturation kinetics. Second order plot of melting data of Experiment II in text.

○ 86% Native as completion

△ 100% Native as completion

## DISCUSSION

The foregoing experiments have shown that renaturation of T7 DNA occurs quite readily in formamide-water-salt solutions at 25°, thus making possible the complete cycle of denaturation and renaturation under non-degradative conditions. The product of renaturation of T7 DNA under the conditions used here was similar but not identical to native T7 DNA.

Methods for accurate study of renaturation kinetics have been outlined and the results of two kinetic experiments presented. The second order rate of disappearance of material which bands at the denatured position in a CsCl density gradient is in agreement with the idea that the two complementary strands come together in a bimolecular reaction as the first step in the renaturation reaction. The fact that the lighter band sharpens toward the native density with time in the renaturing mixture suggests that not all original pairings result in total native register and that false pairings are removed with time in the denaturing medium. The effects of multistrand aggregation could not be assessed in these experiments.

This system appears to be a promising one for the study of renaturation kinetics, and further study of samples renatured at different DNA concentrations by sedimentation velocity as well as by melting and banding techniques should yield valuable insights into the mechanism of the renaturation process.

APPENDIX

Light passing through a refractive index gradient will travel on the path  $x - x_0 = \Theta y + \left( \frac{1}{2n} \frac{dn}{dx} \right) y^2$ , (29), where  $n$  is the refractive index of the solution at the wavelength in question. In an ultracentrifuge cell  $x$  is the distance in the radial direction,  $y$  is distance in the direction normal to the cell windows, and  $\Theta$  is the angle between the entering light beam and the normal to the windows (in the plane defined by the normal to the windows and the radial axis of the cell). Let  $x_0, 0$  and  $x_e, y_e$  be the points at which a light beam enters and leaves the rotating solution, which contains a density gradient. Then  $y_e$  is the thickness of the cell centerpiece and  $x_e - x_0$  is the total  $x$  displacement experienced by light passing through the solution.

The absorption distribution of the light which has passed through the cell will determine the concentration distribution registered on film. The bending of light in the  $x$  direction by a density gradient will cause light to cross isoconcentration surfaces on passing through the cell.

An error is thus introduced into the film record of the concentration distribution in the cell. The particular case of interest for density gradient work is that in which the absorbing material in the cell has a

gaussian distribution  $C = C_0 e^{-\frac{(x - x_c)^2}{2\sigma^2}}$ . In this case the absorption of light which crosses the gaussian distribution upon passing through the cell from  $x_0$  to  $x_e$  is given by the expression

$$\log \frac{I_0}{I} = \text{const} \int_{x_0}^{x_e} e^{-\frac{(x - x_c)^2}{2\sigma^2}} ds$$

where  $ds = \sqrt{dx^2 + dy^2}$ . Evaluation of the integral over the individual paths of light through the cell gives the relative absorbancy for each path as a function of  $x_0$ , the result recorded on film. This absorption distribution may be compared with the concentration distribution in the cell.

As a first approximation to the real case let us first consider the case in which the light traverses the cell in a straight line,  $x - x_0 = ky$ .

For this path  $ds = \sqrt{1 + \left(\frac{1}{k}\right)^2} dx$  so that the absorbancy along a particular path is

$$\log \frac{I_0}{I} = \text{const} \int_{x_0}^{x_e} e^{-\frac{(x - x_c)^2}{2\sigma^2}} dx.$$

The above integral is just the area under the gaussian between  $x_0$  and  $x_e$ , which is readily available in published tables. Absorption distributions as a function of  $x_0$  were plotted for several values of  $\frac{x_e - x_0}{\sigma_{\text{cell}}}$

0.25 and 2, and all were found to be gaussian. Table 1 gives data about the absorption distributions for different values of  $\frac{x_e - x_0}{\sigma_{\text{cell}}}$ . The

lowering of the molecular weight due to the optical distortion is given

in the last column:  $\frac{M_{\text{abs}}}{M_{\text{cell}}} = \frac{\sigma_{\text{cell}}^2}{\sigma_{\text{abs}}^2}$ .

Table 1

$\frac{x_e - x_o}{\sigma_{\text{cell}}}$	$C_{\text{max}}$	$\frac{C_{\text{max}}}{C_{\text{max}}(0)}$	$\frac{\sigma_{\text{abs}}}{\sigma_{\text{cell}}}$	$\frac{M_{\text{abs}}}{M_{\text{cell}}} = \frac{\sigma_{\text{cell}}^2}{\sigma_{\text{abs}}^2}$
0	3989	1.000	1.000	1.000
0.25	3984	.999	1.002	.996
0.50	3948	.990	1.01	.980
1.0	3830	.960	1.04	.924
2.0	3431	.856	1.16	.743

The figures in Table 1 also give the error in densitometry of a film, where  $x_e - x_o$  is the effective slit width of the densitometer,  $\sigma_{\text{cell}}$  is the variance of the film gaussian and  $\sigma_{\text{abs}}$  is the variance of the traced gaussian.

For light which passes through the cell on the path  $x - x_o = ky$  the path on which light is maximally absorbed passes through the cell symmetrically about the center of the gaussian from  $-\frac{x_e - x_o}{2}$  to  $+\frac{x_e - x_o}{2}$ , thus shifting the center of the absorption distribution  $+\frac{x_e - x_o}{2}$ . However, the light beams themselves are shifted  $x_e - x_o$  so there is an apparent shift of center of the gaussian on film of  $-\frac{x_e - x_o}{2}$ .

Let us now consider the actual case for the density gradient where light enters the solution normal to the windows and thus crosses the cell on the path  $x - x_o = ky^2$ . For a CsCl gradient in the ultracentrifuge  $dy \gg dx$  so we may make the approximation  $ds = \sqrt{dx^2 + dy^2} \cong dy$ .

The absorbancy along an individual light path is then

$$\log \frac{I_0}{I} = \text{const} \int_{x_0}^{x_e} e^{-\frac{(x - x_c)^2}{2\sigma^2}} dy.$$

This integral can be approximated as follows:

From the definition of an integral

$$\int_{x_0}^{x_e} e^{-\frac{(x - x_c)^2}{2\sigma^2}} dy = \lim_{\substack{n \rightarrow \infty \\ \max \Delta_i y \rightarrow 0}} \sum_{i=1}^n \left( e^{-\frac{(x - x_c)^2}{2\sigma^2}} \right)_i \Delta_i y$$

where  $\Delta_i y$  is defined as the difference  $y_i - y_{i-1}$

where  $i = 0, 1, 2, \dots, n$  and  $0 = y_0 < y_1 < y_2 < \dots < y_n = y_e$ .

The quantity  $\left( e^{-\frac{(x - x_c)^2}{2\sigma^2}} \right)_i$  is some value of the gaussian between  $x_{i-1}$  and  $x_i$  where  $x_i$  is the value of  $x$  corresponding to  $y_i$ .

Obviously the above limit can be approximated to any desired accuracy by taking sufficiently large  $n$  and small  $\Delta y$ . The absorption distribution for the case of light crossing a gaussian concentration distribution on the path  $x - x_0 = ky^2$  through a distance  $\frac{x_e - x_0}{\sigma} = 1$  was determined by evaluating the absorbancies for eleven individual light paths by the sum

$$\sum_{i=1}^{10} \left( e^{-\frac{(x - x_c)^2}{2\sigma^2}} \right)_i \Delta_i y.$$

The total x displacement of the light was divided into ten equal parts bounded by

$$x_0, x_1, x_2, \dots, x_i, \dots, x_{10} = x_e$$

where  $x_i = x_0 + 0.1 i (x_e - x_0)$ .

Each value of x defines a value of  $y = \left( \frac{(x - x_0)^2}{k} \right)^{\frac{1}{2}}$ , but for convenience

$y_i$  was taken to be the fractional y displacement  $\frac{y}{y_e}$ . Thus the y displacement of the light passing through the solution is divided into ten parts bounded by

$$0 = y_0, y_1, y_2, \dots, y_i, \dots, y_{10} = 1$$

where  $y_i = \frac{\left( \frac{x_i - x_0}{k} \right)^{\frac{1}{2}}}{y_e} = \frac{\left( \frac{0.1 i (x_e - x_0)}{k} \right)^{\frac{1}{2}}}{\left( \frac{x_e - x_0}{k} \right)^{\frac{1}{2}}} = \sqrt{0.1 i}$

Thus the value of  $\Delta_i y = y_i - y_{i-1} = \sqrt{0.1 i} - \sqrt{0.1 (i-1)}$ .

The quantity  $\left( e^{-\frac{(x - x_c)^2}{2 \sigma^2}} \right)_i$  was taken to be the value of the gaussian at  $x = \frac{x_i - x_{i-1}}{2}$ .

The plot against  $x_0$  of the relative absorbancies determined for the eleven paths gave a gaussian curve identical to that obtained for light crossing the gaussian on the path  $x - x_0 = ky$ , except that the relative shift of the maximum was  $-0.33(x_e - x_0)$  (as found by Hearst and Vinograd (29)) rather than the  $-0.5(x_e - x_0)$  found for the linear path. This means that the error calculated for light crossing a gaussian distribution of absorbing material in the cell on a parabolic path is well approximated

by the error on a linear path for values of  $\frac{x_e - x_o}{\sigma_{\text{cell}}}$  up to at least 1 and probably further. Although the error for the parabolic path can be accurately estimated by the above procedure for any value of  $\frac{x_e - x_o}{\sigma_{\text{cell}}}$  if sufficiently large  $i$  is used, it seems reasonable to use the much more readily evaluated errors for a linear path as given in Table 1.

It should be pointed out that the above calculations are made on the assumption that  $\theta = 0$ , that is, that the light enters the solution normal to the windows. It seems likely from the above results that, for small deflections, the apparent decrease in molecular weight due to bending of light is almost solely a function of the maximum value of

$\left| \frac{x - x_o}{\sigma_{\text{cell}}} \right|$  and has very little dependence on the path taken. The maximum

value of  $|x - x_o|$  can be reduced by changing  $\theta$  so that  $x_e = x_o$ . In this case

$$x_e - x_o = \theta y_e - ky_e^2 = 0$$

$$\text{and } \theta = -ky_e.$$

The maximum  $x$  displacement will then be at  $y = \frac{1}{2}y_e$ , the midpoint of the cell, and will equal

$$x - x_o = -ky_e \left(\frac{1}{2}y_e\right) - k\left(\frac{1}{2}y_e\right)^2 = -\frac{1}{4}ky_e^2$$

which is one fourth the  $x$  displacement for the case when  $\theta = 0$ . Thus the optical error due to bending light can be reduced very extensively by the introduction of the proper wedge window into the bottom of the cell.

The quantity  $x_e - x_o$  is evaluated for the conditions used in the work reported here. For light entering the cell normal to the windows  $x_e - x_o = \left(\frac{1}{2n} \frac{dn}{dx}\right) y_e^2$ . For CsCl  $\rho = 10.8601 n - 13.4974$  (27) where  $n$  is the refractive index at 589  $m\mu$  and

$$\left(\frac{dn}{dx}\right)_{589} = .0921 \frac{d\rho}{dx} .$$

At  $\rho = 1.7$ ,  $\frac{d\rho}{dx} = 8.4 \times 10^{-10} \omega^2 x$  (27). Since the wavelength of light in this optical system is around 257  $m\mu$  the refractive index at this wavelength must be used. From (29)

$$\left(\frac{1}{2n} \frac{dn}{dx}\right)_{257} = 1.21 \left(\frac{1}{2n} \frac{dn}{dx}\right)_{589} .$$

The value of  $n_{589} = 1.400$  for a CsCl solution of  $\rho = 1.708$ , the density of T7 DNA, so

$$x_e - x_o = \left(\frac{1}{2n} \frac{dn}{dx}\right)_{257} y_e^2 = 3.34 \times 10^{-11} (\omega^2 x) y_e^2 .$$

At  $x_o = 6.6$  cm the light displacements due to the CsCl gradients in this work were:

Speed	$x_e - x_o$	
	3 mm cell	12 mm cell
25,980 rpm	$1.47 \times 10^{-4}$ cm	$2.35 \times 10^{-3}$ cm
44,770	$4.36 \times 10^{-4}$	$6.99 \times 10^{-3}$

These figures represent the  $x$  displacement by the salt gradient alone, but there is also a refractive index gradient due to compression of the solution. From data of Ifft (81) comparing the elevation of the

schlieren baseline upon coming to speed with the elevation after the salt gradient is established, the bending of light due to the compression gradient and window distortion combined is about 30% of that due to the CsCl gradient at 39,460 rpm. A similar estimate was obtained by us at 44,770 rpm from the displacement of the slit image focused behind the camera lens in the UV system. At speeds around 44,770 rpm the total x displacement of the light upon passing through the solution will be somewhere between that calculated for the salt gradient alone and an amount 30% greater than that.

REFERENCES

1. M. Meselson, F. W. Stahl and J. Vinograd. Proc. Nat. Acad. Sci. (1957) 43, 581-588.
2. J. E. Hearst and J. Vinograd. Proc. Nat. Acad. Sci. (1961) 47, 825-830.
3. J. E. Hearst and J. Vinograd. Proc. Nat. Acad. Sci. (1961) 47, 999-1004.
4. J. E. Hearst and J. Vinograd. Proc. Nat. Acad. Sci. (1961) 47, 1005-1014.
5. J. E. Hearst, J. B. Ifft and J. Vinograd. Proc. Nat. Acad. Sci. (1961) 47, 1015-1025.
6. S. Yeandle. Proc. Nat. Acad. Sci. (1959) 45, 184-188.
7. R. L. Baldwin. Proc. Nat. Acad. Sci. (1959) 45, 939-944.
8. J. E. Hearst. Doctoral dissertation, California Institute of Technology (1961).
9. M. Meselson and F. W. Stahl. Proc. Nat. Acad. Sci. (1958) 44, 671-682.
10. R. Rolfe and M. Meselson. Proc. Nat. Acad. Sci. (1959) 45, 1039-1043.
11. N. Sueoka, J. Marmur and P. Doty. Nature (1959) 183, 1429-1431.
12. N. Sueoka. Proc. Nat. Acad. Sci. (1959) 45, 1480-1490.
13. N. Sueoka. J. Mol. Biol. (1961) 3, 31-40.
14. I. Rubenstein, C. A. Thomas and A. D. Hershey. Proc. Nat. Acad. Sci. (1961) 47, 1113-1122.
15. P. F. Davison, D. Freifelder, R. Hede, and C. Levinthal. Proc. Nat. Acad. Sci. (1961) 47, 1123-1129.

16. J. Cairns. J. Mol. Biol. (1961) 3, 756-761.
17. J. Cairns. Nature (1962) 194, 1274.
18. I. Bendet, E. Schachter, M. A. Lauffer. J. Mol. Biol. (1962) 5, 76-79.
19. A. D. Kaiser and D. S. Hogness. J. Mol. Biol. (1960) 2, 392-415.
20. C. A. Thomas and T. C. Pinkerton. J. Mol. Biol. (1962) 5, 356-372.
21. M. Meselson in The Cell Nucleus (1959) pp. 240-245, The Faraday Society, publ. Butterworth and Co. (Publishers) Ltd., London.
22. P. F. Davison and D. Freifelder. J. Mol. Biol., in press.
23. P. F. Davison. Proc. Nat. Acad. Sci. (1959) 45, 1560-1568.
24. D. Fraser and E. A. Jerrel. J. Biol. Chem. (1953) 205, 291-295.
25. J. D. Mandell and A. D. Hershey. Analyt. Biochem. (1960) 1, 66-77.
26. R. J. L. Allen. Biochem. J. (1940) 34, 858-865.
27. J. B. Ifft, D. H. Voet, and J. Vinograd. J. Phys. Chem. (1961) 65, 1138-1145.
28. R. Trautman. Arch. Biochem. and Biophys. (1960) 87, 289-292.
29. J. E. Hearst and J. Vinograd. J. Phys. Chem. (1961) 65, 1069-1070.
30. H. K. Schachman, L. Gropper, S. Hanlon and F. Putney. Arch. Biochem. and Biophys. (1962) 99, 175-190.
31. P. F. Davison. Personal communication.
32. J. D. Watson and F. H. C. Crick. Nature (1953) 171, 737-738.
33. S. A. Rice and P. Doty. J. Amer. Chem. Soc. (1957) 79, 3937-3947.
34. P. Doty, J. Marmur, J. Eigner and C. Schildkraut. Proc. Nat. Acad. Sci. (1960) 46, 461-476.
35. L. F. Cavalieri and B. H. Rosenberg. Ann. Rev. Biochem. (1962) 31, 247-270.

36. J. Marmur, R. Rownd and C. L. Schildkraut. Submitted to Progress in Nucleic Acid Research, Vol. I, J. N. Davidson and W. E. Cohn, eds. Academic Press, New York.
37. L. F. Cavalieri and B. H. Rosenberg. J. Amer. Chem. Soc. (1957) 79, 5352-5357.
38. P. D. Lawley. Biochim. Biophys. Acta (1956) 21, 481-488.
39. P. Doty, H. Boedtker, J. R. Fresco, R. Haselkorn and M. Litt. Proc. Nat. Acad. Sci. (1959) 45, 482-499.
40. L. F. Cavalieri, M. Rosoff and B. H. Rosenberg. J. Amer. Chem. Soc. (1956) 78, 5239-5247.
41. R. A. Cox and A. R. Peacocke. J. Polymer Science (1957) 23, 765-779.
42. P. Ehrlich and P. Doty. J. Amer. Chem. Soc. (1958) 80, 4251-4255.
43. K. Hamaguchi and E. P. Geiduschek. J. Amer. Chem. Soc. (1962) 84, 1329-1338.
44. G. K. Helmkamp and P. O. P. Ts'o. J. Amer. Chem. Soc. (1961) 83, 138-142.
45. J. Marmur and P. O. P. Ts'o. Biochim. Biophys. Acta (1961) 51, 32-36.
46. E. P. Geiduschek and T. T. Herskovits. Arch. Biochem. Biophys. (1961) 95, 114-129.
47. C. E. Hall and M. Litt. J. Biochem. Biophys. Cytol. (1958) 4, 1-4.
48. N. K. Sarkar and A. L. Dounce. Biochim. Biophys. Acta (1961) 49, 160-169.
49. W. Ginoza and B. H. Zimm. Proc. Nat. Acad. Sci. (1961) 47, 639-652.
50. J. Eigner, H. Boedtker and G. Michaels. Biochim. Biophys. Acta (1961) 51, 165-168.

51. C. A. Thomas and P. Doty. J. Amer. Chem. Soc. (1956) 78, 1854-1860.
52. S. Greer and S. Zamenhof. J. Mol. Biol. (1962) 4, 123-141.
53. J. Applequist. J. Amer. Chem. Soc. (1961) 83, 3158-3159.
54. J. Marmur and P. Doty. Nature (1959) 183, 1427-1429.
55. J. Marmur and P. Doty. J. Mol. Biol. (1962) 5, 109-118.
56. J. Josse, A. D. Kaiser and A. Kornberg. J. Biol. Chem. (1961) 236, 864-875.
57. E. P. Geiduschek. J. Mol. Biol. (1962) 4, 467-487.
58. E. P. Geiduschek. J. Polymer Science (1958) 31, 67-75.
59. W. F. Dove, F. A. Wallace and N. Davidson. Biochem. Biophys. Res. Comm. (1959) 1, 312-317.
60. C. L. Schildkraut, J. Marmur and P. Doty. J. Mol. Biol. (1961) 3, 595-617.
61. K. I. Berns and C. A. Thomas. J. Mol. Biol. (1961) 3, 289-300.
62. M. Beer and C. A. Thomas. J. Mol. Biol. (1961) 3, 699-700.
63. D. Freifelder and P. F. Davison. Biophys. J. (1962) 2, 249-256.
64. E. P. Geiduschek. Proc. Nat. Acad. Sci. (1961) 47, 950-955.
65. J. Marmur and L. Grossman. Proc. Nat. Acad. Sci. (1961) 47, 778-787.
66. J. Marmur and D. Lane. Proc. Nat. Acad. Sci. (1960) 46, 453-461.
67. J. Marmur and P. Doty. J. Mol. Biol. (1961) 3, 585-594.
68. A. W. Kozinski and M. Beer. Biophys. J. (1962) 2, 129-141.
69. L. F. Cavalieri, T. Small and N. Sarkar. Biophys. J. (1962) 2, 339-350.

70. R. M. Herriott. Proc. Nat. Acad. Sci. (1961) 47, 146-153.
71. K. D. Lunan and R. L. Sinsheimer. Virology (1956) 2, 455-462.
72. I. Tinoco. J. Amer. Chem. Soc. (1960) 82, 4785-4790.
73. J. P. Johnston and A. G. Ogston. Trans. Faraday Soc. (1946) 42, 789-799.
74. J. E. Hearst and J. Vinograd. Arch. Biochem. Biophys. (1961) 92, 206-215.
75. E. Burgi and A. D. Hershey. J. Mol. Biol. (1961) 3, 458-472.
76. As quoted in B. S. Friesen and R. L. Sinsheimer. J. Mol. Biol. (1959) 1, 321-328.
77. R. L. Sinsheimer. Personal communication.
78. P. O. P. Ts'o, G. K. Helmkamp and C. Sander. Biochim. Biophys. Acta (1962) 55, 584-600.
79. See for example pp. 447-449 in Technique of Organic Chemistry, Vol. VII, Organic Solvents, (1955), by A. Weissberger, E. S. Proskauer, J. A. Riddick and E. E. Toops, Jr. Interscience Publishers, Inc. London.
80. G. Streisinger, R. S. Edgar and G. H. Denhardt. In preparation.
81. J. B. Ifft. Personal communication.